AA&ES-67-9

Purdue University
School of Aeronautics, Astronautics, and Engineering Sciences
Lafayette, Indiana

NONEQUILIBRIUM RADIATION AND IONIZATION IN SHOCK WAVES

by

Clair E. Chapin

June 1967

This research was sponsored by
The Office of Naval Research (N00014-67-A-0226-0001) and
by the National Aeronautics and Space Administration (NASA 8-11485)

Purdue Research Foundation – Research Projects 4520 and 1492

AA&ES 67-9

NONEQUILIBRIUM RADIATION AND IONIZATION IN SHOCK WAVES

Clair E. Chapin*

June 1967

This research was sponsored by The
Office of Naval Research (N00014-67-A-0226-0001) and
by the National Aeronautics and Space Administration (NASA 8-11485)

* Presently at Lawrence Radiation Laboratory, P.O. Box 808, Livermore, California 94551.

ACKNOWLEDGMENTS

I am grateful to the Office of Naval Research and the National Aeronautics and Space Administration for their financial support.

It is a pleasure to acknowledge Dr. Robert Goulard for his helpful counsel and Mr. H. Frederick Nelson for his capable assistance with some of the calculations.

TABLE OF CONTENTS

TABLE OF CONTENTS
(Continued)

LIST OF TABLES

LIST OF FIGURES

ABSTRACT

Radiation energy transfer and ionization rates in the mixture of atoms, ions and electrons produced by a normal shock wave propagating in cold argon gas are examined. It is shown the gas may be regarded as a combination of two gases, one composed only of electrons and one composed of both atoms and ions. Temperature differences between the electron gas and the atom-ion gas significantly affect radiation and ionization rates in the shock wave.

The analysis uses the ionization rates due to both atom-atom collisions and electron-atom collisions. In addition, photoionization, which is responsible for precursor ionization, is included.

Although argon is not a grey gas, it is shown that the radiation variables may be reduced to the forms they would have if the gas were grey, but with different source functions and attenuation properties. Radiation generated by photoionization and radiative recombination involving excited atomic states escapes ahead of the shock wave and results only in cooling the hot gas. Radiation due to photoionization and recombination involving the ground state is trapped by the cold particles ahead of the shock and causes precursor ionization. Photoexcitation processes (line radiation) are omitted from consideration.

The integral form of the radiation variables causes the equations to be integro-differential. Iterative techniques for solving the

equations are not practical because they converge too slowly. Instead, a combined perturbation-iteration method is used.

The effect of viscosity and heat conduction is to discontinuously change the temperature and density of the gas. Preceding the discontinuity is the precursor region caused by ground state photoionization. After the discontinuity the electron gas is colder than the atom-ion gas. Subsequently the electron gas temperature increases until it becomes equal to the temperature of the atom-ion gas. Finally, after chemical equilibrium has been reached, the gas radiatively cools to its final stage. The ionization rate and precursor ionization are found to be greatly affected by the cool layer of the electron gas following the discontinuity.

Radiation energy transfer has little effect on the ionization rate until equilibrium ionization is approached. The net collisional rates then decrease and the radiative rates become relatively more important. The net effect is to decrease the ionization rate and delay chemical equilibrium.

CHAPTER I

BACKGROUND AND LITERATURE SURVEY

In the last few years there has been a great deal of interest concerning shock waves propagating with sufficient speed that the shocked gas becomes ionized and emits radiation. Shock tube research has shown how elastic and inelastic collisions between electrons, ions, and atoms of the gas influence the ionization process. The role of radiation in the ionization process, however, has never been determined.

In this thesis the effect of radiation energy transfer on the ionization process in shock waves propagating in argon is investigated. It is an especially difficult problem because the radiation energy transfer, the kinetics of ionization and the energy exchange between electrons, atoms and ions in the gas must be considered simultaneously. The frequency dependence of the radiative emission and absorption processes leads to additional difficulties in calculating the radiation energy transfer.

Although the analysis in this thesis is performed for shock waves in argon, its concepts and techniques are generally applicable to chemically reacting, radiating gases.

All shock waves analyzed in this thesis are assumed to be normal and time independent. In the Eulerian frame of reference the three appropriate fluid conservation equations are:

The Conservation of Mass Equation.

$$\frac{d}{dx}(\rho u) = 0 \tag{1.1}$$

In this equation ρ is the mass density of the gas, u is the velocity of an elemental gaseous volume and x is a coordinate parallel to the direction of shock wave propagation. The origin of x is fixed to the shock wave. Values of x increase in a direction opposite to the direction of shock wave propagation as shown on Figure 1.1.

The Conservation of Momentum Equation.

$$\frac{d}{dx}\left[\rho u^2 + p - \sigma\right] = 0 \tag{1.2}$$

Here p is the hydrostatic pressure in the gas and σ is the compressive stress produced in the gas because of its viscosity.

The Energy Conservation Equation.

$$\frac{d}{dx}\left[\rho u \left(h + \tfrac{1}{2}u^2\right) - \sigma u + q\right] = 0 \tag{1.3}$$

The quantity $h = (\epsilon + p)/\rho$ stands for the enthalpy per unit mass of gas, ϵ is the internal energy of the gas per unit volume and q is the net heat flux in the direction of increasing x.

These equations may be integrated once to give

$$\rho u = M \tag{1.4}$$

$$Mu + p - \sigma = P \tag{1.5}$$

$$M\left(h + \tfrac{1}{2}u^2\right) - \sigma u + q = E \tag{1.6}$$

where M, P and E are integration constants. These are the equations which are applied to the analysis of shock wave structure in the simplest

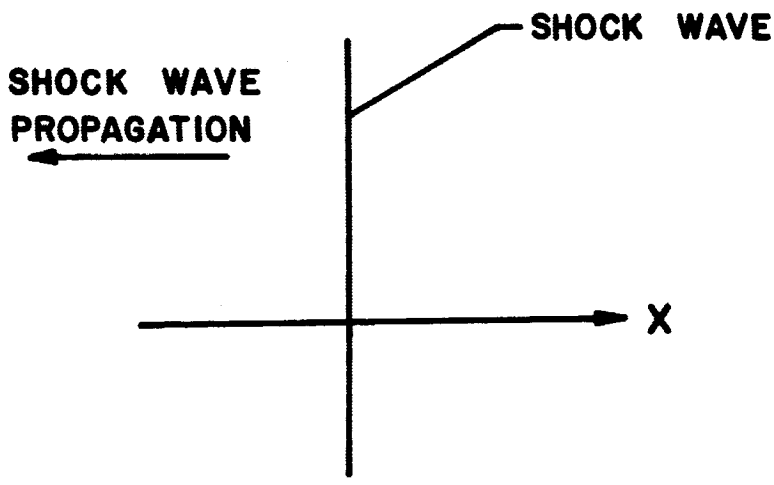

Figure 1.1. Coordinate System.

cases. It is necessary to modify them when the shock wave occurs in a partially ionized gas. This modification is discussed in Chapter II.

The character of the flow in a shock wave is determined by the quantities h, p, σ and q. The way in which these quantities are influenced by viscosity, chemical reactions, radiation and ionization is discussed in the following sections.

Effect of Viscosity

The viscosity of a gas is responsible for the compression and resultant heating which occur in shock waves. At low speeds where the gas is not hot enough to produce changes of state in the gas or emit radiation, it is the only process which occurs. The pressure, enthalpy, compressive stress and heat conduction are then described by the following familiar relations.

$$p = \rho RT \tag{1.7}$$

$$h = C_p T \tag{1.8}$$

$$\sigma = \mu_J \frac{du}{dx} \tag{1.9}$$

$$q = - k_c \frac{dT}{dx} \tag{1.10}$$

Far upstream and far downstream the compressive stress and heat flux are both zero and the initial and final states are related by

$$\rho_- u_- = \rho_+ u_+ = M \tag{1.11}$$

$$Mu_- + p_- = Mu_+ + p_+ \tag{1.12}$$

$$h_- + \tfrac{1}{2} u_-^2 = h_+ + \tfrac{1}{2} u_+^2 \tag{1.13}$$

Subscripts + and - in these equations denote values at + ∞ and - ∞ on the x coordinate.

Mathematically speaking the shock extends from - ∞ to + ∞. In practice the thickness of the viscous shock is often negligibly small. It may then be thought of as producing an instantaneous change in the state of the gas with the initial and final states related by equations (1.11) through (1.13). In mathematical terms the change of state produced by the shock wave may be described as a step function.

Effect of Finite Chemical Rates

The final state reached by the gas in a shock wave can be chemically changed compared to its initial state. Description of chemical changes in shock waves can be very complicated. For example, Sherman [1]* has studied a radiating shock wave in air involving thirty-four reactions. The shock waves studied in this thesis are assumed to propagate in argon. The choice of argon is advantageous because the only chemical process which can occur in argon is ionization. Consequently the chemistry is relatively uncomplicated. Furthermore, because of its wide use in shock tube experiments, the properties of argon are well known.

For ionized argon gas the enthalpy and pressure are given by the following formulas [2].

$$h = \frac{5}{2}(1 + \alpha)\,\rho RT + \alpha R T_{ion} \qquad (1.14)$$

$$p = (1 + \alpha)\,\rho RT \qquad (1.15)$$

---

* Numbers in brackets refer to the Bibliography.

In these equations α is the degree of ionization in the gas

$$\alpha = \frac{n_i}{n_a + n_i} \tag{1.16}$$

where n_i is the number density of ions and n_a is the number density of atoms. T_{ion} is the ionization temperature defined by the requirement that kT_{ion} be the ionization potential. For argon $T_{ion} = 1.82(10^5)$ K.

If the ionization is rapid, the gas may be thought of as instantaneously adjusting to a degree of ionization such that the rate of ionization and the rate of recombination cancel each other. The gas is then said to be in chemical equilibrium. If chemical equilibrium is maintained in the gas, the degree of ionization may be calculated from the Saha equation [2] which for argon may be written

$$\frac{\alpha^2}{1 - \alpha} = \frac{\rho_{ion}}{\rho} \left(\frac{T}{T_{ion}} \right)^{3/2} e^{- T_{ion}/T} \tag{1.17}$$

where ρ_{ion} is a constant which has the value 149.3 gm/cm^3.

However, because of the finite rate at which ionization processes proceed, the changes which would take place in a shock wave if chemical equilibrium were maintained in the gas, may be more rapid than can actually occur. The degree of ionization in this case must be calculated from equations which describe the chemical kinetics of the ionization process. Assuming no diffusion of electrons, conservation of electrons requires

$$\frac{d}{dx} (n_e u) = \dot{n}_{e_{coll}} + \dot{n}_{e_{rad}} \tag{1.18}$$

where n_e is the number density of electrons, $\dot{n}_{e_{coll}}$ is the net rate of production electrons by collisional processes and $\dot{n}_{e_{rad}}$ is the net

rate of production of electrons by radiative processes. If the number density of electrons and ions are equal, the degree of ionization may be written

$$\alpha = \frac{n_i}{n_a + n_i} = \frac{n_e}{n_a + n_i} \doteq \frac{n_e}{\rho / m_a}$$

where m_a is the atomic mass. Equation (1.18) may then be transformed to

$$M \frac{d\alpha}{dx} = m_a(\dot{n}_{e_{coll}} + \dot{n}_{e_{rad}}) \tag{1.19}$$

Collisional ionization occurs by the following reactions:

$$A(p) + \underline{\bar{X}} \rightleftarrows A^+ + \underline{\bar{X}} + e \qquad p = 1,2, \ldots \tag{1.20}$$

$$A(p) + \underline{\bar{X}} \rightleftarrows A(q) + \underline{\bar{X}} \qquad q > p,\ p = 1,2, \ldots \tag{1.21}$$

A represents an argon atom, e an electron and $\underline{\bar{X}}$ stands for a typical reaction partner which could be A, e, or a contaminant species. Bound electron states are indicated by the index p or q with p = 1 corresponding to the ground state.

Radiative ionization is described by a similar set of reaction equations.

$$A(p) + h\nu \rightleftarrows A^+ + e \qquad p = 1,2,3, \ldots \tag{1.22}$$

$$A(p) + h\nu \rightleftarrows A(q) \qquad q > p,\ p = 1,2,3, \ldots \tag{1.23}$$

Continuum radiation is emitted and absorbed by reactions (1.22) and line radiation by (1.23).

Other reactions are possible but the research to be reviewed presently shows them to be of secondary importance for the calculations performed in this thesis.

Detailed expressions for the collisional and radiative ionization rates are developed in Chapter II.

Effect of Radiation

Radiation of the gas in a shock wave can affect shock wave structure by contributing to the ionization process, as just discussed, and by its contribution to the heat flux q. The effect of radiation on pressure and energy density is completely negligible for the calculations performed in this study [3].

The equation of radiation energy transfer appropriate to a one-dimensional geometry is

$$\mu \frac{dI}{dx}(x, \mu, \nu) = - \frac{1}{\ell (x,\nu)} [I(x, \mu, \nu) + S(x, \nu)] \qquad (1.24)$$

The radiation intensity $I(x, \mu, \nu)$ is defined by the requirement that $I(x, \mu, \nu)\ dA\ d\omega\ d\nu$ is the radiation energy which passes through area dA of a surface at x whose normal is parallel to the x axis, within solid angle $d\omega$ of a direction making an angle $\cos^{-1}\mu$ with the x axis, in the frequency interval ν, $\nu + d\nu$, per unit time. The geometry appropriate to this definition is pictured in Figure 1.2.

The source function $S(x, \nu)$ is the radiation intensity at position x, angle $\cos^{-1}\mu$ and frequency ν due to radiation emitted per unit mass of gas at the location of dA. Since emitted radiation is independent of direction, the source function has no dependence on μ.

The penetration length $\ell(x, \nu)$ is the length required for the radiation intensity to decrease by a factor $1/e$ in a gas of constant properties if there is no emission of radiation (as can be seen directly from equation (1.24)). The penetration length is a function of x through its dependence on temperature, density, etc., and it is a function

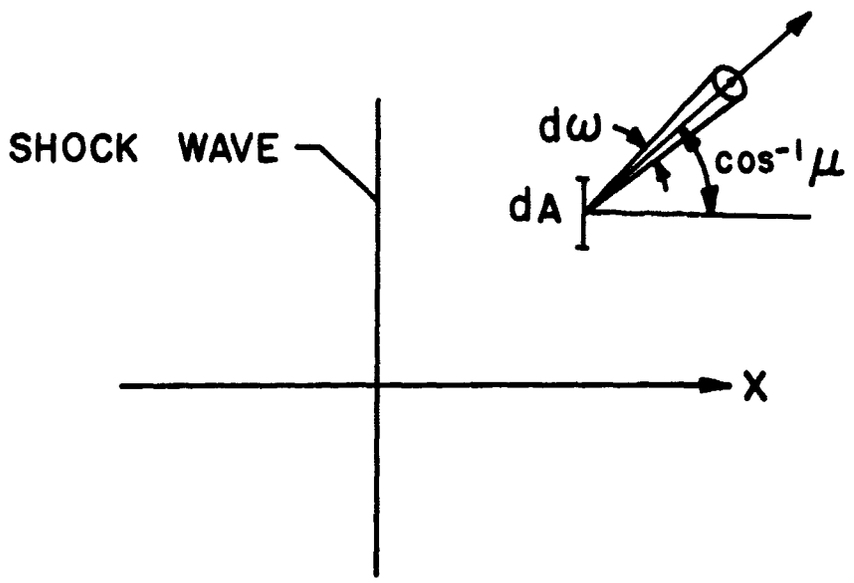

Figure 1.2. Radiation Transfer Geometry.

of frequency through the way in which radiation is created and destroyed by the atoms, ions and electrons in the gas. Detailed formulas for the penetration length are developed in Chapter II.

At the upstream boundary $x = x_-$ the gas is assumed so cold that no radiation is emitted in the positive x direction. At the downstream boundary, the gas is assumed to have constant properties and the intensity is given by the Planck function $B_\nu(T) = 2h\nu^3/c^2(e^{h\nu/kT}-1)^{-1}$ evaluated at the upstream temperature T_+.

$$I(x_-, \mu, \nu) = 0 \qquad \text{for } 0 \leq \mu \leq 1$$
$$I(x_+, \mu, \nu) = B_\nu(T_+) \tag{1.25}$$

Replacing x by the optical length

$$\tau(x, \nu) = \int_0^x \frac{dx'}{\ell(x', \nu)} \tag{1.26}$$

in terms of which equation (1.24) is linear, the solution of equation (1.24) appropriate to the boundary conditions (1.25) is seen to be

$$I(x,\mu, \nu) = \begin{cases} \displaystyle\int_{\tau(x_-,\nu)}^{\tau(x, \nu)} S(x',\nu) \exp\{-[\tau(x, \nu) - \tau(x', \nu)]/\mu\} d\tau(x', \nu)/\mu \\ \qquad\qquad \text{for } 0 \leq \mu \leq 1 \\ B_\nu(T_+)\, e^{-[\tau(x,\nu) - \tau(x_+,\nu)]/\mu} \\ \qquad - \displaystyle\int_{\tau(x,\nu)}^{\tau(x_+,\nu)} S(x,\nu) \exp\{-[\tau(x, \nu) - \tau(x', \nu)]/\mu\} d\tau(x', \nu)/\mu \\ \qquad\qquad \text{for } -1 \leq \mu \leq 0 \end{cases} \tag{1.27}$$

The contribution to the heat flux from radiation in the frequency range ν, $\nu + d\nu$ is

$$q_R(x, \nu) = 2\pi \int_{-1}^{1} \mu \; I(x, \mu, \nu) \, d\mu \tag{1.28}$$

Substitution of (1.27) into this expression gives

$$q_R(x, \nu) = 2\pi \left[\int_{\tau(x_-,\nu)}^{\tau(x_+,\nu)} S(x',\nu)\,\mathrm{sgn}[\tau(x,\nu) - \tau(x',\nu)] E_2(|\tau(x,\nu) - \tau(x',\nu)|) d\tau(x',\nu) \right.$$

$$\left. - E_3[\tau(x_+,\nu) - \tau(x,\nu)] \; B_\nu(T_+) \right] \tag{1.29}$$

where

$$E_n(t) = \int_0^1 \mu^{n-2} \; e^{-t/\mu} \, d\mu \tag{1.30}$$

$$\mathrm{sgn}\,(t-t') = \begin{cases} +1 & \text{if } t' \leq t \\ -1 & \text{if } t' > t \end{cases} \tag{1.31}$$

The location of the downstream boundary x_- will be taken to be $-\infty$ and that of the upstream boundary x_+ will be taken to be $+\infty$. Then equation (1.29) becomes

$$q_R(x, \nu) = 2\pi \int_{-\infty}^{+\infty} S(x',\nu)\,\mathrm{sgn}[\tau(x,\nu) - \tau(x',\nu)] E_2[\,|\tau(x,\nu) - \tau(x',\nu)|\,] d\tau(x',\nu) \tag{1.32}$$

The total contribution to the heat flux due to radiation of all frequencies is found from this by an integration over frequency.

$$q_R(x) = \int_0^\infty q_R(x,\nu) d\nu \tag{1.33}$$

The form of the radiative heat flux q_R considerably complicates the problem because of the frequency integration required in equation (1.33) and because the integrand in equation (1.32) depends on the

temperature, density, etc. of the gas which are not known until the problem is solved. In almost all of the work on radiation shock waves the problem has been simplified by assumptions involving one or both complicating factors.

Effects of Ionization

Ionization in shock waves is responsible for some phenomena which are mentioned here and discussed in greater detail later.

A partially ionized gas is a mixture of atoms, ions, and electrons. In such a mixture it is possible for processes to occur in which one species is preferentially affected.

For example, electrons will lose energy by creating ions through the reaction

$$e + A(p) \rightarrow A^{+} + e + e.$$

It happens that the ways in which electrons can gain energy are much less efficient than the way they lose energy by creating ions. The net result is an energy drain from the electrons. The electrons can be thought of as cooler than other species when ionization is taking place.

The thermal conductivity of electrons is much larger than for other species. Consequently a preferential heat conduction in the electron gas can be expected.

Transport properties are greatly affected by ionization. Viscosity and heat conduction are much different for a slightly ionized gas than one which is fully ionized [4].

Collision processes by which energy and momentum exchange take place also depend on the degree of ionization in the gas. If the

degree of ionization is small, energy and momentum exchange takes place through binary collisions. But when the degree of ionization is large, energy and momentum may be exchanged by interactions involving many particles.

Lastly, the steep concentration gradients in a shock wave will promote diffusion of electrons relative to ions. The resulting charge separation will cause an electric field which can affect the flow.

Literature Survey

The survey presented in this section does not attempt to give an exhaustive account of all the research conducted on radiating, chemically reacting shock waves. Rather, its purpose is to illustrate the experimental and theoretical knowledge which has been gained by such research.

Radiation in Shock Waves

All of the work involving radiation energy transfer in shock waves, with the exception of the work of Clarke and Ferrari [5], has assumed the gas to be grey and the radiation to be emitted in local thermodynamic equilibrium.

A gas is grey when its penetration length may be replaced by an average penetration length which is independent of frequency.

$$\ell(x, \nu) \rightarrow \ell_{avg}(x) \tag{1.34}$$

Local thermodynamic equilibrium means that the source function at any point in the gas is given by the Planck function evaluated at the local gas temperature.

$$S(x, \nu) = B_{\nu}(T) \tag{1.35}$$

With these simplifying assumptions equation (1.33) for the radiative flux becomes

$$q_R = 2\int_{-\infty}^{+\infty} \gamma\, T(x')^4 \operatorname{sgn}[\tau(x) - \tau(x')] E_2(|\tau(x) - \tau(x')|)\, d\tau(x') \qquad (1.36)$$

where γ is the Stefan-Boltzmann constant and

$$\tau(x) = \int_0^x \frac{dx'}{\ell_{avg}(x')} \qquad (1.37)$$

The radiation is characterized by the average penetration length. This is a consequence of the grey gas assumption. When frequency variation of the radiation is considered, there may be no one length which typifies radiation energy transfer. Non-grey radiation energy transfer is considered in Chapter II.

Research on radiating shock waves may be classified by whether the radiation is lost or trapped.

Of course no radiation energy can ever be lost in the sense that it is destroyed. By lost radiation is meant radiation which escapes the system being considered. For example, radiation may be lost from a shock tube to the surrounding laboratory. Loss of radiation energy from a system is referred to as radiation cooling.

Radiation which is not lost but re-absorbed within the shock will be termed trapped radiation. All previous investigations of shock wave structure have considered either trapped radiation or radiation cooling but not both.

Heaslet and Baldwin [6] have obtained solutions for shock waves with trapped radiation. The shock wave is assumed to be inviscid and propagating in a perfect gas. The mathematical problem associated with

the integral form of the radiation flux, which requires the solution to be known before the integrand in equation (1.36) can be calculated, is avoided by what is essentially the differential approximation discussed by Murty [7] and by Goulard and Traugott [8].

Although the problem solved by Heaslet and Baldwin is the least complicated formulation possible which involves trapped radiation, it must still be solved numerically.

If there were no radiation, the solution would be a step function shock wave caused by viscosity and heat conduction in the gas. The nature of the solution depends on the amount of heating which occurs by radiation energy transfer compared to that which occurs by viscous dissipation.

If radiative heating exceeds viscous heating, it is possible to have a shock wave without any discontinuities. The absence of discontinuities shows the viscous effects to be completely negligible . Representative profiles of temperature, velocity and radiated heat flux typical of this kind of shock wave sketched from the solutions obtained by Heaslet and Baldwin are shown in Figure 1.3. Presentation of the results in terms of the optical length can be misleading. If the average penetration length for grey radiation is large, the extent of the shock in terms of the optical length will correspond to a very small distance in terms of the physical length x.

When the radiative heating is not so strong the solution consists of a step function shock imbedded in a larger inviscid region. Profiles typical of this situation, sketched from the solutions of Heaslet and Baldwin, are shown in Figure 1.4.

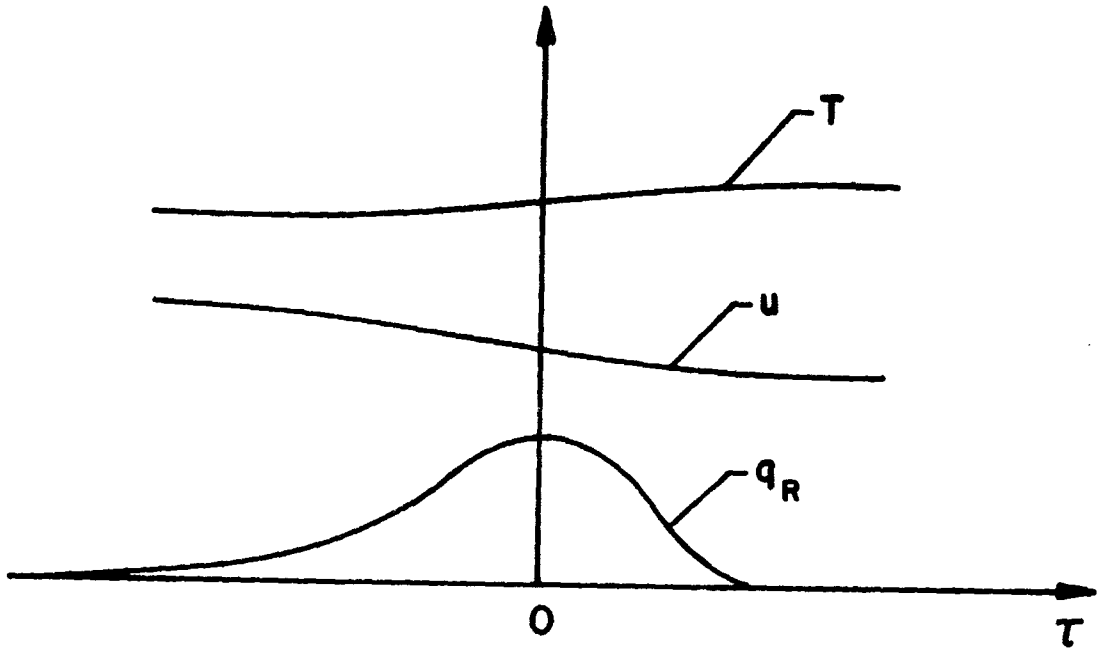

Figure 1.3. Inviscid Radiating Shock Wave.

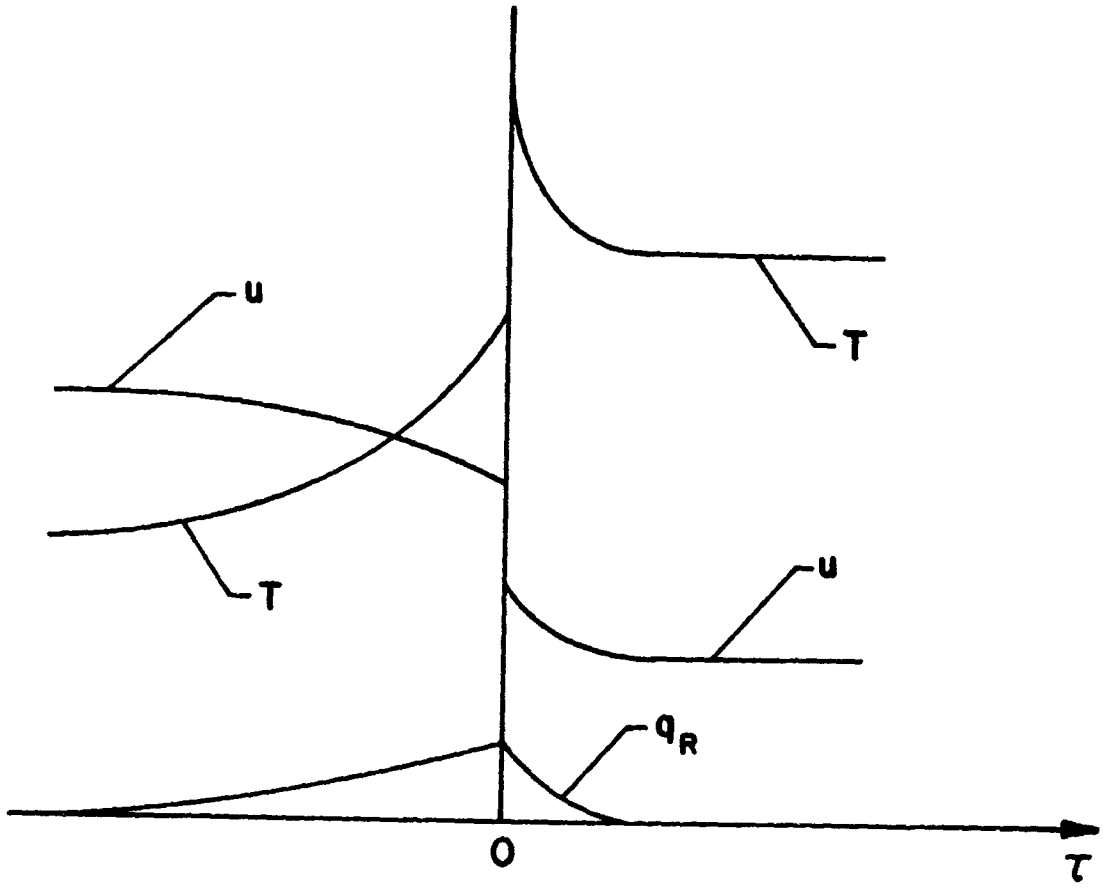

Figure 1.4. Radiating Shock with Discontinuities.

Heaslet and Baldwin assume the viscous portion of the shock in the latter case to be vanishingly thin. Cohen and Clarke [9] and Chow [10] have shown it is a good approximation to consider the shock wave composed of an inviscid region, identical to the solution obtained by Heaslet and Baldwin, in which is imbedded a viscous region, unaffected by radiation, which matches the inviscid solution at its boundaries. This is true as long as the penetration length is large compared to the extent of the viscous region.

Solutions for shock waves with combined radiation and viscosity in which there is no restriction placed on the size of the penetration length compared to the size of the viscous region have been obtained by Traugott [11]. Sen and Guess [12] also solve the combined problem but assume the penetration length to be small compared to the thickness of the viscous region. They then employ the Rosseland approximation to calculate the radiative heat flux.

All of the solutions just mentioned assume the gas is not ionized by the shock wave. Non-grey trapped radiation energy transfer in shock waves with ionization has been investigated by Clarke and Ferrari [5]. Their work is discussed in Chapter II.

Radiation cooling effects in shock tube experiments have been reported by Petschek et al.[13] and Redkobordyi [14].

All of the solutions for radiation cooling assume the shock may be divided into two regions. In the first region ionizational equilibrium is reached and no radiation cooling occurs. That region is followed by the radiation cooling region from which radiation energy is lost. The radiation cooling region is terminated by a cold gas interface or wall.

Petschek et al. [13] calculate profiles in the radiation cooling zone assuming it is optically thin. McChesney and Al-Attar [16] perform a similar calculation except they assume in addition the gas is grey.

In the solution of Pomerantz [17] the gas is assumed to be grey but self absorption is taken into account. In contrast to the optically thin solutions, in which the gas continually cools, cooling stops after a few penetration lengths due to self absorption. A steady state is reached in the radiation cooling region when it is a few penetration lengths thick.

In the case investigated by Pomerantz the radiation cooling region was terminated by a cold gas interface. Yoshikawa and Chapman [18] obtained a solution similar to that of Pomerantz but they terminate the radiation cooling region with a wall. In addition to the radiation which is lost by emission ahead of the shock there is a loss at the wall. Cooling adjacent to the downstream boundary appears to be absent from the solution of Pomerantz.

Chemistry of Ionization

For shock waves in argon, ionization proceeds in a very complicated way. The details of the ionization process are not clearly known.

Petschek and Byron [19] show that more than one reaction is necessary to reach equilibrium ionization. If the electron concentration is sufficiently high, the most probable ionization process is ionization by electron-atom collisions. Petschek and Byron concentrated on investigating this reaction.

They deduced the electron concentration during the approach to equilibrium ionization in argon from measurements with potential probes

placed in their shock tube and from measurements of the continuum radiation intensity. Initially the electron concentration is too low for electron-atom collisions to be important, but later in the ionization process the number of electrons is sufficient for electrom-atom collisions to be the main source of ionization.

Their measured ionization rate is consistent with a two-step reaction scheme consisting of excitation followed by ionization of the excited state.

$$\begin{aligned} e + A &\rightarrow A^* + e \\ e + A^* &\rightarrow A^+ + e + e \end{aligned} \qquad (1.38)$$

Furthermore, their measurements verify that the electrons are not in thermal equilibrium with the atoms as ionization proceeds. This is because each time an electron is produced the electrons collectively lose energy equal to the ionization potential of the atom. The only way in which this energy can be regained is through elastic collisions with the ions and atoms. However, this is an inefficient process because the electron mass is much smaller than the atom mass. On the other hand, energy exchange between the ions and atoms, which have essentially the same mass, is effective. As a result the electrons tend to cool, but the atoms and ions establish an equal and hotter temperature. Petschek and Byron assumed the electrons established thermodynamic equilibrium among themselves at an electron temperature T_e and the atoms and ions established thermodynamic equilibrium among themselves at a temperature T_a. The electron temperature was assumed to be such that the energy lost by electrons through ionizing collisions was just balanced by that gained from elastic collisions with the atoms and ions. Since the reaction

rate is sensitive to the electron temperature, the agreement between measured and calculated rates obtained by Petschek and Byron justified their model of thermal non-equilibrium between the electrons and heavy particles.

Wong [21] has also deduced the electron-atom ionization rate in argon by measuring the electron concentration in the chemical non-equilibrium region of a shock wave using an interferometric technique. He found the electron-atom ionization rate to be more rapid than had been measured by Petschek and Byron. He attributes the larger rate to the onset of one-step electron-atom ionization

$$e + A \rightarrow A^{+} + e + e$$

but it could also be caused by other processes to be discussed presently.

In the early stages of ionization, when the electron concentration is too small to support ionization by electron-atom collisions, other reactions must be responsible for ionization. Petschek and Byron noticed that the time to reach equilibrium ionization was greatly affected by the concentration of impurities present in their shock tube. Accordingly, they suggested that when the electron concentration was small reactions between impurity molecules and argon atoms would be important. However, the concentration of impurities in their experiment was not great enough to account for all of the ionization which takes place in the region of small electron concentration. They speculated that reactions involving atom-atom collisions and radiation in addition to contaminant reactions contributed to the ionization.

Weymann [21] considered the relative importance of contaminant reactions and atom-atom reactions. He showed the contaminant reactions

could be considered independently from reactions between gas atoms because of the much lower concentration of impurities. The impurity reactions were conjectured to occur much more rapidly than atom-atom reactions due to the lower ionization potential of impurity species. He viewed the initial region of ionization as being divided into two regions. In the first region ionization would take place by reactions involving impurity molecules. This would be followed by a much more extensive region where ionization would proceed by reactions involving only gas atoms.

Weymann theorized the most probable atom-atom reaction would be a two-step reaction similar to the two-step reaction investigated by Petschek and Byron.

$$\begin{aligned} A + A &\rightarrow A^* + A \\ A^* + A &\rightarrow A^+ + e + A \end{aligned} \qquad (1.39)$$

The concentration of excited atoms is maintained either because the excited state is metastable or because radiative transitions from this excited state are optically thick. This reaction scheme was experimentally verified by Harwell and Jahn [22] by use of a microwave probe transverse to their shock tube. Great care was taken to reduce the impurity concentration. Only when the impurity level was reduced to a few parts per million did their presence have a negligible effect on the results. Their technique for reducing the impurity level was further refined by Kelly [23] who confirmed the conclusions of Harwell and Jahn and obtained more accurate results.

The contaminant reaction region was investigated in xenon by Hacker and Bloomberg [24] by using the microwave probe along the axis of their shock tube. They found the ionization occurred by a very complicated set of reactions involving contaminant species, xenon atoms and molecules in various states of excitation, and radiation. Contaminant reactions in argon were theoretically discussed by Morgan and Morrison [25] who calculated the time to reach equilibrium ionization in argon shock waves by combining the electron-atom rate of Petschek and Byron and the atom-atom rate of Harwell and Jahn. They attributed the discrepancy between the calculated time and the time observed by Petschek and Byron to contaminant reactions. The calculations made in this thesis assume the argon gas to be absolutely free of impurities.

Bibermann and Yakubov [26] also calculated the time to reach equilibrium ionization by combining electron-atom ionization and atom-atom ionization rates. Experiments show the ionization process actually takes place more quickly than they calculated. They suggested that line radiation from the hot gas following the ionization region excites argon atoms in the ionization region, which are easily ionized, contributing additional electrons and consequently decreasing the time to reach equilibrium. The equilibrium ionization time calculated by including this effect showed much improved agreement with experimentally measured times.

Radiation can affect ionization in still another way by creating electrons ahead of the shock discontinuity. Such electrons have been termed precursor electrons because they occur ahead of what is normally thought of as the shock front. They have been observed in re-entry by

their effect on radar cross section [27], [28], [29], and in shock tubes as described below.

Results of experiments to detect precursor electrons in shock tubes were at first quite confusing. Some care was needed to eliminate extraneous causes of electrons ahead of the shock wave such as the photoemission from the shock tube walls [30], [31]. The early measurements of precursor phenomena seemed to indicate that most of the charged particles ahead of the shock front were electrons [30], [32], [33]. If the photoionization caused the precursors, the number of electrons and ions would be equal. It was proposed that precursors were caused by electrons diffusing ahead of the shock wave. It was thought the severe gradients of electron concentration in the shock wave would cause such a diffusion.

Theoretical investigation of the diffusion hypothesis has been reviewed by Wetzel [34]. All the calculations showed a much smaller electron density ahead of the shock than had been measured. Pipkin [35] argued that the distribution of electrons in small diameter shock tubes, such as had been used for the experiments, produce an electric field vector that is not mainly along the axis of the shock tube as had been assumed in the theoretical work. He analyzed the problem assuming a different configuration of the electric field and, because of its weaker axial component, was able to explain the main features of the experimental results. Appleton [36] claims it is unreasonable to assume that Pipkin's expression for the axial field is valid in the immediate vicinity of the shock. Instead Appleton requires the field to be one-dimensional near the shock and obtains a numerical solution in which the electron

concentration rapidly decreases ahead of the shock, consistent with the earlier theoretical results. Unless a transition to a weak axial field takes place in a short distance ahead of the shock, the diffusion hypothesis cannot be theoretically explained.

Recently Weymann and Holmes [37] and Holmes [38] have repeated the earlier experiments of Weymann with improved measurements. These more recent experiments show that photoionization of the cold gas ahead of the shock by radiation from the hot shocked gas is the principal means of producing precursor electrons. This is consistent with the recent experiment of Zivanovic [39] and Lederman and Wilson [40] who were able to separately measure the photo-electrons and the diffusion electrons ahead of the shock waves. They found only photo-electrons.

These experiments indicate that precursor ionization is caused by radiation from the hot shocked gas.

CHAPTER II

FORMULATION OF EQUATIONS

In this chapter the equations which describe non-grey radiation energy transfer, ionization kinetics, and energy exchange in partially ionized argon are formulated. First the fluid conservation equations for a partially ionized gas are developed. These are then transformed to a non-dimensional form and simplified by eliminating all unimportant terms. Next equations for the ionization rate are developed. Finally expressions are developed which give the non-grey radiation flux and radiative ionization rate. The method of solution is discussed at the end of this chapter.

Conservation Equations for a Partially Ionized Gas

In an un-ionized monatomic gas mass, momentum and energy can be transferred only by the neutral atoms which make up the gas. If the gas is ionized, electrons and ions provide additional ways for mass, momentum and energy to be exchanged. An equation for the conservation of mass, momentum and energy can be written for each species of the gas following the approach used by Appleton and Bray [41]. Let each species be labeled by a subscript λ. The species conservation equations for one-dimensional steady state flow are as follows:

The species mass conservation equation is

$$\frac{d}{dx}\left(\rho_\lambda u_\lambda\right) = \dot{w}_\lambda \qquad (2.1)$$

where $\rho_\lambda = m_\lambda n_\lambda$ is the mass density of species λ, m_λ is the mass of a particle of species λ, n_λ is the number density of species λ, u_λ is the average velocity of species λ, and $\dot{w}_\lambda$ is the mass rate of production of species λ per unit volume per unit time.

$$\dot{w}_\lambda = m_\lambda \dot{n}_\lambda$$

where $\dot{n}_\lambda$ is the net number of species λ produced per unit volume per unit time by all radiative and collisional reactions.

The equation expressing conservation of momentum for species λ is

$$\frac{d}{dx}\left[\rho_\lambda u_\lambda^2 + p_\lambda - \sigma_\lambda\right] = n_\lambda e_\lambda E + \sum_{\lambda'} P_{\lambda\lambda'} + J_\lambda \qquad (2.2)$$

where p_λ is the partial pressure of species λ, σ_λ is the viscous stress tensor component of species λ, e_λ is the charge of a particle of species λ, E is the electric field created by the collective motion of the charged particles, $P_{\lambda\lambda'}$ is the rate of loss of momentum by species λ per unit volume and time due to <u>elastic</u> interactions with particles of species λ', and J_λ is the rate of loss of momentum by species λ per unit volume and time due to <u>inelastic</u> interactions with particles of all other species and the radiation field.

Conservation of energy for species λ is expressed by the following equation.

$$\frac{d}{dx}\left[\left(\epsilon_\lambda + \tfrac{1}{2}\rho_\lambda u_\lambda^2 + p_\lambda - \sigma_\lambda\right) u_\lambda + q_{c_\lambda}\right]$$
$$= n_\lambda e_\lambda E u_\lambda + u_\lambda \sum_{\lambda'} P_{\lambda\lambda'} + \sum E_{\lambda\lambda'} + Q_\lambda \qquad (2.3)$$

where ϵ_λ is the average internal energy per unit volume due to species λ and q_{c_λ} is the conductive heat flux. The first term on the right hand

side of equation (2.3) is the energy dissipated by Joule heating and the second is the rate at which work is done on species λ per unit volume and time due to elastic interactions between species λ and the other species because of the fluid motion of species λ. In the remaining terms $E_{\lambda\lambda'}$ is the rate of energy gain by species λ per unit volume and time due to elastic encounters between species λ and λ' because of thermal motion of the particles and Q_λ is the rate of energy gain by species λ per unit volume and time due to inelastic encounters between species λ and all other species because of the thermal motion of the particles and radiation.

Equations (2.1) and (2.2) may be used to reduce equation (2.3) to the following alternative form

$$\frac{d}{dx}\left(\epsilon_\lambda u_\lambda + q_{c_\lambda}\right) + \left(p_\lambda - \sigma_\lambda\right)\frac{du_\lambda}{dx} = \tfrac{1}{2}u_\lambda^2\dot{w}_\lambda - u_\lambda J_\lambda + \sum_{\lambda'} E_{\lambda\lambda'} + Q_\lambda \qquad (2.4)$$

Elastic Interactions

Assuming that the degree of ionization in the gas is sufficiently small that only binary collisions are important, the following kinetic theory expressions give the net momentum and energy transfer between species λ and λ' [41], [42].

$$P_{\lambda\lambda'} = -\frac{m_\lambda m_{\lambda'}}{m_\lambda + m_{\lambda'}} n_\lambda n_{\lambda'} \int \vec{g} S_{\lambda\lambda'}(g)\, f_\lambda f_{\lambda'}\, d\vec{v}_\lambda d\vec{v}_{\lambda'} \qquad (2.5)$$

$$E_{\lambda\lambda'} = -\frac{m_\lambda m_{\lambda'}}{m_\lambda + m_{\lambda'}} n_\lambda n_{\lambda'} \int \vec{g}\cdot\vec{G}\, S_{\lambda\lambda'}(g)\, f_\lambda f_{\lambda'} d\vec{v}_\lambda d\vec{v}_{\lambda'} - u_\lambda P_{\lambda\lambda'} \qquad (2.6)$$

In these expressions $\vec{g}$ is the relative velocity of the particles before collision, $\vec{G}$ is the center of mass velocity of the particles, f_λ is the

velocity distribution function of species λ, $\vec{v}_\lambda$ is the total velocity of species λ equal to $\vec{u}_\lambda + \vec{c}_\lambda$ where $\vec{c}_\lambda$ is the thermal velocity, and $S_{\lambda\lambda'}$ is the diffusion cross section between species λ and λ'.

It is reasonable to assume the time required for each species to establish a Maxwellian distribution of thermal velocities by self collisions is short compared to the time required to exchange energy with other particles [43]. Accordingly, the velocity distribution function in equations (2.5) and (2.6) are assumed to be Maxwellian at a particular species temperature T_λ. The species temperatures are equal only if thermodynamic equilibrium between the species is established.

In addition to the distribution functions, the cross sections $S_{\lambda\lambda'}$ are needed to evaluate the integrals in equations (2.5) and (2.6). They are given by the following equations [4], [42], [44]-[47].

$$S_{ee} = S_{ei} = \frac{\pi e^4}{2(k\,T_e)^2} \ln\left[\frac{9k^3\,T_e^3}{4\pi\,n_e\,e^6}\right]^{\frac{1}{2}} \tag{2.7}$$

$$S_{ii} = \frac{\pi\,e^4}{2(k\,T_i)^2} \ln\left[\frac{9k^3\,T_i^3}{4\pi\,n_i\,e^6}\right]^{\frac{1}{2}} \tag{2.8}$$

$$S_{aa} = 1.7\,(10^{-14})T_a^{-\frac{1}{6}}\ \text{cm}^2 \tag{2.9}$$

$$S_{ia} = 1.4\,(10^{-14})\ \text{cm}^2 \tag{2.10}$$

$$S_{ea} = \begin{cases} [-.35 + .775\,(10^{-4})T_e]\,10^{-16}\ \text{cm}^2 & \text{if } T_e > 10^4\ ^\circ\text{K} \\ [.39 - .551(10^{-4})T_e + .595(10^{-8})T_e^2]\,10^{-16}\ \text{cm}^2 & \text{if } T_e \leq 10^4\ ^\circ\text{K} \end{cases} \tag{2.11}$$

where the subscripts i, a, and e stand for ions, atoms, and electrons.

Using these cross sections and the Maxwellian velocity distribution functions the integrals in equations (2.5) and (2.6), correct to first order in $(m_e/m_a)^{\frac{1}{2}}$, are [4], [19], [48],[51].

$$P_{ai} = - P_{ia} = - \frac{4}{3} \sqrt{2}\, n_a n_i \left[\frac{m_i}{\pi} k(T_a + T_i) \right]^{\frac{1}{2}} S_{ia}(u_a - u_i) \tag{2.12}$$

$$P_{ae} = - P_{ea} = - \frac{8}{3} \sqrt{2}\, n_a n_e \left(\frac{m_e\, k\, T_e}{\pi} \right)^{\frac{1}{2}} S_{ea}(u_a - u_e) \tag{2.13}$$

$$P_{ei} = - P_{ie} = - \frac{8}{3} \sqrt{2}\, n_i n_e \left(\frac{m_e k\, T_e}{\pi} \right)^{\frac{1}{2}} S_{ei}(u_e - u_i) \tag{2.14}$$

$$E_{ei} = - E_{ie} = - 8 \sqrt{2}\, n_i n_e \left(\frac{m_e k\, T_e}{\pi} \right)^{\frac{1}{2}} \frac{S_{ei}}{m_i} \left[k(T_e - T_i) + \frac{1}{3}(u_e - u_i)(m_i (u_i - u_e) + m_e u_e) \right] \tag{2.15}$$

$$E_{ae} = - E_{ea} = - 8 \sqrt{2}\, n_a n_e \left(\frac{m_e\, k\, T_e}{\pi} \right)^{\frac{1}{2}} \frac{S_{ea}}{m_i} \left[k(T_a - T_e) + \frac{1}{3}(u_a - u_e) m_e u_e \right] \tag{2.16}$$

$$E_{ai} = - E_{ia} = - 2 \sqrt{2}\, n_a n_i \left[\frac{k(T_a + T_i)}{\pi\, m_i} \right]^{\frac{1}{2}} S_{ia} \left[k(T_a - T_i) + \frac{1}{3}(u_a - u_i) m_i u_i \right] \tag{2.17}$$

Pressure, Viscosity and Heat Conduction

The partial pressure p_λ, viscous stress σ_λ and conductive flux q_{c_λ} are assumed to be given by the following familiar formulas.

$$p_\lambda = n_\lambda\, k\, T_\lambda \tag{2.18}$$

$$\sigma_\lambda = \frac{4}{3} \mu_{\sigma_\lambda} \frac{du_\lambda}{dx} \tag{2.19}$$

$$q_{c_\lambda} = - k_{c_\lambda} \frac{dT_\lambda}{dx} \tag{2.20}$$

The viscosity coefficient μ_{σ_λ} and thermal conductivity coefficient k_{c_λ} are given by the following classical expressions [4], [48].

$$\mu_{\sigma_\lambda} = \frac{5\pi}{32} n_\lambda m_\lambda \bar{c}_\lambda \left(\frac{\bar{c}_\lambda}{\omega_\lambda} \right) \tag{2.21}$$

$$k_{c_\lambda} = \frac{15k}{4m_\lambda} \mu_{\sigma_\lambda} \tag{2.22}$$

In these equations $\bar{c}_\lambda$ is the mean thermal velocity of species λ,

$$\bar{c}_\lambda = \left(\frac{8k\, T_\lambda}{\pi\, m_\lambda} \right)^{\frac{1}{2}} \tag{2.23}$$

and ω_λ is the frequency of collisions of species λ with all other particles.

$$\omega_\lambda = \sum_{\lambda'} n_{\lambda'} S_{\lambda\lambda'} \left(\bar{c}_\lambda^2 + \bar{c}_{\lambda'}^2 \right)^{\frac{1}{2}} \frac{2m_{\lambda'}}{m_\lambda + m_{\lambda'}} \tag{2.24}$$

Noting that $m_e/m_a \ll 1$, the viscosity and heat conduction coefficients may be written as follows:

$$\mu_{\sigma_a} = \frac{5}{16 S_{aa}} (\pi\, m_a\, k\, T_a)^{\frac{1}{2}} \left[1 + \frac{n_i S_{ia}}{n_a S_{aa}} \left(\frac{T_a + T_i}{2\, T_a} \right)^{\frac{1}{2}} \right]^{-1} \tag{2.25}$$

$$\mu_{\sigma_i} = \frac{5n_i}{16 S_{ia} n_a} (\pi\, m_i k)^{\frac{1}{2}} T_i \left\{ \left(\frac{T_a + T_i}{2} \right)^{\frac{1}{2}} \left[1 + \frac{n_i S_{ii}}{n_a S_{ia}} \left(\frac{2T_i}{T_a + T_i} \right)^{\frac{1}{2}} \right] \right\} \tag{2.26}$$

$$\mu_{\sigma_e} \tilde{=} 0 \tag{2.27}$$

$$k_{c_a} = \frac{15k}{4\, m_a}\ \mu_{J_a} \tag{2.28}$$

$$k_{c_i} = \frac{15k}{4\, m_i}\ \mu_{J_i} \tag{2.29}$$

$$k_{c_e} = \frac{75}{64\, S_{ee}} \left(\frac{\pi\, k\, T_e}{m_e} \right)^{\frac{1}{2}} k \left[(1+\sqrt{2}) \left(1 + \frac{\sqrt{2}\, S_{ea}\, n_a}{(1+\sqrt{2}) S_{ee}\, n_e} \right) \right]^{-1} \tag{2.30}$$

The relative magnitude of these coefficients depends on the amount of ionization that has taken place through the ratios $n_i s_{ia}/n_a s_{aa}$, $n_i s_{ii}/n_a s_{ia}$, etc.

Inelastic Interactions

Inelastic interactions are collisions in which the internal energy of the collision partners is permanently changed. Each species may gain or lose energy through inelastic collision processes.

Processes of this kind are the inelastic electron-atom (e-A) collision process

$$e + A(1) \rightleftarrows e + A(2)$$

$$e + A(2) \rightleftarrows A^+ + e + e$$

and the inelastic atom-atom (A-A) collision process.

$$A(1) + A(1) \rightleftarrows A(2) + A(1)$$

$$A(1) + A(2) \rightleftarrows A^+ + e + A(1)$$

Particles may also exchange energy with the radiation field.

Consider how the e-A process will affect the particles in a unit volume of gas. There are n_e electrons in the unit volume. Suppose one electron is produced by the e-A process. The electrons which cause the

ionization will lose energy equal to the ionization potential χ plus the energy of the created electron. The average energy of the created electron is $\bar{\xi}$. The original n_e electrons will establish equilibrium by elastic collisions among themselves. Thus the n_e original electrons collectively lose energy $\chi + \bar{\xi}$ in creating one electron of average energy $\bar{\xi}$. There will then be $n_e + 1$ electrons in the unit volume, n_e of which have lost the energy $\chi + \bar{\xi}$ and one which has gained energy $\bar{\xi}$. No energy is lost in the unit volume by equilibrating the created electron since the required energy $\frac{3}{2} k T_e - \bar{\xi}$ will be lost by the original n_e electrons but gained by the created electron. The net energy loss per unit volume is therefore just χ. If $\dot{n}_{eA}$ is the net rate of production of electrons by the e-A process, the total energy loss per unit volume by this means is $-\dot{n}_{eA}\chi$.

Since $\frac{3}{2} k T_a + \frac{1}{2} m_a u_a^2$ is the average energy of an atom, and the e-A process destroys atoms at the rate $-\dot{n}_{eA}$, the atoms will collectively lose energy at the rate $-\dot{n}_{ea} (\frac{3}{2} k T_a + \frac{1}{2} m_a u_a^2)$. Similarly the ion gas will gain energy at the rate $\dot{n}_{ea}(\frac{3}{2} k T_i + \frac{1}{2} m_i u_i^2)$.

Electrons are ineffective in transferring momentum with ions and atoms because of their small mass. Approximately the rate of momentum exchange by the e-A process for the electrons is zero, for the atoms is $-\dot{n}_{eA} m_a u_a$ and for the ions is $\dot{n}_{eA} m_i u_i$.

Similar considerations for the A-A process and radiation lead to the following formulas for the inelastic momentum and energy exchange.

$$J_e = 0 \tag{2.31}$$

$$J_a = - \dot{n} m_a u_a \tag{2.32}$$

$$J_i = \dot{n}\, m_i\, u_i \tag{2.33}$$

$$Q_e = -\dot{n}_{eA}\chi + \dot{n}_{AA}\,\bar{\zeta}_{AA} + \dot{n}_{rad}\,\bar{\zeta}_{rad} \tag{2.34}$$

$$Q_a = -\dot{n}\left(\tfrac{3}{2} k T_a + \tfrac{1}{2} m_a u_a^2\right) - \dot{n}_{AA}(\chi + \bar{\zeta}_{AA}) - \frac{dq_R}{dx} \tag{2.35}$$

$$- \dot{n}_{rad}(\bar{\zeta}_{rad} + \chi)$$

$$Q_i = \dot{n}\left(\tfrac{3}{2} k T_i + \chi + \tfrac{1}{2} m_i u_i^2\right) \tag{2.36}$$

where $\bar{\zeta}_{AA}$ is the average energy of electrons when created by the A-A process, $\bar{\zeta}_{rad}$ is the average creation energy of photoelectrons, $\dot{n}_{AA}$ is the rate of production of electrons by the A-A process, $\dot{n}_{rad}$ is the rate of production of electrons by the radiation field and $\dot{n} = \dot{n}_{eA} + \dot{n}_{AA} + \dot{n}_{rad}$.

The Electric Field

Steep gradients of electron and ion densities in the shock wave will cause diffusion of electrons relative to the ions. The resulting charge separation creates an electric field. The electric field is found from Poisson's equation:

$$\frac{dE}{dx} = 4\pi e\,(n_i - n_e) \tag{2.37}$$

The diffusion is impeded by the electric field it creates. A steady state is reached when the diffusion is just balanced by the drift from the electric field. It is assumed a steady state diffusion is maintained in the shock wave. The net current then is zero.

$$e\, n_i\, u_i - e\, n_e\, u_e = 0$$

or

$$n_i\, u_i = n_e\, u_e \tag{2.38}$$

Internal Energy

The internal energy due to the thermal motion of particles of species λ is $3/2kT_\lambda$ since the particles have a Maxwellian velocity distribution at the temperature T_λ. The internal energies of the atoms, ions and electrons per unit volume are:

$$\epsilon_a = n_a \left(\tfrac{3}{2} k T_a + \psi_a \right) \tag{2.39}$$

$$\epsilon_i = n_i \left(\tfrac{3}{2} k T_i + \chi \right) \tag{2.40}$$

$$\epsilon_e = n_e \tfrac{3}{2} k T_e \tag{2.41}$$

where ψ_a is the average electronic excitation energy of the atoms. For the calculations to be performed ψ_a is negligible compared to the thermal energy of the atom.

Simplified Nondimensional Equations

It will be advantageous to refer the variables to characteristic values in order to aid in the estimation of the relative magnitudes of terms in the equations. Let the characteristic values be denoted by a subscript 0. Then the barred variables

$$\bar{T}_\lambda = \frac{T_\lambda}{T_o}, \quad \bar{u}_\lambda = \frac{u_\lambda}{u_o}, \quad \bar{\rho}_\lambda = \frac{\rho_\lambda}{\rho_o}$$

will all have a value near one. Let ℓ be a length which is typical of the extent of the chemical and radiative portion of the shock wave. It will be on the order of a centimeter for the shock waves to be considered in this thesis. Let $\bar{x} = x/\ell$ be the nondimensional coordinate.

In addition to the length ℓ there are several other characteristic lengths which will appear in the equations. Those which are associated

with the momentum and energy exchange are presented next.

In the course of the presentation to follow it will be shown that charge separation is negligible for the shock waves to be investigated. Then $n_e = n_i$ and the species concentration may be related to the degree of ionization by the following formulas.

$$n_e = n_i = \alpha \frac{\rho}{m_a} \qquad n_a = (1 - \alpha) \frac{\rho}{m_a} \tag{2.42}$$

Using relations (2.42) the lengths characteristic of the energy and momentum exchange processes may be written as follows.

$$\ell_{aa} = \frac{1}{\sqrt{2}\, S_{aa}\, n_a} = \ell^o_{aa} \frac{\bar{T}_a^{1/4}}{(1 - \alpha)\, \bar{\rho}} \tag{2.43}$$

where

$$\ell^o_{aa} = \frac{m_a\, T_o^{1/4}}{\sqrt{2}\, (1.7)(10^{-14})\, \rho_o} \tag{2.44}$$

$$\ell_{ia} = \frac{1}{\sqrt{2}\, S_{ia}\, n_a} = \ell^o_{ia} \frac{1}{(1 - \alpha)\, \bar{\rho}} \tag{2.45}$$

where

$$\ell^o_{ia} = \frac{m_a}{\sqrt{2}\, (1.4)\, 10^{-14}\, \rho_o} \tag{2.46}$$

$$\ell_{ei} = \ell_{ii} = \frac{1}{\sqrt{2}\, S_{ei}\, n_i} = \ell^o_{ei} \frac{\bar{T}_e^2 / \alpha\, \bar{\rho}}{1 + \frac{1}{c_{ei}} \ln (\bar{T}_e^3 / \alpha\, \bar{\rho})} \tag{2.47}$$

where

$$\ell^o_{ei} = \left(\frac{m_a}{m_e} \right)^{\frac{1}{2}} \frac{8(kT_o)^2}{\sqrt{2}\, \pi\, e^4} \frac{m_a}{\rho_o\, c_{ei}} \tag{2.48}$$

and

$$c_{ei} = \ln \left(\frac{9k^3\, T_o^3\, m_a}{4\pi\, \rho_o\, e^6} \right) \tag{2.49}$$

$$\ell_{ea} = \ell^{o}_{ea} \frac{1}{(1-\alpha)\bar{\rho}\,\bar{S}_{ea}(\bar{T}_e)} \tag{2.50}$$

where

$$\ell^{o}_{ea} = \left(\frac{m_a}{m_e}\right)^{\frac{1}{2}} \frac{m_a}{\sqrt{2}\,\rho_o\,S_{ea}(T_o)} \tag{2.51}$$

and $S_{ea}(\bar{T}_e) = S_{ea}(T_e)/S_{ea}(T_o)$. Using the reference values $T_o = 10^4$ °K and a density of $\rho_o = 2.13\ (10^{-5})$, gm/cm^3 (which is the density corresponding to a pressure of 1 cm Hg at a temperature of 300°K) the following values are found.

$$\begin{aligned} \ell^{o}_{aa} &= 1.31\ (10^{-4})\ \text{cm} & \ell^{o}_{ea} &= 14.3\ \text{cm} \\ \ell^{o}_{ia} &= 1.58\ (10^{-4})\ \text{cm} & \ell^{o}_{ei} &= .8\ (10^{-2})\ \text{cm} \\ & & c_{ei} &= 6.86 \end{aligned} \tag{2.52}$$

From these formulas it can be seen that the lengths for heavy particle partners, ℓ_{aa} and ℓ_{ia}, are considerably smaller than those involving electrons, ℓ_{ea} and ℓ_{ei}.

An appropriate nondimensional electric field is

$$\bar{E} = \frac{E}{(k\,T_o/e\,\ell_D)} \tag{2.53}$$

where ℓ_D is the Debye length. In terms of nondimensional variables the Debye length is

$$\ell_D = \ell^{o}_{D} \left(\frac{\bar{T}_e}{\alpha\,\bar{\rho}}\right)^{\frac{1}{2}} \tag{2.54}$$

where

$$\ell^{o}_{D} = \left(\frac{m_a\,k\,T_o}{4\pi\,e^2\,\rho_o}\right)^{\frac{1}{2}} \tag{2.55}$$

For the same values of the reference variable as used above, ℓ_D^o is found to be 1.21 (10^{-6}) cm. The Debye length is much smaller than any other length in the problem.

Substituting the formulas developed in the last section and the nondimensional variables from this section into the electron momentum equation (equation (2.2) with $\lambda = e$) and noting that $m_e \ll m_a$ produces the following equation:

$$\frac{d}{d\bar{x}}(n_e \bar{T}_e) = - n_e \bar{E} \frac{\ell}{\ell_D} + \frac{8}{3\sqrt{\pi a}} \left[\frac{\ell}{\ell_{ea}} (\bar{u}_a - \bar{u}_e) + \frac{\ell}{\ell_{ei}} (\bar{u}_e - \bar{u}_i) \right] \quad (2.56)$$

where the parameter $a = kT_0/m_a u_0^2$ is a typical ratio of thermal to kinetic energy of the particles. Since $\ell_D \ll \ell$, the first term on the right hand side will be the dominant term in the equation. Unless the gradients in n_e and T_e are large the electric field must be small in order to preserve the equality. It will be assumed that E is small throughout the region which has characteristic length ℓ. Equations (2.37) and (2.38) then show that there is no charge separation and no diffusion of electrons relative to ions.

$$n_i = n_e \quad (2.57)$$

$$u_i = u_e \quad (2.58)$$

This justifies the previous use of relations (2.42) which will be used frequently in the equations which follow.

Consider now the equation obtained by adding the electron momentum equation to the ion momentum equation. This is found by summing equation (2.2) over the electron and ion species. Using the result just obtained,

$n_i = n_e$ and $u_i = u_e$, and the formulas specified in the previous sections, the nondimensional form of this equation is found to be

$$\frac{\alpha}{a}\frac{d}{d\bar{x}}(\bar{\rho}\,\bar{u}_e^2) + \frac{d}{d\bar{x}}\left[\alpha\,\bar{\rho}\,(\bar{T}_e + \bar{T}_i) - \frac{5}{12}\sqrt{\frac{2\pi}{a}}\,\alpha\,\bar{\rho}\,\frac{\ell_{ia}}{\ell}\,\frac{T_i\,\frac{d\bar{u}_e}{d\bar{x}}}{\left(\frac{\bar{T}_a + \bar{T}_i}{2}\right)^{\frac{1}{2}}\left(1 + \frac{\ell_{ia}}{\ell_{ii}}\left\{\frac{2\,\bar{T}_i}{\bar{T}_a + \bar{T}_i}\right\}^{\frac{1}{2}}\right)}\right]$$

$$= \frac{4}{3}\sqrt{\frac{a}{\pi}}\,(\bar{u}_a - \bar{u}_e)\,\alpha\,\bar{\rho}\left[2\,\frac{\ell}{\ell_{ea}}\,\bar{T}_e^{\frac{1}{2}} + \frac{\ell}{\ell_{ia}}\,(\bar{T}_a + \bar{T}_i)^{\frac{1}{2}}\right] \qquad (2.59)$$

Since the ratio $\frac{\ell}{\ell_{ia}}$, which appears on the right hand side of the equation, is very large, the mean atom velocity u_a must be very nearly the same as the mean electron velocity u_e in order that the equality be true. Consequently there is negligible diffusion of the species relative to each other.

$$\bar{u}_a = \bar{u}_e = \bar{u}_i = \bar{u} \qquad (2.60)$$

The nondimensional form of the ion energy equation (equation (2.3) with $\lambda = 1$) is:

$$\frac{3}{2}\,\alpha\,\bar{\rho}\bar{u}\,\frac{d\bar{T}}{d\bar{x}} - \frac{d}{d\bar{x}}\left[\frac{75}{16}\sqrt{2\pi a}\,\frac{\ell_{ia}}{\ell}\,\alpha\,\bar{\rho}\,\frac{\bar{T}_i\,\frac{d\bar{T}_i}{d\bar{x}}}{\left(\frac{\bar{T}_a + \bar{T}_i}{2}\right)^{\frac{1}{2}}\left[1 + \frac{\ell_{ia}}{\ell_{ii}}\left(\frac{2\bar{T}_i}{\bar{T}_a + \bar{T}_i}\right)^{\frac{1}{2}}\right]}\right]$$

$$+ \alpha \bar{\rho} \frac{d\bar{u}}{d\bar{x}} - \frac{5}{16} \sqrt{\frac{2\pi}{a}} \frac{\ell_{ia}}{\ell} \alpha\bar{\rho} \frac{\bar{T}_i \left(\frac{d\bar{u}}{d\bar{x}}\right)^2}{\left(\frac{\bar{T}_a + \bar{T}_i}{2}\right)^{\frac{1}{2}} \left[1 + \frac{\ell_{ia}}{\ell_{ii}} \left(\frac{2\bar{T}_i}{\bar{T}_a + \bar{T}_i}\right)^{\frac{1}{2}}\right]}$$

$$= 8\sqrt{\frac{a}{\pi}} \frac{\ell}{\ell_{ei}} \alpha \bar{\rho} (\bar{T}_e - \bar{T}_i) + \frac{\dot{n}}{\dot{N}} \bar{T}_{ion}$$

$$+ 2 \sqrt{\frac{a}{\pi}} \frac{\ell}{\ell_{ia}} \alpha \bar{\rho} (\bar{T}_a + \bar{T}_i)^{\frac{1}{2}} (\bar{T}_a - \bar{T}_i) \qquad (2.61)$$

where $\dot{N} = \frac{\rho_o/m_a}{\ell/u_o}$ is a characteristic convective rate.

The largest term on the left hand side of this equation is of order α. On the right hand side of the equation the term containing the ratio $\frac{\ell}{\ell_{ia}}$ and the term containing the chemical reaction rate $\dot{n}$ will have the largest values. If the chemical rate were zero, the atom temperature and the ion temperature would have to be very nearly equal to preserve the equality since the ratio $\frac{\ell}{\ell_{ia}}$ is very large. However, if the chemical rate is sufficiently high, the atom and ion temperature can differ. For the shock waves which are considered in this thesis the chemical rates are sufficiently small that differences in the atom and ion temperatures are negligible. Accordingly, it is assumed that

$$\bar{T}_a = \bar{T}_i \qquad (2.62)$$

The assumptions just discussed greatly simplify the problem for they have reduced the dependent variables to the following five quantities: α, $\bar{\rho}$, $\bar{u}$, $\bar{T}_a$, and $\bar{T}_e$. The equations which will be used to calculate these variables will be the total conservation equations, the electron energy equation and electron mass conservation equation.

The total conservation equations are obtained by summing equations (2.1), (2.2) and (2.3) over all species.

The nondimensional form of the total mass conservation equation is

$$\bar{\rho}\,\bar{u} = C_M = 1 \tag{2.63}$$

The constant C_M is chosen to be one. This means that the reference quantities must be chosen such that $\rho_o u_o$ is equal to ρu at some point in the shock wave.

After summing equation (2.2) over all species, substituting the nondimensional variables and integrating once, the following equation which governs the transfer of momentum is found.

$$\frac{1}{\bar{\rho}} + \alpha\,\bar{\rho}\,(\bar{T}_a + \alpha\,\bar{T}_e) - \frac{4}{3}\sqrt{2\kappa a}\left[(1-\alpha)\,\bar{\rho}\,\bar{T}_a^{\frac{1}{2}}\,\frac{\ell_{aa}/\ell}{1+\ell_{aa}/\ell_{ia}} + \alpha\bar{\rho}\,\frac{\ell_{ia}/\ell}{1+\ell_{ia}/\ell_{ii}}\right]\frac{d\bar{u}}{d\bar{x}} = C_P$$

where C_P is the integration constant. The last term in this equation is the viscous stress. This term is negligible since the ratios $\frac{\ell_{aa}}{\ell}$ and $\frac{\ell_{ia}}{\ell}$ are very small and the velocity gradient $\frac{d\bar{u}}{d\bar{x}}$ is assumed not to be large. The equation of momentum transfer for the gas is therefore

$$\frac{1}{\bar{\rho}} + a\,\bar{\rho}\,(\bar{T}_a + \alpha\,\bar{T}_e) = C_P \tag{2.64}$$

The equation of total energy conservation is obtained in a manner similar to that used to derive the total momentum conservation equation. The result is

$$\frac{5}{2}(\bar{T}_a + \alpha \bar{T}_e) + \alpha \bar{T}_{ion} + \frac{1}{2a\bar{\rho}^2} + \frac{q_R}{a \rho_o u_o^3}$$

$$- \frac{5}{12}\sqrt{\frac{2\pi}{a}} \left\{ \frac{\ell_{aa}/\ell}{1 + \ell_{aa}/\ell_{ia}} (1 - \alpha)\bar{\rho}\, \bar{T}_a^{\frac{1}{2}} + \frac{\ell_{ia}/\ell}{1 + \ell_{ia}/\ell_{ii}} \alpha \bar{\rho} \bar{T}_a^{\frac{1}{2}} \right\} \bar{u} \frac{d\bar{u}}{d\bar{x}}$$

$$- \frac{75}{64}\sqrt{2\pi a} \left[\frac{\ell_{aa}/\ell}{1 + \ell_{aa}/\ell_{ia}} (1 - \alpha)\bar{\rho}\, \bar{T}_a^{\frac{1}{2}} + \frac{\ell_{ia}/\ell}{1 + \ell_{ia}/\ell_{ii}} \alpha \bar{\rho}\, \bar{T}_a^{\frac{1}{2}} \right] \frac{d\bar{T}_a}{d\bar{x}}$$

$$- \frac{75}{64}\sqrt{2\pi a} \frac{\ell_{ee}/\ell}{(1 + \sqrt{2})\left(1 + \frac{\sqrt{2}}{1 + \sqrt{2}} \frac{\ell_{ee}}{\ell_{ea}}\right)} \alpha \bar{\rho}\, \bar{T}_e^{\frac{1}{2}} \frac{d\bar{T}_e}{d\bar{x}} = C_E \qquad (2.65)$$

where C_E is a constant resulting from the integration of equation (2.3). The last two terms represent thermal heat conduction in the gas and the one preceding these represents viscous dissipation. The terms containing the ratios $\frac{\ell_{aa}}{\ell}$ and $\frac{\ell_{ia}}{\ell}$ are clearly negligible but the term containing the gradient in electron temperature can be important. This term represents heat conduction in the electron gas. Its larger magnitude reflects the fact that the electrons are good conductors of heat. As can be seen from equation (2.47), the quantity $\alpha \frac{\ell_{ee}}{\ell}$, which is the magnitude of this term, is sufficiently small for the range of variables of interest in this thesis that heat conduction in the electron gas may be neglected. The equation of energy conservation then reduces to the following form.

$$\frac{5}{2}(\bar{T}_a + \alpha \bar{T}_e) + \alpha \bar{T}_{ion} + \frac{1}{2a\bar{\rho}^2} + \frac{q_R}{a \rho_o u_o^3} = C_E \qquad (2.66)$$

Equation (2.4) evaluated for $\lambda = e$ is the equation which describes the energy balance for the electrons. Substituting the formulas developed in the preceding sections into this equation and noting that $m_e/m_a \ll 1$, the following nondimensional form of the electron energy equation will be found.

$$\frac{3}{2}\alpha \frac{d\bar{T}_e}{d\bar{x}} - \frac{d}{d\bar{x}}\left[\frac{75}{64}\sqrt{2\pi a} \frac{\ell_{ee}/\ell}{(1+\sqrt{2})\left(1+\frac{\sqrt{2}}{1+\sqrt{2}}\frac{\ell_{ee}}{\ell_{ea}}\right)} \alpha \bar{\rho}\, \bar{T}_e^{\frac{1}{2}} \frac{d\bar{T}_e}{d\bar{x}} \right]$$

$$+ \alpha \bar{\rho}\, \bar{T}_e \frac{d\bar{u}}{d\bar{x}} = 8\sqrt{\frac{a}{\pi}}\left(\frac{\ell}{\ell_{ea}} + \frac{\ell}{\ell_{ei}}\right) \alpha \bar{\rho}\, \bar{T}_e^{\frac{1}{2}} (\bar{T}_a - \bar{T}_e) - \frac{\dot{n}_{eA}}{\dot{N}} \bar{T}_{ion}$$

$$+ \frac{\dot{n}_{AA}}{\dot{N}} \frac{\zeta_{AA}}{kT_o} + \frac{\dot{n}_{rad}}{\dot{N}} \frac{\bar{\zeta}_{rad}}{kT_o} - \frac{\dot{n}}{\dot{N}} \frac{3}{2} \bar{T}_e \qquad (2.67)$$

Conduction and convection of energy in the electron gas is described by the terms on the left hand side of this equation. The gain in energy of the electrons by elastic interactions, inelastic interactions, and the creation of electrons by ionizing reactions is accounted for by the terms on the right hand side of the equation.

When the rate of production of electrons is sufficiently slow the right hand side of equation (2.67) reduces to the single term

$$8\sqrt{\frac{a}{\pi}}\left(\frac{\ell}{\ell_{ea}} + \frac{\ell}{\ell_{ei}}\right) \alpha \bar{\rho}\, \bar{T}_e^{\frac{1}{2}} (\bar{T}_a - \bar{T}_e)$$

This term represents the energy gained by electrons because of elastic interactions between the electrons, ions and atoms.

Jaffrin [4] has studied shock waves in ionized argon assuming the rate of production of electrons to be zero. Equation (2.67) reduces to the electron energy equation used by Jaffrin when the rate of production of electrons is zero. In addition Jaffrin neglects the radiative heat flux q_R. He finds the shock wave consists of a region of the order ℓ_{ee} thick in which the electrons are heated by conduction and elastic interactions with ions and atoms. Imbedded in the region where heating of the electrons takes place is a much smaller region of the order ℓ_{ia} or ℓ_{aa} thick in which the atoms and ions experience a viscous shock.

For the shock waves studied in this thesis the rate of production of electrons is not negligibly small. Heating of the electrons by conduction and convection, however, is negligible because either α is small, or $\alpha \frac{\ell_{ee}}{\ell}$ is small or the gradients in T_e and u are small. Consequently the electron energy equation reduces to

$$8\sqrt{\frac{a}{\pi}}\left(\frac{\ell}{\ell_{ea}}+\frac{\ell}{\ell_{ei}}\right)\alpha\,\bar{\rho}\,\bar{T}_e^{\frac{1}{2}}\,(\bar{T}_a-\bar{T}_e)-\frac{\dot{n}_{eA}}{\dot{N}}\,\bar{T}_{ion}+\frac{\dot{n}_{AA}}{\dot{N}}\,\frac{\bar{\zeta}_{AA}}{kT_o}$$

$$+\frac{\dot{n}_{rad}}{\dot{N}}\,\frac{\bar{\zeta}_{rad}}{kT_o}-\frac{\dot{n}}{\dot{N}}\frac{3}{2}\,\bar{T}_e=0 \qquad (2.68)$$

When all ionization processes except the electron atom ionization process are ignored equation (2.68) reduces to the equation used by Petschek and Byron [19] to describe the energy balance of the electrons.

The final equation needed to completely determine the problem is the mass conservation equation for the electrons (equation (2.1) with $\lambda = e$). The nondimensional form of this equation is

$$\frac{d\alpha}{d\bar{x}} = \frac{\dot{n}}{\dot{N}} \tag{2.69}$$

Summary of Equations

The simplified nondimensional equations which are used in this thesis to describe shock waves in radiating and ionizing argon are:

The total mass conservation equation.

$$\bar{\rho}\,\bar{u} = 1 \tag{2.63}$$

The total momentum conservation equation.

$$\frac{1}{\bar{\rho}} + a\,\bar{\rho}\,(\bar{T}_a + \alpha\,\bar{T}_e) = C_P \tag{2.64}$$

The total energy conservation equation.

$$\frac{5}{2}(\bar{T}_a + \alpha\,\bar{T}_e) + \alpha\,\bar{T}_{ion} + \frac{1}{2a\,\bar{\rho}^2} + \frac{q_R}{a\,\rho_o\,u_o^3} = C_E \tag{2.66}$$

The electron energy conservation equation.

$$8\sqrt{\frac{a}{\pi}}\left(\frac{\ell}{\ell_{ea}} + \frac{\ell}{\ell_{ei}}\right)\alpha\,\bar{\rho}\,\bar{T}_e^{\frac{1}{2}}\,(\bar{T}_a - \bar{T}_e) - \frac{\dot{n}_{eA}}{\dot{N}}\,\bar{T}_{ion} + \frac{\dot{n}_{AA}}{\dot{N}}\,\frac{\bar{\zeta}_{AA}}{kT_o} + \frac{\dot{n}_{rad}}{\dot{N}}\,\frac{\bar{\zeta}_{rad}}{kT_o} - \frac{\dot{n}}{\dot{N}}\,\frac{3}{2}\,\bar{T}_e = 0 \tag{2.68}$$

The electron mass conservation equation.

$$\frac{d\alpha}{d\bar{x}} = \frac{\dot{n}}{\dot{N}} \tag{2.69}$$

It remains to give detailed expressions for the ionization rates and the radiative heat flux. This is done in the following two sections.

Ionization Rates

In order to compute the rates $\dot{n}_{eA}$, $\dot{n}_{AA}$ and $\dot{n}_{rad}$ it is necessary to know the population of all electronic energy levels of the atom which contribute to the rates. In many instances one process, for example, electron collisions, is dominant in populating these states and a Boltzmann distribution of the population of excited levels can be assumed.

However, in the present problem no one process is necessarily dominant in populating all the electronic states of the atom. For example the upper levels might be affected most by collisions of the atom with electrons, but the ground level population might be affected most by radiative interactions.

In theory it is necessary to calculate the population distribution of the atom by solving a rate equation for each level, taking into account all the ways by which the population of that level can be changed. Such a calculation has been performed for atomic hydrogen (the only gas for which the collisional and radiative cross sections are known in sufficient detail) assuming the upper states of the atom to be in statistical equilibrium [52] - [56].

A detailed analysis of the population of excited levels in argon cannot be made because of an insufficient knowledge of the necessary data. Even if all the necessary data were available it would be desirable to simplify the calculation by making a reasonable model of the actual case.

The model employed in this thesis is based on the fact that electron-atom collision rates greatly exceed other rates for those

levels which are close to the ionization limit of the atom [52]- [58]. Consequently these levels will establish equilibrium with the electrons. Since the excited states of the argon atom are all within about 4 ev of the ionization limit, the excited states of the argon atom are assumed to be in thermodynamic equilibrium with the electrons.

Since the excited states are in equilibrium with the electrons, their net rate of production of electrons is zero. All of the free electrons must be supplied by the ground level. Ground state electrons are released by electron-atom collisions, atom-atom collisions and radiative interactions.

The collisional reactions depleting the ground state are

$$A(1) + A \underset{K_A(2,1)}{\overset{K_A(1,2)}{\rightleftharpoons}} A(2) + A \tag{2.70}$$

$$A(1) + e \underset{K_e(2,1)}{\overset{K_e(1,2)}{\rightleftharpoons}} A(2) + e \tag{2.71}$$

where index 1 denotes the ground state and index 2 the excited state. These reactions are followed by a rapid ionization from the excited state.

The rate of change of population of state 2 due to atom-atom collisions is

$$\dot{n}(2) = K_A(1,2)\, n_a\, n(1) - K_A(2,1)\, n(2)\, n_a - \dot{n}_+(2)$$

where $\dot{n}_+(2)$ is the rate of ionization from state 2. Since state 2 is in equilibrium with the electrons, its net ionization rate must be zero. Consequently the rate of ionization by atom-atom collisions is

$$\dot{n}_{AA} = K_A(1,2)\, n_a\, n(1) - K_A(2,1)\, n(2)\, n_a \qquad (2.72)$$

where the rate coefficient $K_A(1,2)$ is shown in Appendix A to be

$$K_A(1,2) = \frac{2C_A}{\sqrt{\pi\, m_A}} (k\, T_a)^{3/2} \left(\frac{T_{ex}}{T_a} + 2 \right) e^{-T_{ex}/T_a} \qquad (2.73)$$

In equation (2.73) $T_{ex} = 1.34(10^5)$ °K is the excitation temperature for the first excited state of the argon atom and $C_A = 7.5(10^{-8})\text{cm}^2/\text{erg}$ is a constant used in the expression for the atom-atom excitation cross section.

At equilibrium $\dot{n}_{AA}$ must be zero and the population of the atomic levels must be given by a Boltzmann distribution at the atom temperature T_a. In the limit of equilibrium equation (2.73) shows that $K_A(1,2)$ is related to $K_A(2,1)$ by

$$K_A(1,2) = \left[\frac{n(2)}{n(i)} \right]_{E,T_a} K_A(2,1) = \frac{g_2}{g_1}\, e^{-T_{ex}/T_a} K_A(2,1) \qquad (2.74)$$

where g_ℓ is the degeneracy of state ℓ. Consequently the atom-atom ionization rate may be written as

$$\dot{n}_{AA} = K_A(1,2)\, n_a n(1) \left[1 - \frac{n(2)/n(1)}{[n(2)/n(1)]_{E,T_e}} \right]$$

$$= K_A(1,2)\, n_a n(1) \left[1 - \frac{n(2)}{n(1)} \frac{g_1}{g_2} e^{T_{ex}/T_a} \right] \qquad (2.75)$$

Since state 2 is in equilibrium with the electrons, its population may be found from the Saha equation.

$$\frac{n_e^2}{n(2)} = \frac{2(2\pi\, m_e\, k\, T_e)^{3/2}}{g_2 h^3}\, e^{-\chi_2/kT_e}$$

where χ_2 is the ionization potential of state 2.

The population of state 1 which would exist if it were in equilibrium with the electrons, $n(1)_{E,\,T_e}$, is found from the following similar equation

$$\frac{n_e^2}{n(1)_{E,\,T_e}} = \frac{2(2\pi\, m_e\, k\, T_e)^{3/2}}{g_1 h^3}\, e^{-\chi/kT_e}$$

Therefore the ratio of the population of states 1 and 2 may be written as

$$\frac{n(2)}{n(1)} = \frac{n(1)_{E,T_e}}{n(1)} \frac{g_2}{g_1}\, e^{-T_{ex}/T_e}$$

The first excited level of the argon atom is separated from the ground state by an energy gap of about 11.8 ev. Because of this large energy gap, it is a good approximation that

$$n(1) = n_a = (1 - \alpha)\ \rho/m_a \tag{2.76}$$

$$n(1)_{E,T_e} = n_{a_{E,T_e}} = [1 - \alpha_E(T_e)]\ \rho/m_a \tag{2.77}$$

where $\alpha_E(T_e)$ is the degree of ionization which would exist if the gas were in equilibrium at the electron temperature and is given by the following formula.

$$\frac{\alpha_E^2(T_e)}{1 - \alpha_E(T_e)} = \frac{\rho_{ion}}{\rho} \left(\frac{T_e}{T_{ion}}\right)^{3/2} e^{-T_{ion}/T_e} \tag{2.78}$$

The ratio of the population of states 1 and 2 may then be written as

$$\frac{n(2)}{n(1)} = \frac{1 - \alpha_E(T_e)}{1 - \alpha} e^{-T_{ex}/T_e} \frac{g_2}{g_1} \tag{2.79}$$

Using equation (2.79) in equation (2.75) the atom-atom ionization rate is

$$\dot{n}_{AA} = (1 - \alpha)^2 \left(\frac{\rho}{m_a}\right)^2 K_A(1,2) \left[1 - \frac{1 - \alpha_E(T_e)}{1 - \alpha} e^{-T_{ex}\left(\frac{1}{T_e} - \frac{1}{T_a}\right)}\right] \tag{2.80}$$

In a similar way the electron-atom ionization rate is

$$\dot{n}_{eA} = \left(\frac{\rho}{m_a}\right)^2 K_e(1,2)\, \alpha\, (\alpha_E(T_e) - \alpha) \tag{2.81}$$

where $K_e(1,2)$ is the forward reaction rate constant for the electron-atom reaction. It is shown in Appendix A to be

$$K_e(1,2) = 2C_E \sqrt{\frac{2}{\pi m_e}} (kT_e)^{3/2} \left(\frac{T_{ex}}{T_e} + 2\right) e^{-T_{ex}/T_e} \tag{2.82}$$

In equation (2.82) $C_e = 4.4\ (10^{-6})$ cm^2/erg is a constant used in the formula for the electron-atom excitation cross section.

When the degree of ionization is small the atom-atom rate is larger than the electron-atom rate. By substituting equation (2.80) into equation (2.68) and assuming the degree of ionization is small, it can be seen that as the degree of ionization decreases the electron temperature also decreases. Consequently for small degrees of ionization the collisional ionization rate reduces to

$$(\dot{n}_{AA} + \dot{n}_{eA})_{\alpha \to 0} = (1 - \alpha)^2 \left(\frac{\rho}{m_a}\right) K_A(1,2)$$

It may be that just behind the viscous shock the degree of ionization is so small that there are insufficient electrons to establish equilibrium with the excited states of the atom. Equation (2.79) is

then invalid. Just behind the viscous shock, however, it will be true that

$$\frac{n(2)/n(1)}{[n(2)/n(2)]_{E,T_a}} \ll 1$$

and equation (2.75) shows that the collisional rate will be the same as the expression just given for low degrees of ionization. Therefore although equations (2.80) and (2.81) are invalid for very small degrees of ionization, their limiting values are correct. Consequently the ionization rates will be assumed to be those given by equations (2.80) and (2.81) for all degrees of ionization.

In the equations developed in the last section the ionization rate always appears divided by the characteristic convection rate $\dot{N}$. Dividing equations (2.80) and (2.81) by $\dot{N}$ and expressing the result in terms of nondimensional variables gives the following equations.

$$\frac{\dot{n}_{AA}}{\dot{N}} = \frac{\ell}{\ell_{AA}} (1-\alpha)^2 \bar{\rho}^2 \bar{T}_a^{3/2} \left(\frac{\bar{T}_{ex}}{\bar{T}_a} + 2 \right) \left[e^{-\bar{T}_{ex}/\bar{T}_a} - \frac{1-\alpha_E(T_e)}{1-\alpha} e^{-\bar{T}_{ex}/\bar{T}_e} \right] \tag{2.83}$$

$$\frac{\dot{n}_{eA}}{\dot{N}} = \frac{\ell}{\ell_{eA}} \alpha [\alpha_E(T_e) - \alpha] \bar{\rho}^2 \bar{T}_e^{3/2} \left(\frac{\bar{T}_{ex}}{\bar{T}_e} + 2 \right) e^{-\bar{T}_{ex}/\bar{T}_e} \tag{2.84}$$

where ℓ_{AA} and ℓ_{eA} are characteristic reaction lengths given by

$$\ell_{AA} = \frac{\sqrt{\pi}}{2C_A \rho_o u_o^2 a^{3/2}} = \frac{C_e}{C_A} \sqrt{\frac{2m_a}{m_e}} \ell_{eA} \tag{2.85}$$

Notice that the electron-atom rate depends on the electron temperature and the atom-atom rate depends primarily on the atom temperature. When equilibrium is reached $T_e = T_a$ and $\alpha = \alpha_E(T_e)$. The rates then are zero.

The radiation ionization rate is derived after the next section.

Non-Grey Radiation Energy Transfer

The ways in which radiative interactions take place in a monatomic gas are described by the following reaction equations.

$$A(p) + h\nu \rightleftharpoons A^+ + e \qquad p = 1,2,3 \tag{2.86}$$

and

$$A(p) + h\nu \rightleftharpoons A(q) \qquad q > p \qquad p = 1,2,3 \tag{2.87}$$

where A(p) denotes an atom excited to the p^{th} electronic state.

Appendix B shows it is possible to write a radiation transfer equation for each of the radiative reactions in equations (2.86) and (2.87) and each radiation transfer equation has the same form as equation (1.24). Let the radiative reactions be labeled by the subscript j. The radiation transfer equation which corresponds to reaction j is

$$\mu \frac{dI_j}{dx}(x,\mu,\nu) = -\frac{1}{\ell_j(x,\nu)} [I(x, \mu, \nu) - S_j(x, \nu)] \tag{2.88}$$

The meaning of the terms in this equation is exactly the same as for the corresponding terms in equation (1.24) except they apply to the j^{th} reaction only. For example $I_j(x, \mu, \nu)$ is the intensity of radiation from the jth reaction alone.

The total intensity is the sum of the individual intensities from all the radiative reactions.

$$I(x, \mu, \nu) = \sum_j I_j(x, \mu, \nu) \tag{2.89}$$

If equation (2.86) is summed over all the radiative reactions, equation (1.24) is obtained.

$$\sum_j \mu \frac{dI_j(x, \mu, \nu)}{dx} = \mu \frac{dI(x, \mu, \nu)}{dx} = -\frac{1}{\ell(x,\nu)} [I(x,\mu, \nu) - S(x, \nu)]$$

where the penetration length $\ell(x,\nu)$ and the source function $S(x,\nu)$ are the following functions of the penetration lengths $\ell_j(x,\nu)$ and source functions $S_j(x,\nu)$ for the individual radiative reactions.

$$\frac{1}{\ell(x,\nu)} = \sum_j \frac{1}{\ell_j(x,\nu)} \tag{2.90}$$

$$S(x,\nu) = \sum_j \frac{\ell(x,\nu)}{\ell_j(x,\nu)} S_j(x,\nu) \tag{2.91}$$

Once the individual penetration lengths $\ell_j(x,\nu)$ and source functions $S_j(x,\nu)$ have been specified, equations (2.90) and (2.91) can be used in equations (1.26) and (1.32) to calculate the radiative heat flux.

For the photoionization reactions (2.86) the following formulas for the individual penetration lengths and source functions are derived in Appendix B.

$$\frac{1}{\ell_p(x,\nu)} = B_{pc}(\nu) n(p) \left[1 - \frac{n(p)_E}{n(p)} e^{-h\nu/kT_e}\right] \tag{2.92}$$

$$S_p(x,\nu) = \frac{n(p)_E}{n(p)} \frac{2h\nu^3}{c^2} \left(e^{h\nu/kT_e} - \frac{n(p)_E}{n(p)} \right) \qquad (2.93)$$

where $n(p)_E$ is the population of atoms in state p which would exist if level p were in equilibrium with the electrons and ions. It is found from the following formula.

$$\frac{n_e n_i}{n(p)_E} = \frac{2(2\pi m_e k T_e)^{3/2}}{h^3 g_p} e^{-\chi_p/k T_e} \qquad (2.94)$$

In equation (2.94) χ_p is the ionization energy at level p and g_p is the degeneracy of state p.

The quantities $B_{pc}(\nu)$ in equation (2.92) represent cross sections for photoionization from level p. In the derivation of equations (2.92) and (2.93) the electron energy was assumed to have a Boltzmann distribution at temperature T_e.

As in the sections on ionization rates all but the ground state are assumed to be in equilibrium with the electrons.

$$n(p)_E = n(p) \qquad p = 2,3,4, \ldots$$

and for the ground state

$$n(1) \doteq n_a$$

$$\frac{n(1)_E}{n(1)} \doteq \frac{1 - \alpha_E(T_e)}{1 - \alpha}$$

Using these simplifications the penetration length and source function for photoionization from the ground state are found to be

$$\frac{1}{\ell_1(x,\nu)} = B_{1C}(\nu)\, n_a \left[1 - \frac{1 - \alpha_E(T_e)}{1 - \alpha} e^{-h\nu/kT_e} \right] \qquad (2.95)$$

$$S_1(x, \nu) = \frac{1 - \alpha_E(T_e)}{1 - \alpha} \frac{2h\nu^3}{c^2} \left(e^{-h\nu/kT_e} - \frac{1 - \alpha_E(T_e)}{1 - \alpha} \right)^{-1} \qquad (2.96)$$

The source function given by equation (2.96) differs appreciably from the Planck function only when $\alpha_E(T_e)$ is near one and $\alpha \neq \alpha_E(T_e)$.

For photoionization from excited states the following formulas are found.

$$\frac{1}{\ell_p(x,\nu)} = B_{pc}(\nu)\, n(p)\, (1 - e^{-h\nu/kT_e}) \quad p = 2,3,4 \ldots \qquad (2.97)$$

$$S_p(x,\nu) = \frac{2h\nu^2}{c^2} (e^{h\nu/kT_e} - 1)^{-1} = B_\nu(T_e) \quad p = 2,3,4 \ldots \qquad (2.98)$$

It is to be expected that the source function for photoionization from excited states, equation (2.98), is the Planck function since the excited state atoms have been assumed to be in equilibrium with the electrons.

The penetration lengths and source functions for the photoionization reactions (2.87) are shown in Appendix B to be

$$\frac{1}{\ell_{pq}(x,\nu)} = n(p)\, B_{pq}\, \beta_{pq}(\nu) \left[1 - \frac{n(q)}{n(p)} \frac{g_p}{g_q} \right] \qquad (2.99)$$

$$S_{pq}(x,\nu) = \frac{n(q)}{n(p)} \frac{g_p}{g_q} \frac{2h\nu^3}{c^2} \left(1 - \frac{n(q)}{n(p)} \frac{g_p}{g_q} \right)^{-1} \qquad (2.100)$$

where B_{pq} is the total transition probability for the transition between states p and q, and $\beta_{pq}(\nu)$ is the line shape function.

Separation of Radiative Interactions

Radiation energy transfer is combined in the sense that the total penetration length and source function depend on the penetration lengths

and source functions for each of the individual radiative interactions as shown by equations (2.90) and (2.91).

However, if for some range of frequencies one penetration length is significantly smaller than all the others, the term in the summation containing that penetration length will be dominant. For example if $\ell_k(x,\nu)$ is considerably smaller than all other penetration lengths for the frequency range $\nu_a \leq \nu \leq \nu_b$, equations (2.90) and (2.91) will simplify to

$$S(x,\nu) = S_k(x,\nu) \qquad \nu_a \leq \nu \leq \nu_b \qquad (2.101)$$

$$\frac{1}{\ell(x,\nu)} = \frac{1}{\ell_k(x,.)} \qquad \nu_a \leq \nu \leq \nu_b \qquad (2.102)$$

These equations show radiation would be transferred in the frequency range $\nu_a \leq \nu \leq \nu_b$ as if the k^{th} reaction were the only radiative interaction taking place.

If the penetration length $\ell_k(x,\nu)$ is assumed to be vanishingly small compared to the scale of variation of gas properties, equations (1.26) and (1.32) show the radiative flux for the k^{th} reaction is zero. Consequently reactions for which the penetration lengths are vanishingly small may be eliminated from the summations in equations (2.90) and (2.91).

Radiative reactions for which the penetration lengths are very large may also be neglected since terms for which the penetration lengths are large will not contribute to the summations in equations (2.90) and (2.91).

Line Radiation. The photoexcitation reactions (2.87) produce line radiation. Many of the lines may be eliminated from consideration because the atomic levels from which the excitation proceeds are not populated. Equation (2.99) shows the penetration length is then very large.

For those lines produced by photoexcitation from populated states the penetration length at the line center is usually vanishingly small and radiation energy transfer in the center of the line may be ignored. However, the penetration length in the line wings may be such that radiation energy transfer is important.

Murty [15] has examined line radiation in the precursor region ahead of shock waves in hydrogen. He finds the excitation of atoms caused by the line radiation to be important to the ionization process far ahead of the shock front. Biberman and Yakubov [26] have concluded that radiative excitation of atoms affects the approach to equilibrium ionization for shock waves in argon.

However, it is advantageous to determine the effect of continuum radiation without the considerable complication which accompanies the analysis of line radiation, For this reason further consideration of line radiation is omitted.

Continuum Radiation. The cross section for photoionization from the ground state, $B_{1C}(\nu)$, is zero for frequencies less than the frequency of the ionization edge, $\nu_1 = \chi/h$. Consequently for frequencies in the range $0 \leq \nu \leq \nu_1$ only the radiation due to photoionization from excited atomic states takes place. Equations (2.90), (2.91), (2.97), and (2.93) then give

$$S(x,\nu) = B_\nu(T_e) \qquad 0 \leq \nu < \nu_1 \tag{2.103}$$

$$\frac{1}{\ell(x,\nu)} = (1 - e^{-h\nu/kT_e}) \sum_{p \geq 2} B_{pc}(\nu)\, n(p) \tag{2.104}$$

Shock tube experiments in argon show the continuum radiation is well represented by the Unsöld formula [13], [14], [57]. The basic assumption used to obtain the Unsöld formula is that all the excited levels are hydrogenic and closely spaced. Mies [58] and Dronov et al. [59] improve this model by assuming all the levels to be hydrogenic except for certain lower lying states which are treated in more detail. In view of the good agreement of the Unsöld formula the refinements of Mies and of Dronov et al. need not be used for the shock waves of interest in this thesis.

The Unsöld formula predicts the emitted radiation is constant at all frequencies. Since the radiation must decay at the higher frequencies, the radiation predicted by the Unsöld formula is usually terminated at some rather arbitrary cutoff frequency. However, in the formulas developed below, which are based on the same assumptions as the Unsold formula, the radiation properly decays at the higher frequencies.

Assuming the excited states are hydrogenic, the Menzel and Pekeris formula [60] for the photoionization cross section may be used in equation (2.104) to give

$$\frac{1}{\ell(x,\nu)} = \frac{c^2}{2h\nu^3} e^{h\nu/kT_e} n_e^2 \frac{h^3 K Z_{eff}^4}{2(2\pi m_e kT_e)^{3/2}} \sum_{p \geq 2} \frac{1}{p^3} e^{-\eta/kT_e} \tag{2.105}$$

where $K = \frac{he^2}{m_e c^3} \frac{2^6}{3\sqrt{3}} R_Y$, R_Y is the Rydberg constant, Z_{eff} is the effective nuclear charge, G the Gaunt factor, η the energy of the photoelectron. The summation over the atomic state in equation (2.103) is to be carried out at constant frequency. Consequently, the electron energy is limited to values consistent with the requirement that the transition energy, $h\nu$, be a constant

$$h\nu = \chi_p + \eta = \text{constant} \tag{2.106}$$

where χ_p is the energy of level p below the ionization limit

$$\chi_p = \frac{h R_Y Z_{eff}^2}{p^2} \tag{2.107}$$

Assume the states are closely spaced down to a level χ_M below the ionization limit and regard the quantum number p as continuously distributed in this range. Then from equations (2.107) it follows that

$$d\chi = - \frac{2h R Z_{eff}^2}{p^3} dp$$

and since $h\nu = \text{constant} = \chi + \eta$

$$d\chi = - d\eta$$

The maximum electron energy consistent with equation (2.106) is that corresponding to $\chi = 0$ and is

$$\eta_{max} = h\nu$$

The minimum allowed electron energy consistent with equation (2.106) is that corresponding to the largest value of χ which is χ_M.

$$\eta_{min} \begin{cases} = 0 & \text{if } h\nu < \chi_M \\ = h\nu - \chi_M & \text{if } h\nu > \chi_M \end{cases}$$

Substitution of these results into equation (2.103) gives

$$\frac{1}{\ell(x,\nu)} = \frac{c^2}{2h\nu^3} e^{h\nu/kT_e} n_e^2 \frac{h^3}{2(2\pi m_e kT_e)^{3/2}} \frac{KZ_{eff}^2}{2hR} \int_{\eta_{min}}^{\eta_{max}} G\, e^{-\eta/kT_e} d\eta$$

Assuming the Gaunt factor to have a constant value and performing the integration the result is

$$\frac{1}{\ell(x,\nu)} = \frac{K'}{B_\nu(T_e)} \frac{n_e^2 Z_{eff}^2}{\sqrt{T_e}} Gf \qquad (2.108)$$

where

$$K' = \frac{16}{3\sqrt{6}} \sqrt{\frac{\pi}{k}} \frac{e^6}{m_e^{3/2} c^3} = 5.44\ (10^{-39})$$

$$f \begin{cases} = 1 & \text{if } \nu < \nu_M = \chi_M/h \\ = \dfrac{B_\nu(T_e)}{B_{\nu_M}(T_e)} \left(\dfrac{\nu_M}{\nu}\right)^3 & \text{if } \nu \geq \nu_M = \chi_M/h \end{cases}$$

At frequencies less than the frequency ν_M the penetration length given by formula (2.108) is the same as that which would be found from the Unsold formula. At frequencies greater than ν_M the penetration length given by equation (2.108) differs from the Unsold result by the factor f. Similarly for frequencies less than ν_M, the intensity of emitted radiation, which is $B_\nu(T_e)/\ell(x,\nu)$, is independent of frequency, but for frequencies greater than ν_M the intensity of emitted radiation decays as $1/\nu^3$. The penetration length has a marked frequency dependence

through the Planck function and the factor f.

Now consider ground state photoionization. The cross section for photoionization from the ground state of argon has been experimentally determined [61]. It can be roughly represented by

$$B_{1C}(\nu) \begin{cases} = 0 & \text{if } \nu < \nu_1 = \chi/h \\ = B_0 \left(\frac{\nu}{\nu_1} \right)^2 & \text{if } \nu \geq \nu_1 = \chi/h \end{cases} \tag{2.109}$$

where $B_0 = 35(10^{-18})$ cm^2 is the cross section at the ionization threshold.

For frequencies equal to and larger than ν_1, the penetration length for photoionization from the excited states, equation (2.108), will be very large. Consequently excited state photoionization may be neglected compared to the ground state photoionization when $\nu \geq \nu_1$.

Collecting the results of this section, the penetration length and source function to be used in the calculation of the radiative flux are

$$S(x,\nu) \begin{cases} = B_\nu(T_e) & \text{if } 0 \leq \nu \leq \nu_1 \\ = \frac{1 - \alpha_E(T_e)}{1 - \alpha} \frac{2h\nu^3}{c^2} \left(e^{h\nu/kT_e} - \frac{1 - \alpha_E(T_e)}{1 - \alpha} \right)^{-1} & \text{if } \nu \geq \nu_1 \end{cases} \tag{2.110}$$

$$\frac{1}{\ell(x,\nu)} \begin{cases} = \dfrac{K'}{B_\nu(T_e)} \dfrac{n_e^2 Z_{eff} G}{\sqrt{T_e}} & \text{if } 0 \le \nu \le \nu_M \\ = \dfrac{K'}{B_{\nu_M}(T_e)} \dfrac{n_e^2 Z_{eff} G}{\sqrt{T_e}} \left(\dfrac{\nu_M}{\nu}\right)^3 & \text{if } \nu_M \le \nu \le \nu_1 \\ = n_a B_o \left(\dfrac{\nu}{\nu_1}\right)^2 \left[1 - \dfrac{1 - \alpha_E(T_e)}{1 - \alpha} e^{-h\nu/kT_e}\right] & \text{if } \nu \ge \nu_1 \end{cases} \tag{2.111}$$

Clarke and Ferrari [5] have also studied non-grey radiation energy transfer in shock waves with ionization. Their work differs from this study in that they use different reactions to describe the collisional ionization process; they assume the electron and atom temperatures are equal and they neglect photoionization from excited states.

Reduction to Grey Radiation

Non-grey radiation energy transfer can be reduced to an equivalent grey radiation energy transfer if the penetration length can be written as a function of x times a function of ν. Assuming this write

$$\ell(x, \nu) = \theta(x)\, \phi(\nu) \tag{2.112}$$

The contribution to the radiative heat flux in the frequency range $\nu_a \le \nu \le \nu_b$ is

$$Q_{ab}(x) = \int_{\nu_a}^{\nu_b} q_R(x, \nu) d\nu \tag{2.113}$$

where $q_R(x, \nu)$ is given by equation (1.32). Using equation (2.112) in equations (1.26) and (1.32) and reversing the order of integration in equation (1.32), equation (2.113) may be written as

$$Q_{ab}(x) = 2\pi \int_{-\infty}^{\infty} \operatorname{sgn}[\tau(x) - \tau(x')] J_{ab}(x,x')\, d\tau(x') \tag{2.114}$$

where $J_{ab}(x, x')$ is the following integral

$$J_{ab}(x, x') = \int_0^1 d\mu \int_{\nu_a}^{\nu_b} d\nu \; \frac{S(x',\nu)}{\phi(\nu)} \; e^{\frac{-|\tau(x) - \tau(x')|}{\mu \phi(\nu)}} \tag{2.115}$$

and $\tau(x)$ is an optical length which is independent of frequency.

$$\tau(x) = \int_0^x \frac{dx'}{\theta(x')} \tag{2.116}$$

Equation (2.114) for the radiative heat flux is in the form expected for a grey gas where J is to be interpreted as a combined attenuation function and source function.

Consider the frequency range $\nu_1 \leq \nu < \infty$. Noting that $h\nu/kT_e \ll 1$, equations (2.110) and (2.111) give the following relations

$$\theta(x) = \frac{1}{n_a B_o}$$

$$\phi(\nu) = \left(\frac{\nu}{\nu_1}\right)^2$$

$$S(x,\nu) = \frac{1 - \alpha_E(T_e)}{1 - \alpha} \; \frac{2h\nu^3}{c^2} \; e^{-h\nu/kT_e(x)}$$

Using these formulas the function $J(x, x')$ may be written as

$$J_{1\infty}(x, x') = \nu_1 \frac{1 - \alpha_E(T_e)}{1 - \alpha} B_{\nu_1}(T_e) \int_0^1 d\mu \int_0^\infty d\Delta(1+\Delta)\, e^{-\frac{h\nu_1}{kT_e}\Delta - \frac{|\tau(x) - \tau(x')|}{\mu(1+\Delta)^2}}$$

where Δ is defined by

$$\nu = \nu_1(1 + \Delta)$$

Since $(h\nu_1 / kT_e)$ is large, the main contribution to the integral will be for small values of Δ. Assuming $\Delta \ll 1$ and $\frac{h\nu_1}{kT_e} \gg |\tau(x) - \tau(x')|$, $J_{1\infty}(x, x')$ simplifies to

$$J_{1\infty}(x,x') = \frac{1 - \alpha_E(T_e)}{1 - \alpha} \frac{kT_e}{h} B_{\nu_1}(T_e)\, E_2(|\tau(x) - \tau(x')|)$$

Equation (2.114) then gives the radiative heat flux in the frequency range $\nu_1 \leq \nu < \infty$ as

$$Q_{1\infty}(x) = 2\pi \int_{-\infty}^{\infty} \frac{1 - \alpha_E(T_e)}{1 - \alpha} B_{\nu_1}(T_e) \frac{kT_e}{h} \operatorname{sgn}[\tau(x) - \tau(x')] E_2[|\tau(x) - \tau(x')|]\, d\tau(x') \qquad (2.117)$$

This expression is in the form of the radiative heat flux for a grey gas with an equivalent grey source function

$$\frac{1 - \alpha_E(T_e)}{1 - \alpha} B_{\nu_1}(T_e) \frac{kT_e}{h}$$

and optical thickness

$$\tau(x) = \int_0^x \frac{dx'}{n_a(x')\, B_o} \qquad (2.118)$$

A similar reduction can be carried out for the frequency range $\nu_M \leq \nu < \nu_1$. Assuming the Gaunt factor G and effective charge Z_{eff}

to be one, and noting that $\frac{h\nu}{kT_e} \gg 1$, the following relations are found from equations (2.110) and (2.111).

$$\theta(x) = \frac{B_{\nu_M}(T_e)}{K'} \frac{\sqrt{T_e}}{n_e^2}$$

$$\phi(\nu) = \left(\frac{\nu}{\nu_M} \right)^3$$

$$S(x,\nu) = \frac{2h\nu^3}{c^2} e^{-h\nu/kT_e}$$

Substituting these relations into equation (2.114) gives the radiative heat flux from the frequency range $\nu_M \leq \nu < \nu_1$ as

$$Q_{M1}(x) = 2\pi \int_{-\infty}^{\infty} B_{\nu_M}(T_e) \frac{kT_e}{h} \operatorname{sgn}[\tau'(x) - \tau'(x')] E_2[|\tau'(x) - \tau'(x')|] d\tau'(x') \tag{2.119}$$

where $\tau'(x)$ is the following optical thickness

$$\tau'(x) = \int_0^x \frac{K' n_e^2(x')}{B_{\nu_M}[T_e(x')] T_e^{\frac{1}{2}}(x')} dx' \tag{2.120}$$

For frequencies between 0 and ν_M the penetration length is not exactly separable into a function of x times a function of ν because the combination $\frac{h\nu}{kT_e(x)}$ occurs in the Planck function. However, the penetration length may be written in an approximate form which is separable. The penetration length in this frequency range is

$$\ell(x,\nu) = \frac{\sqrt{T_e}}{K' n_e^2} \frac{B_\nu(T_e)}{1 - e^{-h\nu/kT_e}}$$

$$= \frac{\sqrt{T_e}\, B_M(T_e)}{K' n_e^2} \frac{r(h\nu/kT_e)}{1 - e^{-h\nu/kT_e}}$$

where $B_M(T_e)$ is the maximum value of the Planck function at the electron temperature T_e. It is a function only of the electron temperature and is given by

$$B_M(T_e) = 1.421436 \frac{2(kT_e)^3}{(hc)^2} \tag{2.121}$$

The ratio of the Planck function to its maximum value is $r\left(\frac{h\nu}{kT_e}\right)$ which is a function only of $\frac{h\nu}{k T_e}$.

$$r\left(\frac{h\nu}{kT_e}\right) = \frac{B_\nu(T_e)}{B_M(T_e)} = \frac{1}{1.421436} \frac{\left(\frac{h\nu}{kT_e}\right)^3}{e^{h\nu/kT_e} - 1} \tag{2.122}$$

Approximately, the penetration length is

$$\ell(x,\nu) = \frac{\sqrt{T_e}\ B_M(T_e)}{K'\ n_e^2} \frac{r\left(\frac{h\nu}{kT_{av}}\right)}{1 - e^{-h\nu/k\ T_{av}}} \tag{2.123}$$

where T_{av} is a suitably chosen average temperature.

Using the approximate penetration length the following relations are obtained.

$$\theta(x) = \frac{\sqrt{T_e}\ B_M(T_e)}{K'\ n_e^2}$$

$$\phi(\nu) = \frac{r(h\nu/hT_{av})}{1 - e^{-h\nu/kT_{av}}}$$

$$S(x,\nu) = B_\nu(T_e) \doteq B_M(T_e)\ r\left(\frac{h\nu}{kT_{av}}\right)$$

Substituting these formulas into equation (2.115) gives

$$J_{oM}(x,x') = B_M[T_e(x')] \int_o^1 d\mu \int_o^{\nu_M} d\nu \, (1 - e^{-\frac{h\nu}{kT_{av}}}) \cdot$$

$$\cdot e^{-\frac{|\tau''(x) - \tau''(x')|}{\mu \, r(h\nu/kT_{av})}} (1 - e^{-\frac{h\nu}{kT_{av}}})$$

$$= \frac{kT_{av}}{n} B_M[T_e(x')] \int_o^1 d\mu \int_o^{h\nu_M/kT_{av}} d\zeta (1 - e^{-\zeta}) \, e^{-\frac{|\tau''(x) - \tau''(x')|}{\mu \, r(\zeta)}} (1 - e^{-\zeta})$$

$$= \frac{kT_{av}}{h} B_M [T_e(x')] \, F[|\tau''(x) - \tau''(x')|]$$

where, noting that $\frac{h\nu_M}{k} = T_{ex}$, the function F may be written

$$F(t) = \int_o^{T_{ex}/T_{av}} d\zeta (1 - e^{-\zeta}) E_2 \left[t \, \frac{(1 - e^{-\zeta})}{r(\zeta)} \right] \qquad (2.124)$$

and τ'' is the following frequency independent optical thickness

$$\tau''(x) = \int_o^x \frac{K' \, n_e^2(x') \, dx'}{\sqrt{T_e(x')} \; B_M [T_e(x')]} \qquad (2.125)$$

The contribution to the radiative heat flux from the frequency range $0 \leq \nu \leq \nu_M$ is therefore

$$Q_{oM}(x) = 2\pi \int_{-\infty}^{\infty} B_M(T_e) \, \frac{kT_{av}}{h} \, \text{sgn} \, [\tau''(x) - \tau''(x')] F[|\tau''(x) - \tau''(x')|] \, d\tau''(x') \qquad (2.126)$$

Although equation (2.126) has the form of a radiative heat flux for a grey gas, it does not have the attenuation function E_2 appropriate to a grey gas. Instead the radiation is attenuated

according to the function F.

The attenuation function F was evaluated on an IBM 7094 computer. The results for T_{av} equal to ten thousand and thirty thousand degrees Kelvin are shown on Figure 2.1. The grey gas attenuation function E_2 is also shown for comparison. F is much more sharply peaked for small values of its argument than is E_2. Both functions rapidly diminish as their arguments increase. At the larger values of the arguments shown in the figure, F becomes independent of T_{av}.

The differences between the functions F and E_2 show that the widely practiced procedure of using frequency averaged penetration lengths in grey gas radiation energy transfer equations in order to approximate the radiation energy transfer in a non-grey gas may be erroneous because the grey gas attenuation function may be improper.

The total radiative heat flux is given by the sum of equations (2.117), (2.119), and (2.126). Dividing the total radiative heat flux by $\rho_o u_o^3$, which is the way in which it appears in equation (2.66), and expressing the result in terms of the non-dimensional variables, the following formulas for the radiative heat flux are obtained.

$$\frac{q_R}{\rho_o u_o^3} = \Gamma [\bar{Q}_{oM}(\bar{x}) + \bar{Q}_{M1}(\bar{x}) + \bar{Q}_{1\infty}(\bar{x})] = \Gamma \bar{q}_R \qquad (2.127)$$

where $\Gamma = \frac{\gamma' T_o^4}{\rho_o u_o^3}$ is a characteristic ratio of radiated energy to convected energy and $\gamma' = \frac{30}{\pi^4}(1.421436)\gamma$. γ is the Stefan-Boltzmann constant. The separate terms in this equation are

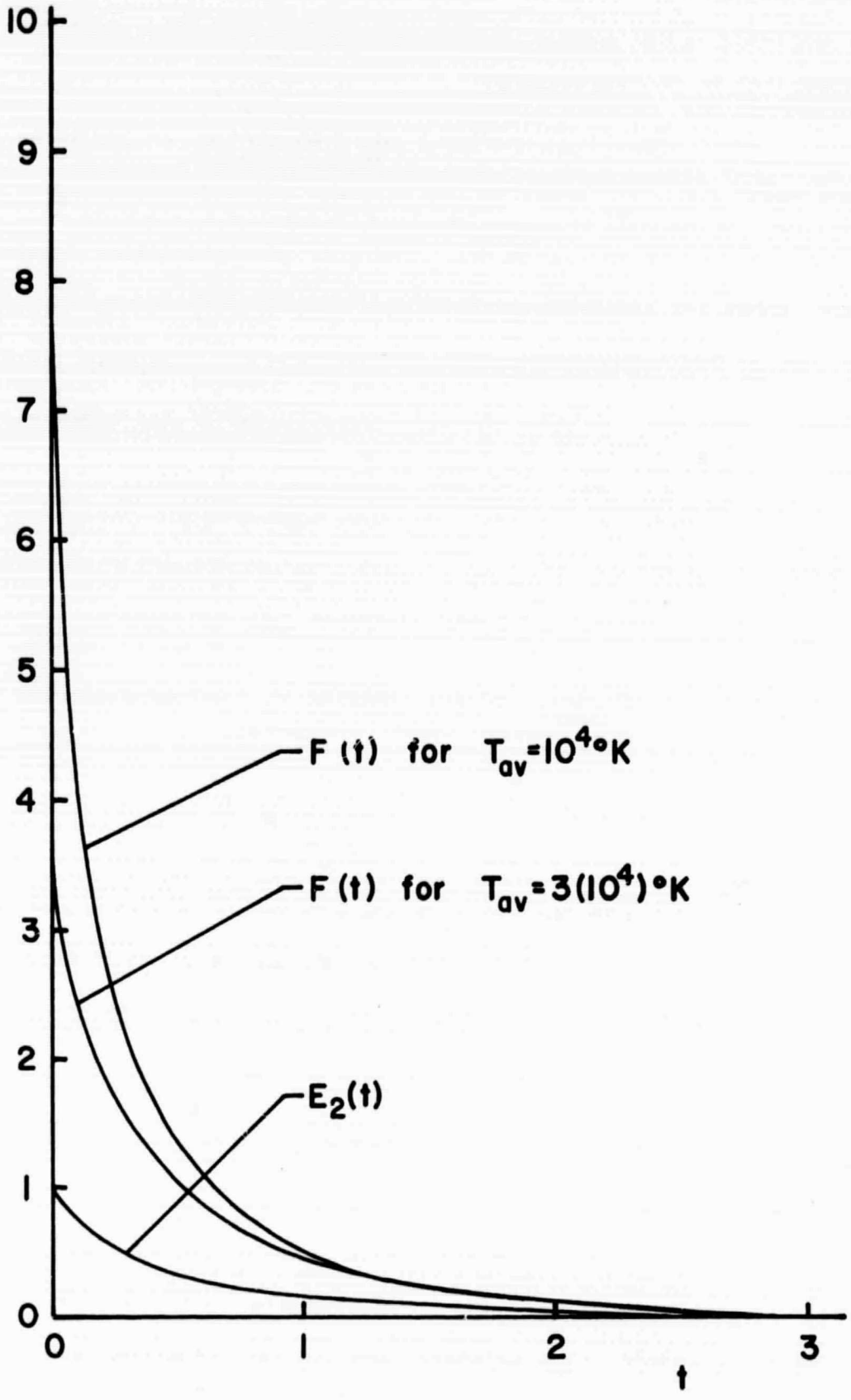

Figure 2.1. Attenuation Function F.

$$\bar{Q}_{1\infty}(\bar{x}) = \frac{\ell}{\ell_g} \int_{-\infty}^{\infty} \bar{\rho}\,[1 - \alpha_B(\bar{T}_e)]r\left(\frac{\bar{T}_{ion}}{\bar{T}_e}\right)\bar{T}_e^4\ \mathrm{sgn}[\tau(x)-\tau(x')]E_2[|\tau(\bar{x}) - \tau(\bar{x}')|]d\bar{x}' \qquad (2.128)$$

$$\bar{Q}_{M1}(\bar{x}) = \frac{\ell}{\ell_{ex}} \int_{-\infty}^{\infty} \alpha^{2-2}\bar{\rho}\sqrt{\bar{T}_e}\,\mathrm{sgn}\,[\tau'(\bar{x})- \tau'(\bar{x}')]E_2[|\tau'(\bar{x})-\tau'(\bar{x}')|]d\bar{x}' \qquad (2.129)$$

$$\bar{Q}_{oM}(\bar{x}) = \frac{\ell}{\ell_{ex}} \int_{-\infty}^{\infty} \alpha^{2}\bar{\rho}^{-2}\sqrt{\bar{T}_e}\ \mathrm{sgn}[\tau''(\bar{x})-\tau''(\bar{x}')\ ]F[|\tau''(\bar{x})-\tau''(\bar{x}')|]d\bar{x}' \qquad (2.130)$$

In these equations ℓ_g is a characteristic length for the ground state photoionization process and ℓ_{ex} is a characteristic length for photoionization from excited states.

$$\ell_g = \frac{1}{\frac{\rho_o}{m_a} B_o} \qquad \ell_{ex} = \frac{\sqrt{T_o}\ B_M(T_o)}{K'(\rho_o/m_a)^2} \qquad (2.131)$$

In terms of the nondimensional variables the optical thicknesses are

$$\tau(\bar{x}) = \frac{\ell}{\ell_g} \int_o^{\bar{x}} (1 - \alpha)\ \bar{\rho}\ d\bar{x}' \qquad (2.132)$$

$$\tau'(\bar{x}) = \frac{\ell}{\ell_{ex}} \int_o^{\bar{x}} \frac{\alpha^2\ \bar{\rho}^{-2}}{\bar{T}_e^{7/2}}\ \frac{d\bar{x}'}{r(\bar{T}_{ex}/\bar{T}_e)} \qquad (2.133)$$

$$\tau''(\bar{x}) = \frac{\ell}{\ell_{ex}} \int_o^{\bar{x}} \frac{\alpha^2\ \bar{\rho}^{-2}}{\bar{T}_e^{7/2}}\ d\bar{x}' \qquad (2.134)$$

It should be noticed that these equations depend only on the electron temperature, not the atom temperature. Thermal nonequilibrium of the gas will therefore affect the radiative flux.

The Radiative Ionization Rate

The rate of radiative energy absorption per unit volume of gas in the frequency range ν, $\nu + d\nu$ is $-\frac{dq_R(x,\nu)}{dx}$. Since the line radiation has been ignored, all the radiative energy that is absorbed must produce ionizations. Each absorption process, that is, each ionization, requires energy $h\nu$. The total rate of production of photo-electrons is therefore

$$\dot{n}_{rad} = -\int_0^\infty \frac{1}{h\nu} \frac{dq_R(x,\nu)}{dx} d\nu = -\frac{d}{dx}\int_0^\infty \frac{q_R(x,\nu)}{h\nu} d\nu$$

Except for the factor $\frac{1}{h\nu}$, the integral in this equation is just like that in equation (2.113). Consequently the procedures used in the last section to evaluate the integral in equation (2.113) are applicable this integral. In terms of the nondimensional variables the radiative ionization rate ratioed to the characteristic convective rate $\dot{N}$ is found to be

$$\frac{\dot{n}_{rad}}{\dot{N}} = -\frac{\Gamma}{a}\frac{d}{d\bar{x}}\left[\frac{\bar{Q}_{1\infty}(\bar{x})}{\bar{T}_{ion}} + \frac{\bar{Q}_{M1}(\bar{x})}{\bar{T}_{ex}} + \frac{\bar{Q}'_{oM}(\bar{x})}{\bar{T}_{av}}\right] \qquad (2.135)$$

where $\bar{Q}'_{oM}$ is the same as $\bar{Q}_{oM}$ given in equation (2.130) except that the attenuation function F is to be replaced by the function F' written below.

$$\bar{Q}'_{oM}(\bar{x}) = \frac{\ell}{\ell_{ex}}\int_{-\infty}^{\infty} \alpha^2 \bar{\rho}^2 \sqrt{\bar{T}_e}\ \mathrm{sgn}\,[\tau''(\bar{x}) - \tau''(\bar{x}')]\ F'[|\tau''(\bar{x}) - \tau''(\bar{x}')|]d\bar{x}' \qquad (2.136)$$

$$F'(t) = \int_0^{\bar{T}_{ex}/\bar{T}_{av}} d\zeta\ \frac{(1 - e^{-\zeta})}{\zeta}\ E_2\left[t\ \frac{(1 - e^{-\zeta})}{r(\zeta)}\right] \qquad (2.137)$$

Numerical evaluation of F' shows it to be similar to the function F as may be seen in Figure 2.2.

Method of Solution

The radiation flux and the radiative ionization rate are in the form of integrals which have integrands containing variables which are not known until the problem has been solved. Yet the problem may not be solved until the radiation flux and radiative ionization rate are known. This dilemma is avoided by using a starting solution to calculate the radiative terms. The equations are then solved using the radiative terms determined by the starting solution. The resulting solution is used to re-evaluate the radiative terms which are then used to generate still another solution and so forth.

The starting solution which was used is that obtained by omitting all radiative terms from the equations. The radiative terms determined from this radiationless solution may not be directly used in the equations to generate another solution because this procedure does not converge to the true solution rapidly enough to be practical. Instead the radiative terms obtained from the radiationless solution are inserted in the equations and multiplied by factors which make them artificially small but not negligible. The factors are chosen so that the next solution does not appreciably differ from the starting solution. This procedure is repeated, each time increasing the factors which multiply the radiative terms. In this way a series of solutions are generated, each of which is not greatly different from the preceding solution. When the factors are one the true solution is obtained by iteration.

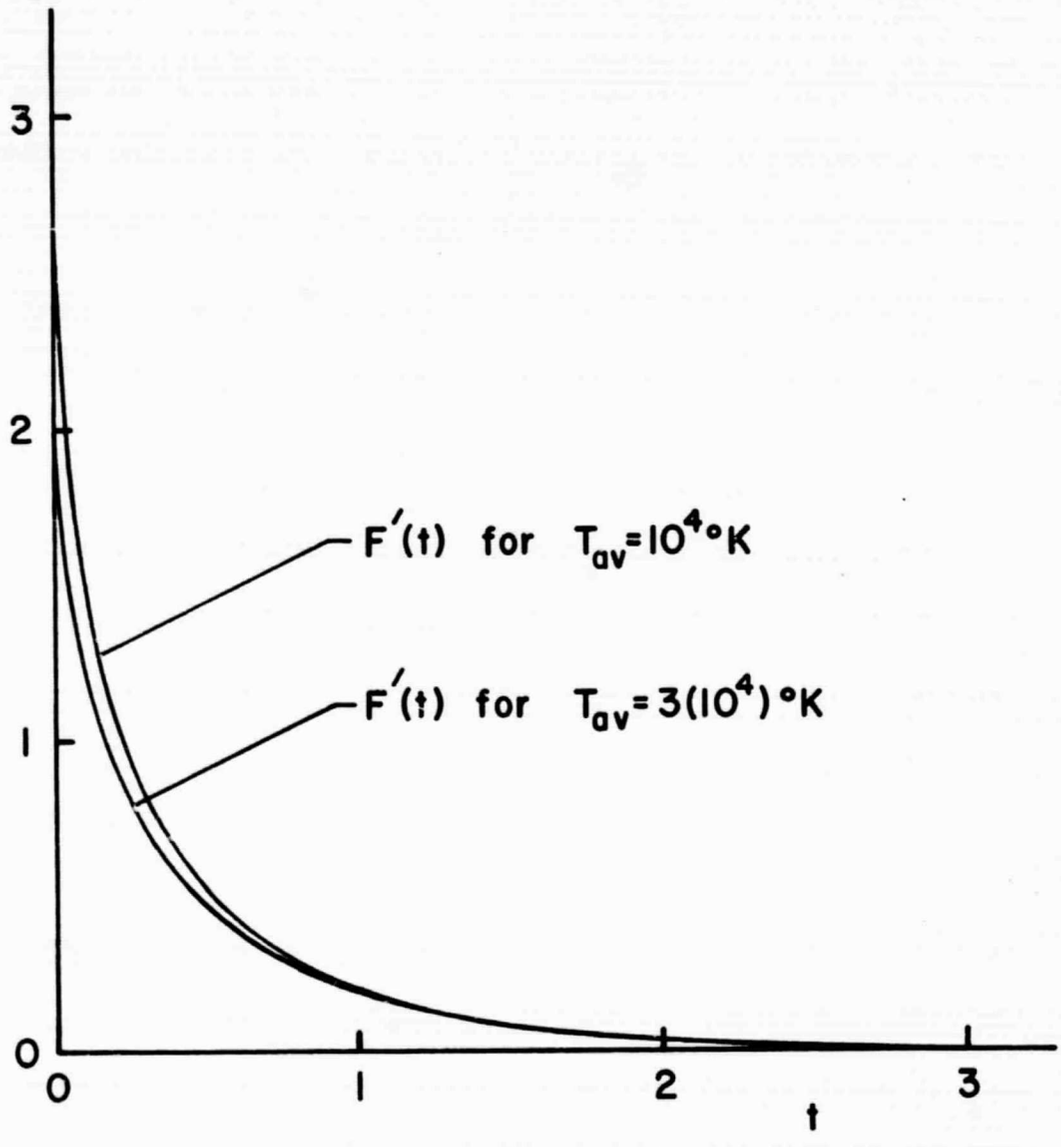

Figure 2.2. Special Function F'.

Knowing the values of the variables at an initial point $\bar{x}_i$, the values of the variables at any point $\bar{x}$ may be found as follows.

Using equation (2.135) the electron mass conservation equation (2.69) becomes

$$\alpha(x) = \alpha_i + \frac{\Gamma}{a}\left[\frac{\bar{Q}_{1\infty}(\bar{x}_i) - \bar{Q}_{1\infty}(\bar{x})}{\bar{T}_{ion}} + \frac{\bar{Q}_{M1}(\bar{x}_i) - \bar{Q}_{M1}(\bar{x})}{\bar{T}_{ex}} + \frac{\bar{Q}'_{oM}(\bar{x}_i) - \bar{Q}'_{oM}(\bar{x})}{\bar{T}_{av}}\right]$$

$$+ \int_{\bar{x}_i}^{\bar{x}} \left(\frac{\dot{n}_{eA} + \dot{n}_{AA}}{\dot{N}}\right) d\bar{x}' \qquad (2.138)$$

where α_i is the initial value of the degree of ionization and the terms $\bar{Q}_{1\infty}$, $\bar{Q}_{M1}$, and $\bar{Q}'_{oM}$ are to be regarded as known functions of $\bar{x}$ from the preceding solution. The integral in equation (2.138) was evaluated using a standard Runge-Kutta integration procedure. The integrand of this integral is found from equations (2.83) and (2.84). It must be evaluated at the values of α and $\bar{x}$ generated by the Runge-Kutta method. This is accomplished in the following way.

Equations (2.64) and (2.66) may be combined to give

$$\bar{\rho}(\bar{x}) = \frac{5C_p}{4a(C_E - \alpha\bar{T}_{ion} - \frac{\Gamma}{a}\bar{q}_R)}\left[1 + \left\{1 - \frac{32a(C_E - \alpha\bar{T}_{ion} - \frac{\Gamma}{a}\bar{q}_R)}{25\,C_p^2}\right\}^{\frac{1}{2}}\right] \qquad (2.139)$$

$$\bar{T}_a + \alpha\bar{T}_e = (C_p - \frac{1}{\bar{\rho}})\frac{1}{a\bar{\rho}} \qquad (2.140)$$

The density $\bar{\rho}$ can be calculated from equation (2.139) using the values of α and $\bar{x}$ generated from the Runge-Kutta integration procedure ($\bar{q}_R$ is a known function of $\bar{x}$ from the preceding solution). Then equation (2.140) can be used with the electron energy equation

(2.68) to give $\bar{T}_e$ and $\bar{T}_a$.

The average energies $\bar{\zeta}_{AA}$ and $\bar{\zeta}_{rad}$ which appear in the electron energy equation are shown in Appendix C to be of the order kT_e or less. When the electron-atom rate $\dot{n}_{eA}$ is the dominant rate, the terms in the electron energy equation which contain the average energies are completely negligible. Just behind the viscous shock front the atom-atom rate will be the dominant rate. There will then be some error in determining the electron temperature if the terms containing $\bar{\zeta}_{AA}$ and $\bar{\zeta}_{rad}$ are omitted from the electron energy equation. However, when the atom-atom rate is the dominant ionization rate an accurate determination of the electron temperature is unimportant because then the atom-atom ionization rate is independent of the electron temperature. In the precursor region, where only the radiative rate is important, the electron temperature need not be calculated because the degree of ionization in the precursor region is so small that the terms containing the electron temperature are eliminated from the equations. Consequently the terms containing the average energies $\bar{\zeta}_{AA}$ and $\bar{\zeta}_{rad}$ were omitted from the electron energy equation.

The constants C_P and C_E are, of course, determined from the initial conditions at point $\bar{x}_i$.

Theoretically the initial conditions are known at $\bar{x} = -\infty$ ahead of the shock wave. To start a numerical solution of the problem, however, initial conditions must be known at a finite distance in front of the shock wave. In order to find the conditions at a finite distance ahead of the shock wave from those which are known at $-\infty$, an analytical solution valid far ahead of the shock wave is used.

In the precursor region far ahead of the shock wave the gas will be cold. The temperature will be so low that the radiative ionization rate will be much larger than the collisional ionization rate. Furthermore, the number of excited atoms will be small and consequently the radiation emitted by electron recombination to excited states in the shocked gas will not be absorbed. Accordingly equation (2.69) can be integrated to read

$$\alpha + \frac{m_a}{\rho_o u_o} \int_{\nu_1}^{\infty} \frac{d\nu}{h\nu} \, q_R(x,\nu) = \text{constant} \tag{2.141}$$

In the far precursor region the emitted radiation will be negligible compared to the absorbed radiation. Consequently equation (1.24), the radiative transfer equation, becomes

$$\mu \frac{dI(x, \mu, \nu)}{d\tau(x, \nu)} = - I(x, \nu, \mu) \tag{2.142}$$

The radiation intensity at x = 0 is found from equation (1.37) to be

$$I(0,\mu,\nu) \quad \begin{cases} = - \int_o^{\infty} S(x', \nu) e^{-\tau(x,\nu)/\mu} \frac{d\tau}{\mu}(x',\nu) & \text{if } -1 \leq \mu \leq 0 \\ = 0 & \text{if } 0 < \mu \leq 1 \end{cases} \tag{2.143}$$

The solution of equation (2.142) with the requirement that the solution at x = 0 be given by equation (2.143) is

$$I(x, \mu, \nu) = I(0, \mu, \nu) e^{-\tau(x, \nu)/\mu} \tag{2.144}$$

Using the Eddington approximation the radiative flux can be related to the average intensity as follows.

$$q_R(x,\nu) = 2\pi \int_{-1}^{1} \mu\, I(x,\ \mu,\nu)\, d\mu = 4\pi\ \bar{\mu}\, \bar{I}\ (x,\nu) \qquad (2.145)$$

where $\bar{\mu}$ is an average value for μ, assumed to be $\frac{2}{3}$, and the average intensity, $\bar{I}$, is defined by

$$\bar{I}(x,\nu) = \frac{1}{2} \int_{-1}^{1} I(x,\ \mu,\ \nu)d\mu \qquad (2.146)$$

Equation (2.142) may be integrated over μ to give

$$\frac{dq_R(x,\nu)}{d\tau(x,\nu)} = 4\pi\ \frac{d\bar{I}(x,\nu)}{d\tau(x,\nu)} = -\ 4\pi\ \bar{I}(x,\nu)$$

The solution to this equation is

$$\bar{I}(x,\nu) = \bar{I}\ (\ 0,\nu)\ e^{-\ \tau(x,\nu)/\bar{\mu}} \qquad (2.147)$$

Collecting these results the integral in equation (2.141) may be written as

$$\frac{m_a}{\rho_o\, u_o} \int_{\nu_1}^{\infty} \frac{d\nu}{h\nu}\ q_R(x,\nu) = \frac{m_o}{\rho_o u_o}\ 2\pi \int_{\nu_1}^{\infty} \frac{d\nu}{h\nu}\, e^{-\tau(x,\nu)/\bar{\mu}} \int_{o}^{1} d\mu\ .$$
$$\cdot \int_{o}^{\infty} S(x',\nu)\, e^{-\tau(x',\nu)/\mu}\ \frac{d\tau\ (x',\nu)}{\mu}$$

Using the penetration lengths and source function appropriate to frequencies greater than ν_1 from equations (2.110) and (2.111) this may be written in the form

$$\frac{m_a}{\rho_o u_o} \int_{\nu_1}^{\infty} \frac{d\nu}{h\nu}\ q_R(x,\nu) = \frac{\Gamma}{a}\ e^{-\tau(\bar{x})/\bar{\mu}}\ \frac{\bar{Q}_{1\infty}(o)}{\bar{T}_{ion}} \qquad (2.148)$$

In this equation all quantities have been referred to the known initial conditions at $\bar{x} = -\infty$

$$\rho_o = \rho(-\infty), \quad T_o = T(-\infty), \quad u_o = u(-\infty), \text{ etc.}$$

except Γ and the variables in the integrand of $\bar{Q}(o)$ which are referred to values typical of the hot shocked gas downstream from the precursor region. Using ℓ_g for the characteristic length ℓ, the optical thickness which appears in equation (2.148) may be written as

$$\tau(\bar{x}) = \int_o^{\bar{x}} (1 - \alpha)\, \bar{\rho}\, d\bar{x} \tag{2.149}$$

In a similar way, the radiative flux is found to be

$$q_R(\bar{x}) = 4\pi \int_{\nu_1}^{\infty} \bar{I}(x,\nu)\, d\nu = e^{-\tau(\bar{x})/\bar{\mu}} \frac{\Gamma}{a} \bar{Q}_{1M}(o)$$

The degree of ionization in the precursor region far ahead of the shock will be negligible compared to one. Since the electron temperature always appears in the equations multiplied by the degree of ionization, the electron temperature may be omitted from consideration in the far precursor region. The equations become

$$\frac{1}{\bar{\rho}} + a\, \bar{\rho}\, \bar{T}_a = C_p \tag{2.150}$$

$$\frac{5}{2} \bar{T}_a + \alpha\, \bar{T}_{ion} + \frac{1}{2a\, \bar{\rho}^2} + \frac{\Gamma}{a} e^{-\tau/\bar{\mu}} Q_{1\infty}(o) = C_E \tag{2.151}$$

$$\alpha + \frac{\Gamma}{a} e^{-\tau/\bar{\mu}} \frac{\bar{Q}_{1\infty}(o)}{\bar{T}_{ion}} = \text{constant} \tag{2.152}$$

At $\bar{x} = -\infty$, $\bar{\rho} = \bar{T}_a = 1$. The solution to these equations is

$$\bar{\rho}(\bar{x}) = \bar{T}_a(\bar{x}) = 1 \tag{2.153}$$

$$\alpha = \alpha(o)\, e^{-\tau(\bar{x})/\bar{\mu}} \tag{2.154}$$

$$\alpha(o) = -\frac{\Gamma}{a\,\bar{T}_{ion}}\,\bar{Q}_{1\infty}(o) \tag{2.155}$$

This solution gives the finite value of $\bar{x}$ needed to start the solution and the initial values for $\bar{\rho}$, $\bar{T}_a$ and α in terms of the ratio $\alpha/\alpha(o)$ at which the solution is to be started and the flux integral $\bar{Q}_{1M}(o)$.

The full equations are then integrated, using the procedure previously discussed, to the point $\bar{x} = 0$, where the gas passes through a shock wave caused by viscosity and heat conduction effects. The radiative flux is constant and no ionization takes place across the viscous shock wave. The fluid conservation equations then give the jump conditions.

$$\rho(o^+) = 4\,\rho(o^-)$$

$$\alpha(o^+) = \alpha(o^-)$$

$$T_a(o^+) + \alpha\, T_e(o^+) = \frac{3}{16}\,\frac{m_a\, u^2(-\infty)}{k}\left[\frac{\rho(-\infty)}{\rho(o^-)}\right]^2$$

where the $-$ and $+$ signs denote values just before and just after the shock respectively. The last equation must be solved with the electron energy equation to get $T_a(o^+)$ and $T_e(o^+)$.

From behind the shock the equations are integrated until equilibrium is reached to within some predetermined accuracy. The

definition of equilibrium used for the calculations was that the degree of ionization equal the local equilibrium degree of ionization within five percent and the electron and atom temperatures be equal within one percent. The equations are very difficult to integrate near equilibrium because then the ionization rates are sensitive to small changes in the variables.

After equilibrium has been reached the degree of ionization can be calculated from the Saha equation, and the system of equations becomes entirely algebraic. The variables change in this region because of radiation cooling. The radiative cooling continues until a steady state is reached.

In this way a new solution is generated from the preceding solution. This process is repeated, each time increasing the factor which multiplies the radiative terms, until the factor is one and the solutions converge. Successive steps for the Mach number 18 solution presented in Chapter III are shown in Appendix D.

CHAPTER III

RESULTS AND DISCUSSION

Computer codes using the method of solution outlined in the previous chapter were developed and calculations were carried out on an IBM 7094 computer.

The argon gas ahead of the shock wave was taken to be at a pressure of 1 cm Hg and 300°K temperature. Calculations were performed for shock waves having Mach numbers of 12, 18, and 30, which correspond to shock velocities of 3.87, 3.81 and 9.68 mm/μ sec respectively.

The reference state used for the calculations was that given by the strong shock Rankine-Hugoniot relations applied to the cold gas far ahead of the shock wave. The reference values found by this procedure are shown in Table 3.1.

Table 3.1. Reference Conditions.

	$\rho_o(10^5)$ (gm/cm^3)	u_o (m_m/μ sec)	$T_e(10^{-4})$ °K	α_o	Γ	a
M = 12	1.090	.7581	1.096	.0344	7.533	3.968
M = 18	17.74	.6984	1.425	.2028	16.91	6.078
M = 30	25.29	.8167	1.987	.7487	28.11	6.202

These reference conditions give the characteristic lengths shown in Table 3.2.

Table 3.2. Characteristic Lengths

	ℓ_{AA} (cm)	$\ell_{eA}(10^4)$ (cm)	$\ell_g(10^2)$ (cm)	ℓ_{ex} (cm)
M = 12	2.387	1.305	1.739	1.791
M = 18	.9112	.4981	1.068	1.693
M = 30	.4536	.2480	.7494	2.674

At each Mach number solutions were first obtained by neglecting thermal nonequilibrium and radiation effects. Then the calculations were again performed with thermal nonequilibrium, or radiation, or both included in the analysis. In this way the effects of radiation and thermal nonequilibrium can be evaluated by comparing the solutions obtained when radiation and thermal nonequilibrium have been included with the solutions obtained when radiation and thermal nonequilibrium have been excluded.

Radiationless, Thermal Equilibrium Solutions

When radiation is omitted from the analysis and the electron and atom temperatures are assumed to be equal the solutions shown in Figures 3.1, 3.2 and 3.3 are found.

The temperature and density are to be read from the linear scale on the left. The electron-atom and atom-atom ionization rates are shown divided by the total ionization rate just after the viscous shock, $\dot{n}_s$. The ionization rates are to be read from the logarithmic scale at the right as is the ratio α/α_o.

Two scales are used on the abscissa. For the extent of the first scale the atom-atom ionization rate exceeds the electron-atom ionization rate and the characteristic length is chosen to be ℓ_{AA}. For the extent

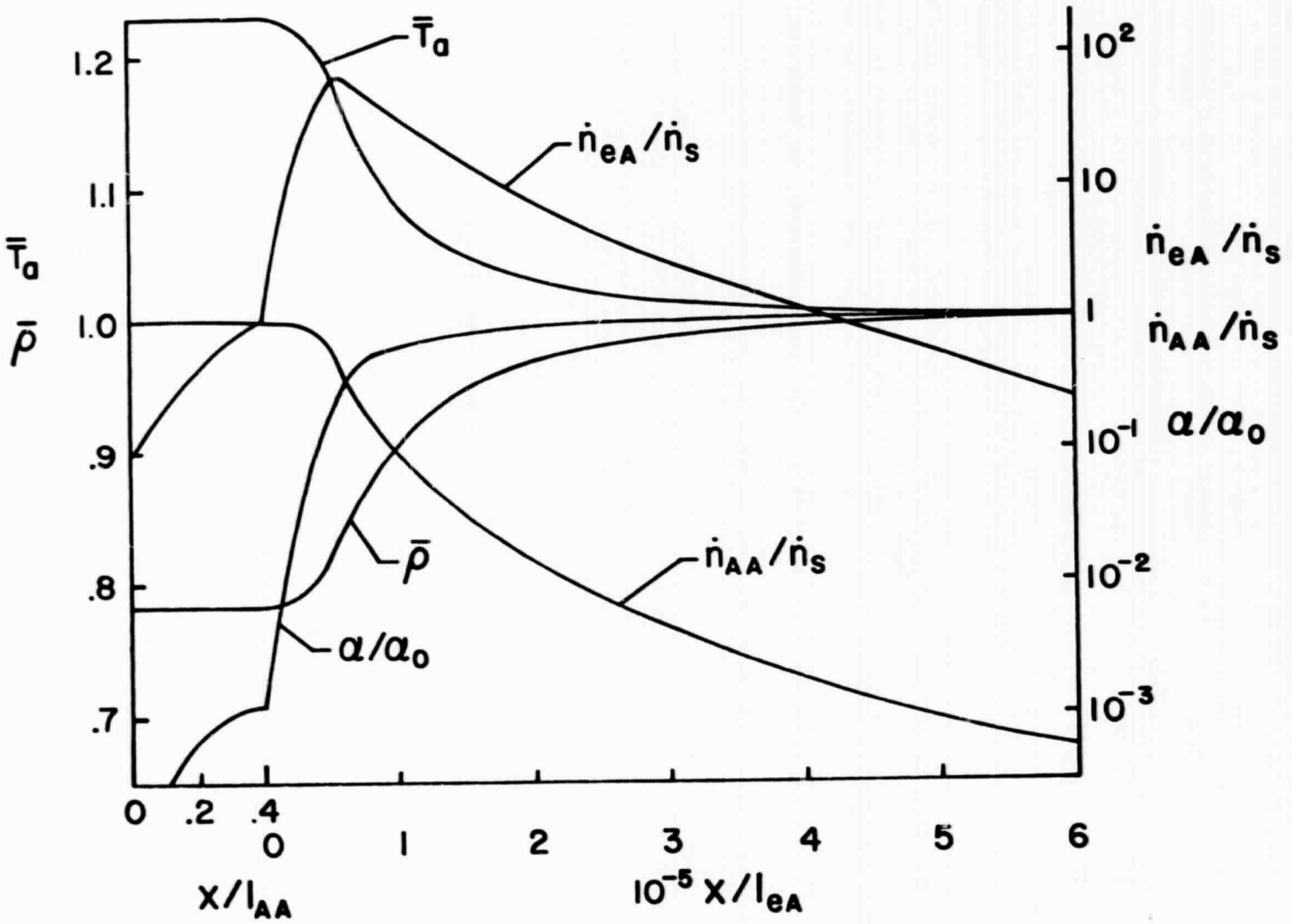

Figure 3.1. M = 12 Radiationless Shock Wave with $T_e = T_a$.

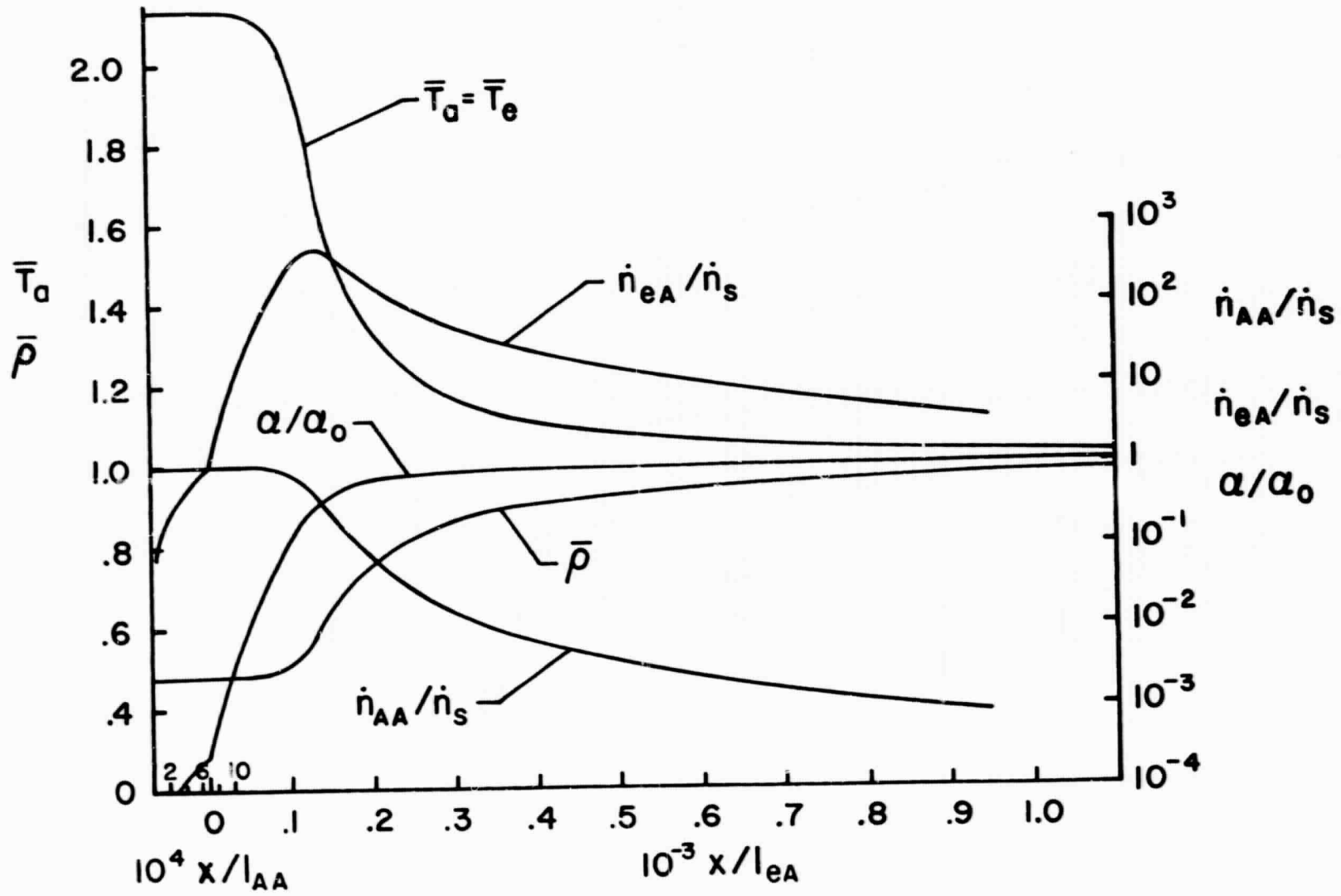

Figure 3.2. M = 18 Radiationless Shock Wave with $T_e = T_a$.

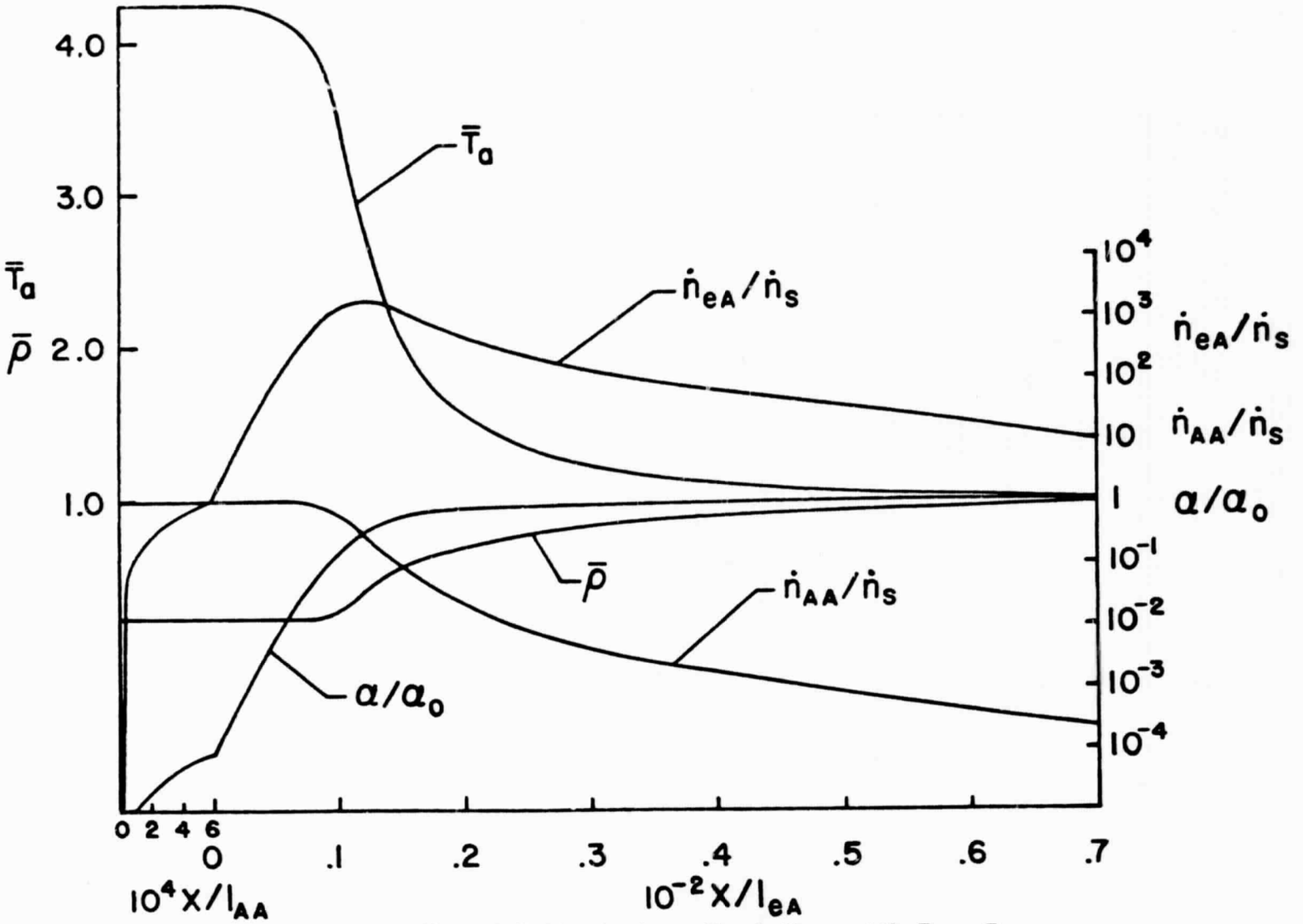

Figure 3.3. M = 30 Radiationless Shock Wave with $T_e = T_a$.

of the following scale the electron-atom rate exceeds the atom-atom rate and the characteristic length is taken to be ℓ_{eA}. The portion of the shock wave where the atom-atom ionization rate is dominant is small compared to the portion where the electron-atom rate is dominant. The length of the region in which the atom-atom rate is dominant, x_{AA}, and the length of the following region in which the electron-atom rate is dominant, x_{eA}, is shown in Table 3.3. The region where the e-A process is dominant is terminated when the degree of ionization is within 5% of the local equilibrium degree of ionization.

Table 3.3. Length of A-A and e-A Regions for Radiationless Shock Wave with $T_e = T_a$.

	x_{AA}(cm)	x_{eA}(cm)
M = 12	.9571	56.3
M = 18	$6.38(10^{-4})$	$8.71(10^{-2})$
M = 30	$2.72(10^{-5})$	$1.92(10^{-3})$

In all cases the e-A ionization rate quickly rises to a peak value and then slowly diminishes. The peak and decrease in the rate is due to the increased importance of recombination as an equilibrium degree of ionization is approached. The A-A ionization is unimportant except right behind the viscous shock.

The behavior of the other variables follows that of the e-A ionization rate, a region of abrupt change followed by a much slower variation. The shock waves all have long tails where the values attained by the variables are close to their final values.

Thermal Equilibrium with Trapped Radiation

For the solutions shown in Figures 3.4, 3.5 and 3.6 the only radiation process allowed was photoionization from the ground state. This radiation is completely absorbed in the shock wave, i.e., the radiation is trapped. As in the last section the gas is assumed to be in thermal equilibrium and the electron temperature is equal to the atom temperature. These same assumptions were used in the solutions obtained by Clarke and Ferrari [5].

Ionization takes place in the precursor region due to the absorption of the radiation emitted by the gas behind the viscous shock at $x = 0$. The degree of ionization in the precursor region is shown divided by the degree of ionization at the viscous shock wave, α_s, in Figures 3.4, 3.5 and 3.6 and is to be read from the logarithmic scale at the extreme left. The abscissa in the precursor region is x divided by the ground state characteristic length evaluated for conditions at $x - \infty$, $\ell_g = .08878$ cm. The precursor degree of ionization is shown on a larger scale in Figure 3.7 where it can be seen that the variation of the degree of ionization is nearly exponential except close to the viscous shock wave and in the far precursor region.

Because of the precursor ionization the atom-atom rate behind the viscous shock at $x = 0$ is much less than the electron-atom rate. In contrast to the radiationless solutions discussed in the last section there is no region where the atom-atom ionization rate is the dominant rate. The peak value of the electron-atom rate is reduced and slightly shifted, but it still has the same features as for the radiationless case, a rapid rise to a peak value followed by a region where it slowly decreases.

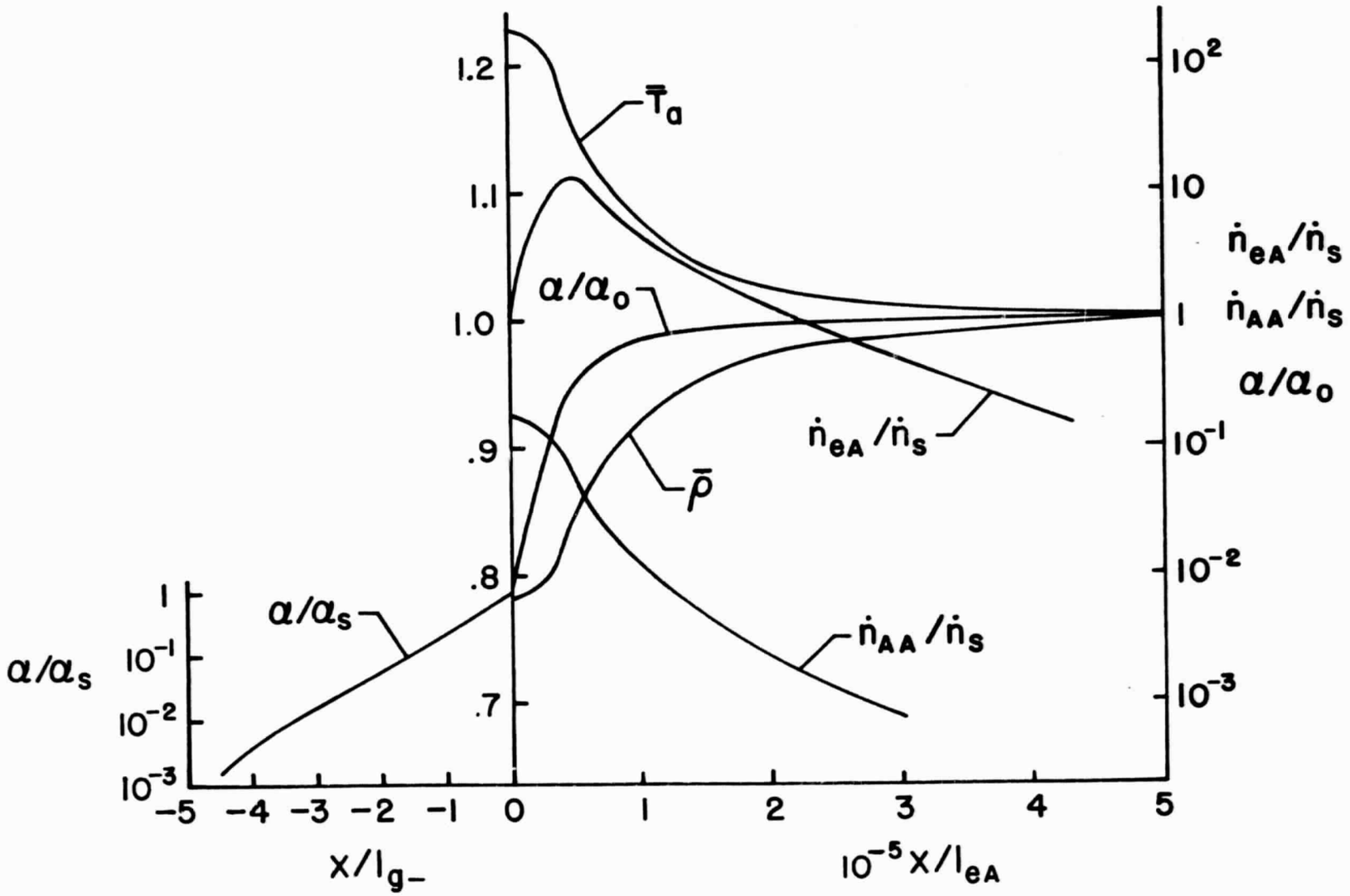

Figure 3.4. M = 12 Trapped Radiation Shock Wave with $T_e = T_a$.

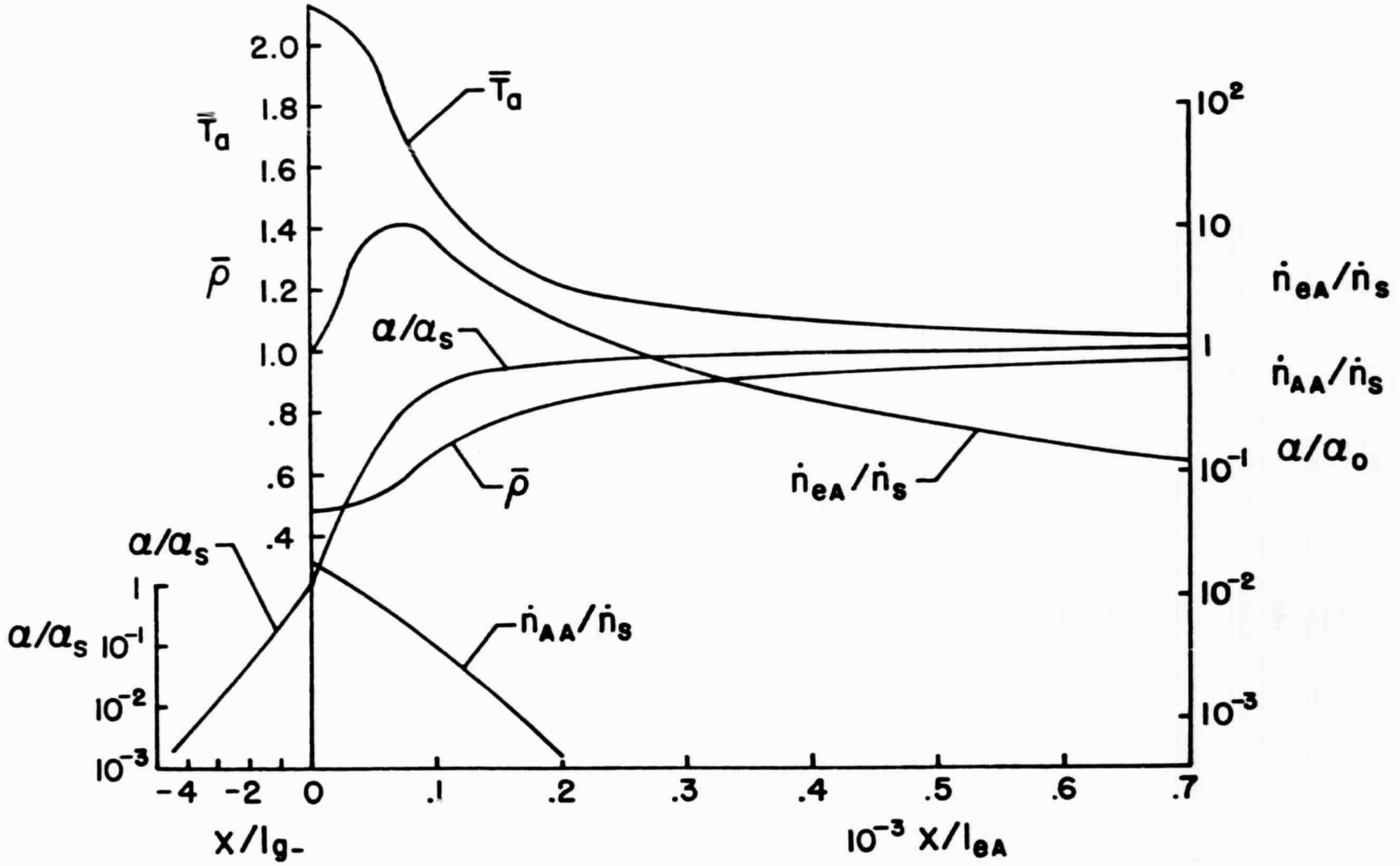

Figure 3.5. M = 18 Trapped Radiation Shock Wave with $T_e = T_a$.

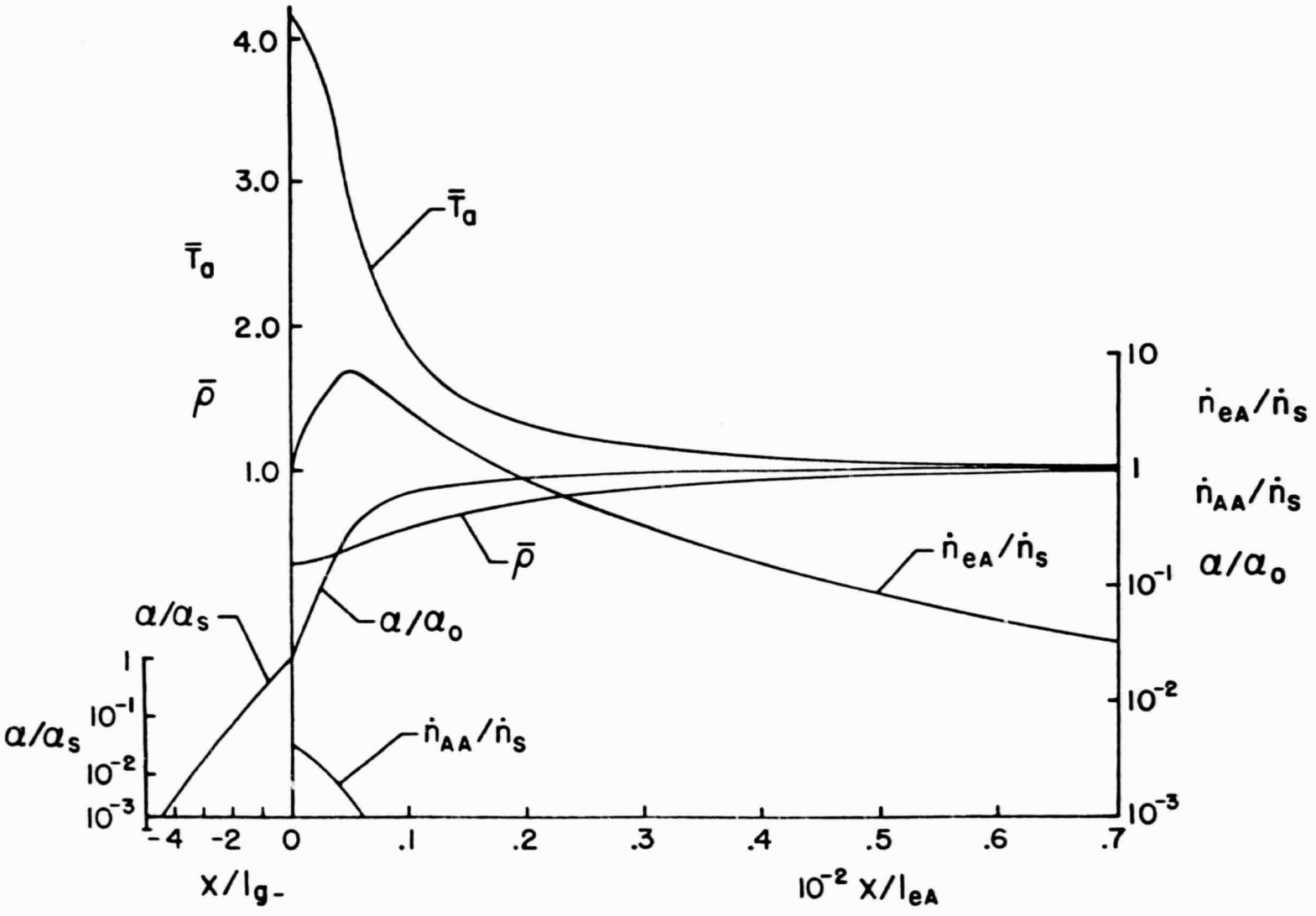

Figure 3.6. M = 30 Trapped Radiation Shock Wave with $T_e = T_a$.

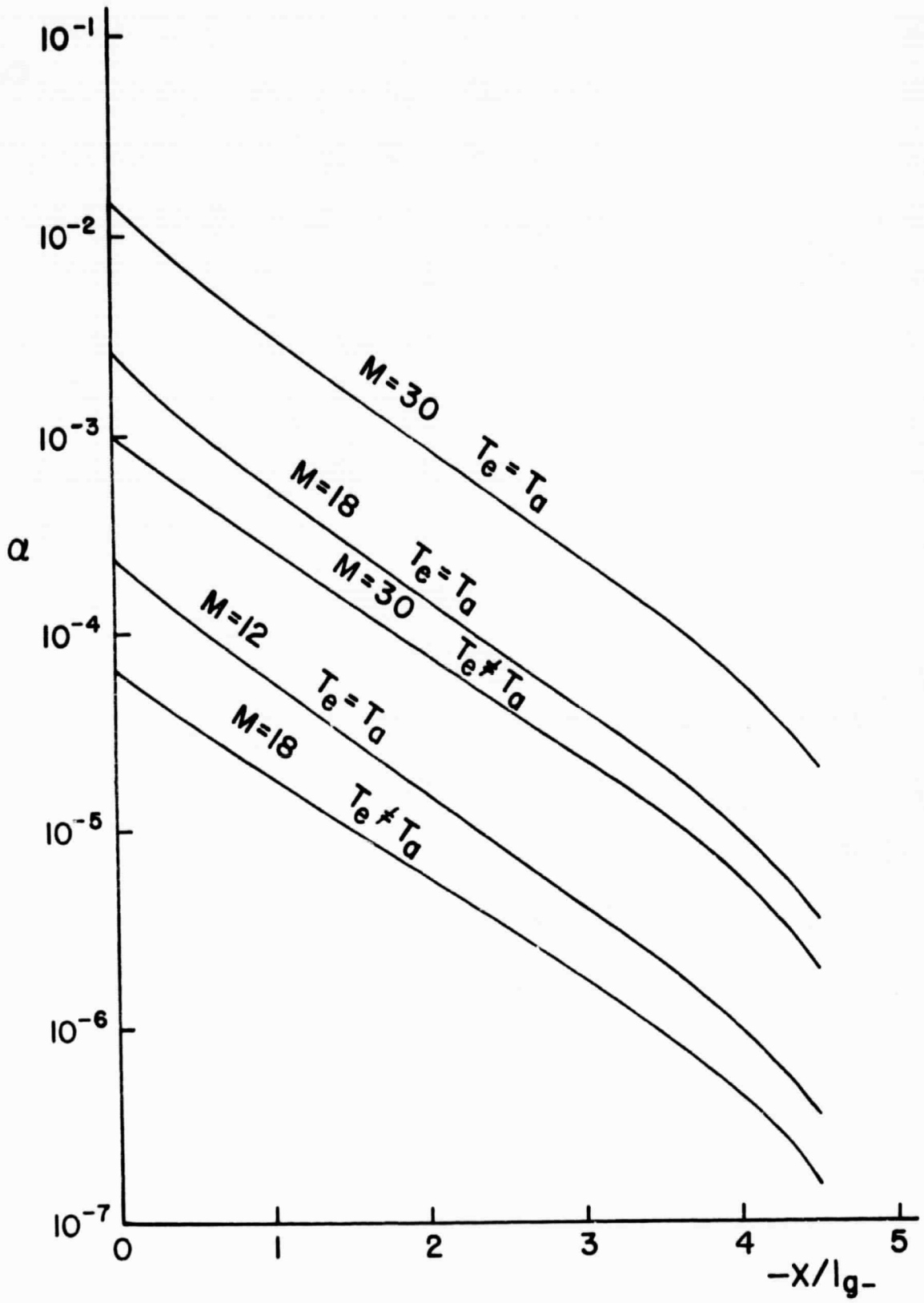

Figure 3.7. Precursor Degree of Ionization.

The distance required for the degree of ionization to come within 5% of its local equilibrium value is only slightly different than when trapped radiation is excluded from consideration as in the last section. The distances are 56.3, $8.97(10^{-2})$ and $1.84(10^{-3})$ cm including trapped radiation compared to 57.3, $8.77(10^{-2})$ and $1.95(10^{-3})$ cm when trapped radiation is excluded, for Mach numbers 12, 18 and 30 respectively.

Thermal Nonequilibrium with Trapped Radiation

As in the last section the only radiation process which is considered in the calculations is photoionization from the ground state. However, the gas is not assumed to be in thermal equilibrium and the electron temperature may be different than the atom temperature. The solutions obtained by employing this model are shown in Figures 3.8, 3.9 and 3.10.

The electron temperature is much less than the atom temperature right behind the viscous shock. It then rises and becomes equal to the atom temperature farther downstream.

The electron-atom ionization rate depends principally on the electron temperature. The lower electron temperature causes the electron-atom rate to be considerably reduced from the value it would have if the electron temperature were equal to the atom temperature. Because of the lower e-A ionization rate, the point at which the e-A rate attains its peak value is much farther downstream from the corresponding point when thermal equilibrium is assumed. Also the length of the region where the atom-atom rate is dominant, x_{AA}, and the length of the following region where the electron-atom rate is dominant, x_{eA}, are much greater than the corresponding lengths when thermal equilibrium

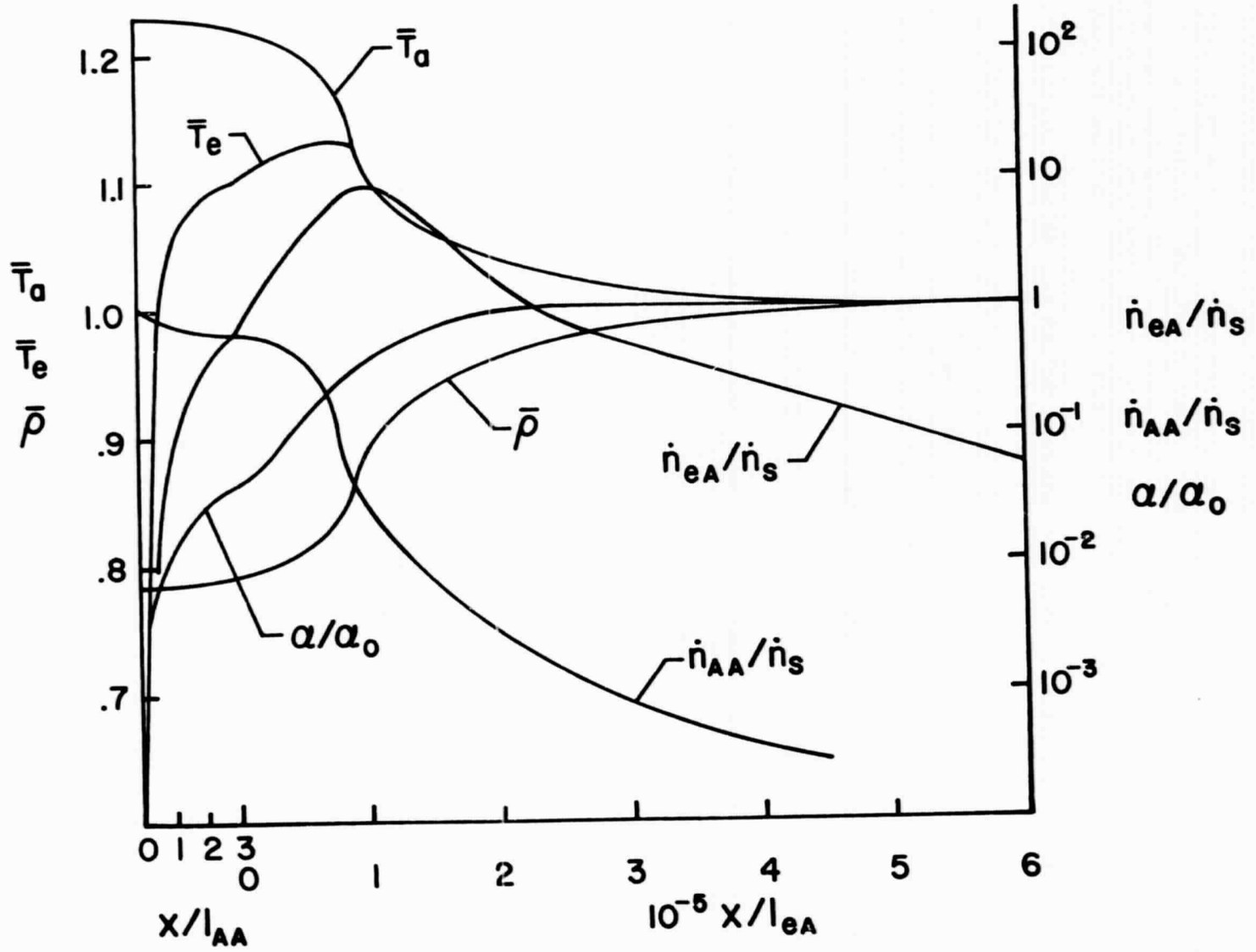

Figure 3.8. M = 12 Trapped Radiation Shock Wave with $T_e \neq T_a$.

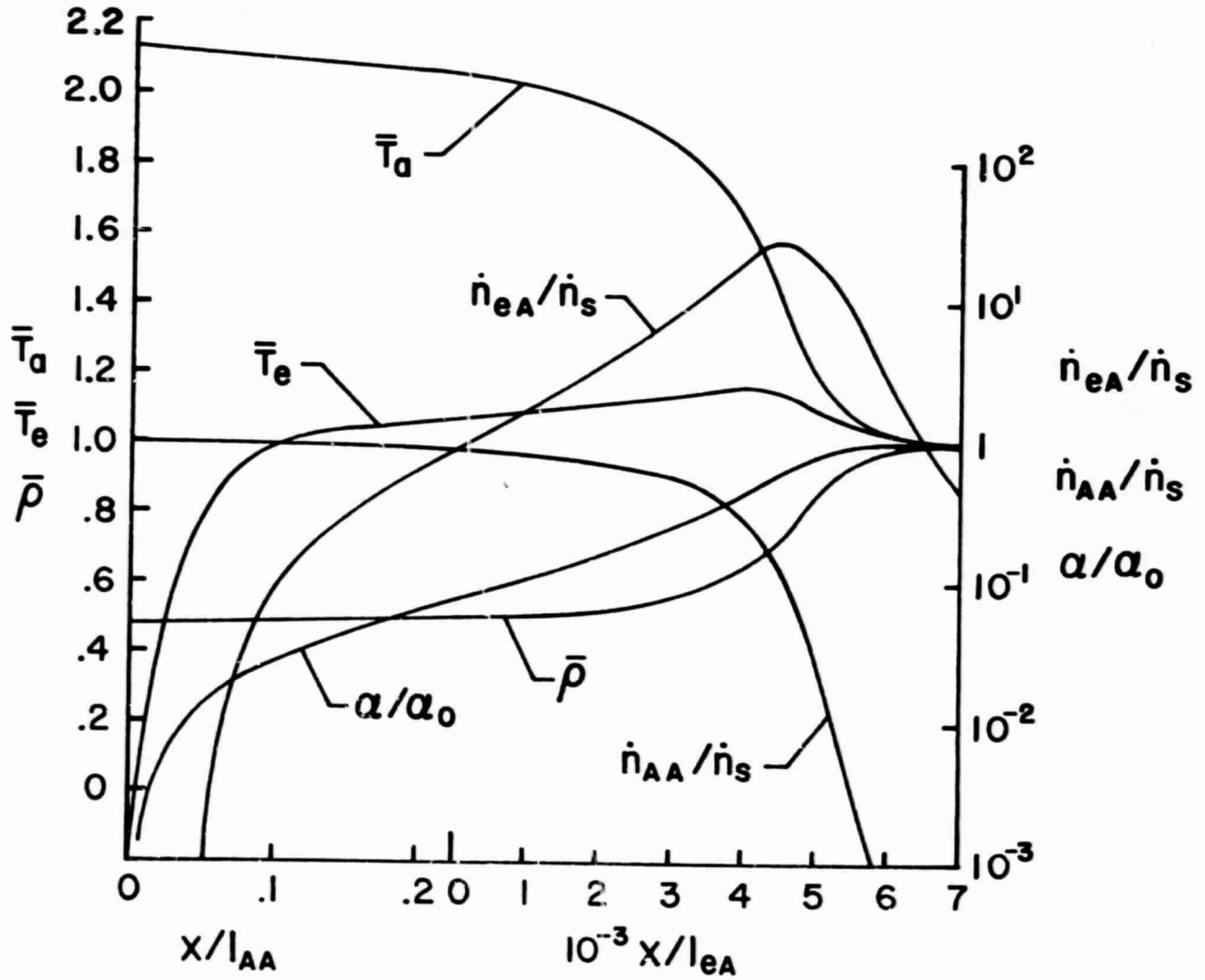

Figure 3.9. M = 18 Trapped Radiation Shock Wave with $T_e \neq T_a$.

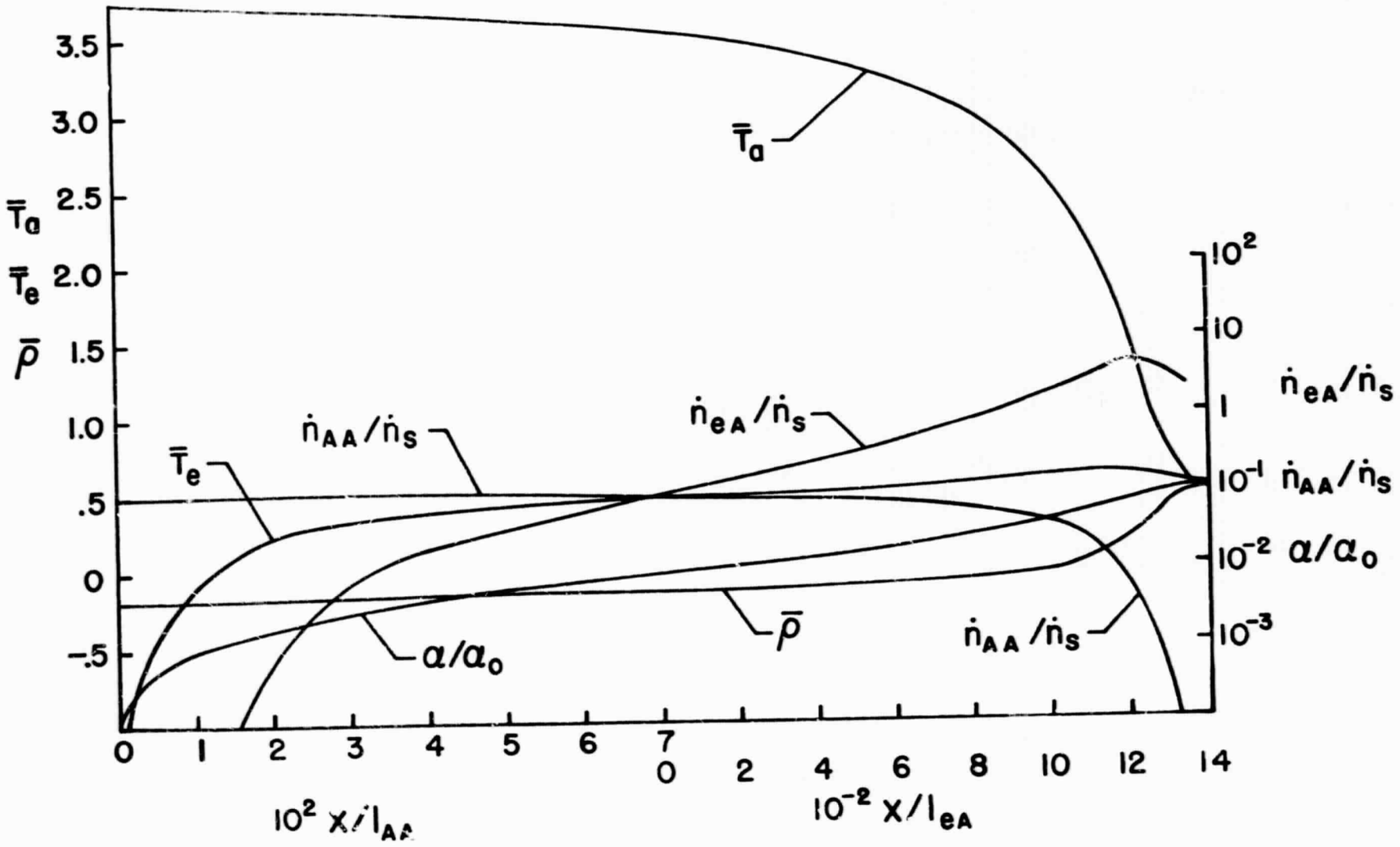

Figure 3.10. M = 30 Trapped Radiation Shock Wave with $T_e \neq T_a$.

is assumed. These lengths are shown in Table 3.4.

Table 3.4. Length of A-A and e-A regions for Trapped Radiation Shock Waves with $T_e \neq T_a$.

	x_{AA} (cm)	x_{eA} (cm)
M = 12	7.17	64.2
M = 18	.205	.349
M = 30	3.18 (10^{-2})	3.47 (10^{-2})

Because of the lower electron temperature the intensity of the radiation emitted from the gas just behind the viscous shock will be significantly less than the intensity of radiation which would be emitted were the gas in thermal equilibrium. The penetration length for ground state continuum radiation is less than or of the order of the length required for the electron temperature to become equal to the atom temperature and all of the ground state continuum radiation is emitted into the precursor region from right behind the viscous shock. Consequently the intensity of ground state continuum radiation is reduced. The precursor ionization for Mach number 12 is so much curtailed it is negligible. For the Mach numbers 18 and 30 reduced precursor ionization occurs. The degree of ionization produced by the Mach numbers 18 and 30 thermal non-equilibrium shock wave is shown in Figure 3.7.

The preceding results show the ratio of the penetration length to the length required for the electron temperature to attain the atom temperature is an important parameter in analyzing the precursor ionization caused by emission of ground state continuum radiation. It can also

be an important parameter in determining precursor ionization due to emission of radiation caused by other radiative reactions involving electrons.

Since the calculations show precursor ionization due to emission of ground state continuum radiation is negligible at Mach number 12, and considerable precursor ionization is measured at Mach numbers and pressures similar to those used in the calculations, [37], [38], [40], precursor ionization must be caused by some other radiative reaction.

Thermal Nonequilibrium with Complete Radiation

The analysis of this section includes radiation resulting from photoionization and radiative recombination involving excited bound states of the atom in addition to the radiation due to photoionization and radiative recombination involving only the atomic ground state which was considered in the previous section. The equations then include the integrals specified by equations (2.129) and (2.130).

The gas is not assumed to be in thermal equilibrium and the electron and atom temperatures may be different. Since the radiation integrals in equations (2.129) and (2.130) depend on the electron temperature, as do the equivalent optical thicknesses given by equations (2.133) and (2.134), the contribution of these terms is affected by the thermal nonequilibrium of the gas. Equations (1.26), (2.133) and (2.134) show the effect of lowering the electron temperature, all other factors being the same, is to decrease the penetration lengths of the excited state continuum radiation. Equations (2.129) and (2.130) show the excited state continuum radiative flux will be reduced if the electron temperature is lowered. Accordingly the radiative flux and

penetration lengths of the excited states continuum radiation is changed by the cool layer of electron gas just behind the shock discontinuity when thermal equilibrium is not established.

The solution for a Mach number 18 shock wave is shown in Figure 3.11. It consists of an atom-atom ionization region and an electron-atom ionization region, just like the corresponding solution without the excited state continuum radiation shown in Figure 3.9, followed by a radiation cooling region. The length ℓ'' chosen to nondimensionalize the coordinate x in the radiation cooling region is a typical penetration length for the continuum radiation in the frequency range $0 \leq \nu \leq \nu_M$. It is the distance in the uniform slab which would result after the shock if there were no radiation cooling for the optical thickness τ'' to be one. For the Mach number 18 shock wave $\ell'' = 42.7$ cm. The optical thickness τ' corresponding to continuum radiation in the frequency range $\nu_M \leq \nu \leq \nu_1$ is always much larger than τ'' and the radiative flux term Q_{M1} is negligible compared to Q_{oM}.

Up to the beginning of the radiation cooling region the solution is almost identical to that found excluding the excited states continuum radiation. At the beginning of the radiation cooling region the solutions for these two cases are within 1% of agreement. The equilibrium degree of ionization, however, is very sensitive to small changes in the solution and at the beginning of the radiation cooling zone, where without the excited states continuum radiation the solution was within 5% of the equilibrium degree of ionization, the degree of ionization is only within about 9% of the equilibrium degree of ionization. Furthermore, as equilibrium is approached, the collisional

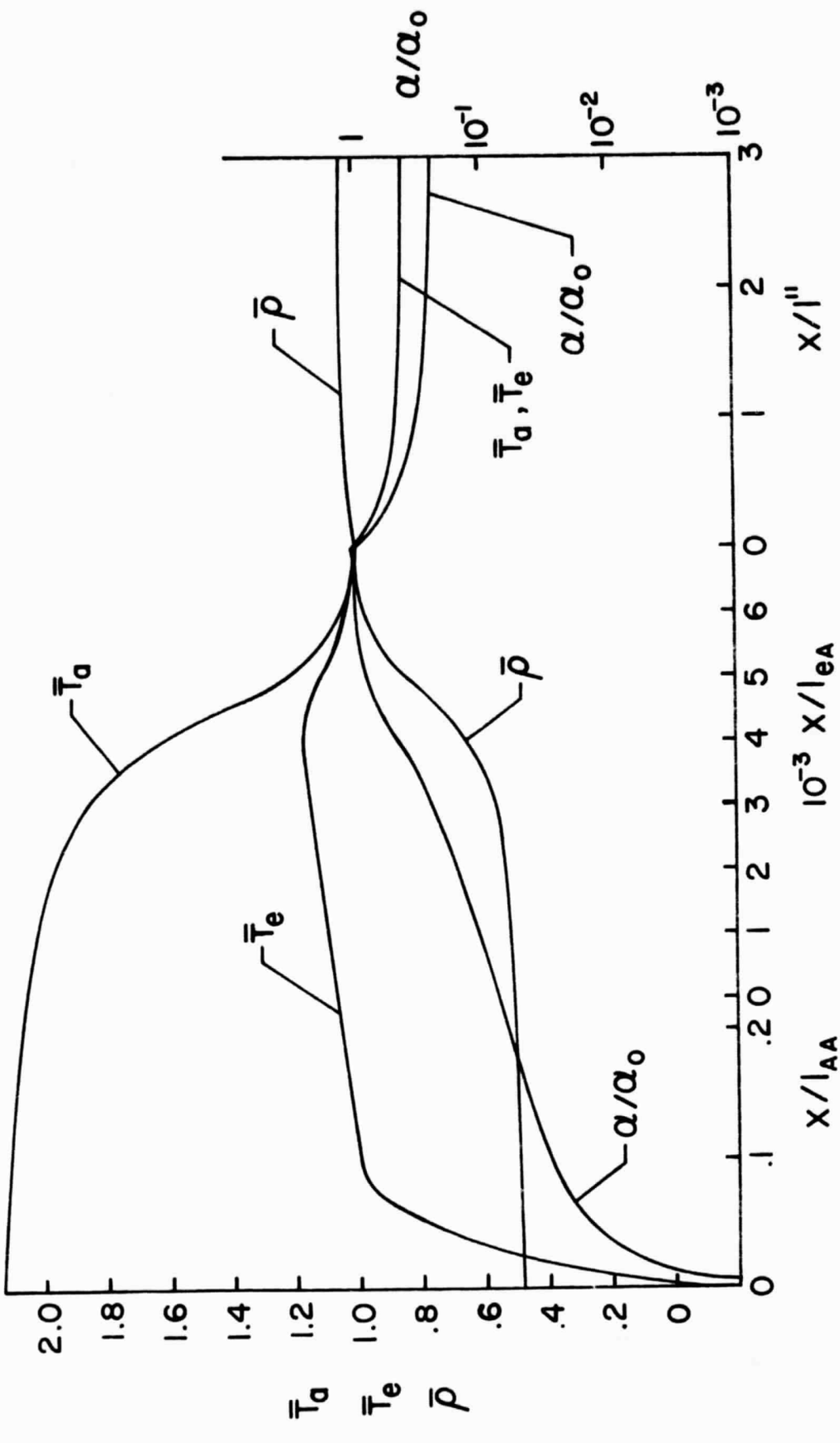

Figure 3.11. M = 18 Shock Wave with Radiation Cooling.

ionizational rate becomes small and the radiative rate becomes relatively more important. The radiative rate is a recombination rate. It opposes the collisional ionization rate. As a result the point at which the degree of ionization reaches 5% of its equilibrium value is considerably delayed. For the solution shown in Figure 3.11 this point is at $x/\ell'' = .1045$ which is 4.46 cm from the end of the e-A region where the 5% equilibrium point was attained when excited state continuum radiation was excluded from the analysis. The end of the e-A region is .545 cm. from the shock wave discontinuity and corresponds to 3.38 μsec. laboratory time. This compares well with the time to reach equilibrium ionization measured by Petschek and Byron [19] of 6.5 μsec. and that measured by Wong [20] of 4.7 μsec. The analytical solution of this section suggests, however, there is an extensive region beyond this point where the gas has not attained equilibrium, but is near equilibrium.

The distance to reach an equilibrium degree of ionization calculated in this section is that corresponding to T_{av} = 30,000 °K. This is a conservative estimate. Smaller values of T_{av} will result in longer distances to reach an equilibrium degree of ionization. Since line radiation, which has been excluded from the analysis, can cause an increased ionization rate and shorten the distance required to reach an equilibrium degree of ionization, the extent of the chemical nonequilibrium region is uncertain. It is clear, however, the relative magnitudes of collisional and radiative ionization rates are important when chemical equilibrium is approached.

CHAPTER IV

SUMMARY AND CONCLUSIONS

A gas, initially composed only of atoms, becomes a mixture of atoms, ions, and electrons in the process of ionization by a shock wave. The ways in which mass, momentum and energy may be transferred within such a mixture are different than for the unionized gas. The shock wave is profoundly affected if the transfer processes occur slowly compared to ionization. This is indeed the situation for the shock waves investigated in this thesis. The electrons lose translational energy in the process of ionizing neutral atoms. Furthermore, since electrons are inefficient in exchanging energy with the atoms and ions, they regain energy slowly, being effectively insulated from the atoms and ions. On the other hand the atoms and ions readily exchange energy. In this situation the gas may be thought of as a combination of two component gases, a gas composed of only electrons and a gas composed of both atoms and ions. The temperature of the electron gas may be different from that of the atom-ion gas, that is, the electron gas and the atom-ion gas may not be in thermal equilibrium. The inability of the electron gas and the atom-ion gas to establish equilibrium greatly affects the rate of ionization and radiative emission behind the shock wave.

Viscosity and heat conduction are changed by ionization. The electron gas is an especially good conductor of heat. For the shock waves of interest in this thesis, viscosity and heat conduction effects

are only important in a very thin portion of the shock wave. In this case the effect of viscosity and heat conduction can be thought of as discontinuously changing the temperatures and density at a point in the gas. Following the discontinuity the atom-ion gas cools because it loses energy by creating further ions, heating the electron gas and by emitting radiation. The temperature of the electron gas, however, is less than that of the atom-ion gas after the discontinuity. Subsequently there is a net gain of energy by the electron gas, heating it until thermal equilibrium is established with the atom-ion gas.

Two collisional processes are responsible for ionization, the atom-atom process and the electron-atom process. The rate of ionization due to the atom-atom process depends on the properties of the atom-ion gas, but the rate of ionization due to the electron-atom process depends on the properties of the electron gas. Since the electron gas is cooler than the atom-ion gas, the ionization rate due to the electron-atom process will be retarded compared to the rate which would be predicted assuming the electron gas and the atom-ion gas were in thermal equilibrium. The results presented in Chapter III show the ionization is significantly different in these two cases.

The grey gas assumption implies that radiation energy transfer can be described by a single frequency independent penetration length. For argon, however, there are many different penetration lengths because there are many possible radiative interactions which can occur. Consequently a grey gas model for argon is open to question.

The excited states of argon are closely spaced within a few electron volts of the ground state ionization limit. It follows that

the energy levels may be approximated as continuously distributed and hydrogenic. The radiation energy transfer due to photoionization and radiative recombination of all the excited states may then be found by integrating over the continuously distributed levels. The resulting radiation transfer equation has a marked frequency dependence. It agrees with the Unsöld result for small values of frequency, but at large values of frequency, where the Unsöld model fails, it has the proper form. For the shock waves considered in this thesis the penetration length for photoionization and radiative recombination from the excited states is large compared to lengths typical of other processes which may take place. In the precursor region it may be regarded as infinitely large. Consequently continuum radiation caused by photoionization and radiative recombination of the excited states results only in the radiation cooling of the gas behind the discontinuity. The penetration length for photoionization and radiative recombination of the ground state, however, is sufficiently small that the continuum radiation from the ground state is trapped, causing precursor ionization.

The total radiative flux and the radiative ionization rate are in the form of multiple integrals. These integrals can be reduced to the form they would have if the gas were grey, but the source functions and attenuation functions contained in these integrals in general are not those of a grey gas. Consequently the practice of using grey radiation transfer formulas to describe radiation energy transfer in a non-grey gas is not justified for the shock waves investigated in this thesis.

Radiation energy transfer depends on the behavior of the electron gas. Just after the shock discontinuity the radiative flux is less than the value it would have if thermal equilibrium were established, because the electron temperature there is less than the atom temperature. For the calculations performed in this thesis all of the radiation which is trapped in the precursor region comes from the cool layer of electron gas just behind the shock discontinuity. Consequently the precursor ionization is much reduced from that which would be estimated if thermal equilibrium were established. In fact the precursor ionization for the Mach number 12 shock wave is found to be negligibly small because thermal equilibrium is not established. Consequently the measured precursor ionization [37], [38], [40], for Mach numbers near 12 is not caused by continuum radiation trapped in the precursor region.

The penetration length for radiation caused by photoionization from the ground state is independent of temperature, but the penetration length for radiation caused by photoionization from excited states depends on the temperature of the electron gas. The excited state penetration length is an equivalent penetration length for photoionization for <u>all</u> excited levels and <u>all</u> possible frequencies of radiation. As shown by equation (2.111) it depends on the number density of electrons and is proportional to the electron temperature. As a result the penetration length for excited state continuum radiation is much smaller in the cool layer of electron gas near the shock wave discontinuity than it would be if the thermal equilibrium were established. This layer is therefore much more absorbent when thermal equilibrium is not established in the shock wave.

Radiation energy transfer, therefore, depends on the relative extent of the thermal and chemical nonequilibrium regions compared to the penetration lengths of radiative processes. The extent of the thermal and chemical nonequilibrium regions is reduced when the Mach number is increased.

Radiation has little effect on the ionization until equilibrium ionization is approached. Then the collisional rates decrease and the radiative rate becomes relatively more important. Since the radiative rate opposes the collisional rates the effect is to delay the point at which equilibrium ionization will be reached. There is an extensive region where the gas properties are nearly constant but not in chemical equilibrium. Since photoexcitation processes, which could increase the ionization rate and cause equilibrium to be reached more quickly, have been excluded from the calculations, the existence of the quasi-equilibrium region is questionable. It is certain, however, that the rate of ionization near equilibrium ionization is a delicate balance of collisional and radiative ionization rates.

BIBLIOGRAPHY

BIBLIOGRAPHY

1. M. T. Sherman, "Radiation-Coupled Chemical Nonequilibrium Normal Shock Waves," G. E. Missile and Space Div. Report R 66SD17 (1966).

2. F. A. Goldsworthy, "On the Dynamics of an Ionized Gas," in Progress in Aeronautical Sciences, (Pergamon, N. Y., 1961).

3. R. Goulard, "Similarity Parameters in Radiation Gas Dynamics," in High Temperatures in Aeronautics, (Pergamon, N. Y., 1962).

4. M. Y. Jaffrin, "Shock Structure in a Partially Ionized Gas," Phys. Fluids 8, 606 (1965).

5. J. H. Clarke and C. Ferrari, "Gas Dynamics with Nonequilibrium Radiative and Collisional Ionization," Phys. Fluids 8, 2121 (1965).

6. N. A. Heaslet and B. S. Baldwin, "Predictions of the Structure of Radiation Resisted Shock Waves," Phys. Fluids 6, 781 (1963).

7. S. S. Murty, "Approximations On Angular Distribution of Intensity of Thermal Radiation," Int. J. Heat and Mass Transfer 18, 1203 (1965).

8. R. Goulard and S. G. Traugott, "Radiation Fronts in Gasdynamics," Proceedings of the XIth International Congress for Applied Mechanics, Munich, August 1964.

9. I. M. Cohen and J. H. Clarke, "Influence of Viscosity on Shock Waves Structured by Radiation," Phys. Fluids 8, 1278 (1965).

10. R. R. Chow, "Effect of Thermal Radiation on Thin Shock Structure," AIAA J. 3, 973 (1965).

11. S. C. Traugott, "Shock Structure in a Radiating Heat Conducting and Viscous Gas," Phys. Fluids 8, 834 (1965).

12. H. K. Sen and A. W. Guess, "Radiation Effects in Shock Wave Structure," Phys. Rev. 108, 560 (1957).

13. H. E. Petschek, P. H. Rose, H. S. Glick, A. Kane and A. Kantrowitz, "Spectroscopic Studies of Highly Ionized Argon Produced by Shock Waves," J. Appl. Phys. 26, 83 (1955).

14. Yu. N. Redkoboradyi and V. I. Fedulov, Bolometer Measurement of Emission from Argon Ionized by a Shock Wave," Sov. Phys. Tech. Phys. 10, 1275 (1960).

15. S. S. R. Murty, "Effect of Line Radiation on Precursor Ionization," Proceedings of the Symposium on Interdisciplinary Aspects of Radiative Energy Transfer, Philadelphia, Pa., Feb. 1966.

16. M. McChesney and Z. Al-Attar, "Continuum Radiation Losses in Shock Heated Argon," JQSRT 5, 553 (1965).

17. J. Pomerantz, "The Influence of the Absorption of Radiation in Shock Tube Phenomena," JQSRT 1, 185 (1961).

18. K. K. Yoshikawa and D. R. Chapman, "Radiative Heat Transfer and Absorption Behind Hypersonic Normal Shock Waves," NASA TN D-1424 (1962).

19. H.H. Petschek and S. Byron, "Approach to Equilibrium Ionization Behind Strong Shock Waves in Argon," Ann. Phys. (New York) 1, 270 (1957).

20. H. Wong, "Interferometric Study of Thermal Equilibration of a Shock Heated Plasma," Ph. D. Thesis, Stanford University, 1956.

21. H. D. Weymann, "On the Mechanism of Thermal Ionization Behind Strong Shock Waves," Institute for Fluid Dynamics and Applied Mathematics, U. Maryland Tech. Note BN-144 (1958), also AD 202 113.

22. K. E. Harwell and R. G. Jahn, "Initial Ionization Rates in Shock Heated Argon, Krypton and Xenon," Phys. Fluids 7, 514 (1964).

23. A. J. Kelly, "Atom-Atom Ionization Cross Sections of the Noble Gases - Argon, Krypton and Xenon," J. Chem. Phys. 45, 1723 (1966).

24. L. Wetzel, "Far Flow Approximations for Precursor Ionization Profiles," AIAA J. 2, 1208 (1964).

25. E. J. Morgan and R. D. Morrison,"Ionization Rates Behind Strong Shock Waves in Argon," Phys. Fluids 8, 1008 (1965).

26. L. M. Biberman and I. T. Yakubov, "Approach to Ionization Equilibrium Behind the Front of a Shock Wave in an Atomic Gas," Sov. Phys. Tech. Phys. 8, 1002 (1964).

27. J. S. Hey, S. J. Parsons and G. S. Stewart, "Radar Observations of the Giacobinal Meteor Shower, 1964," Mon. Not. Roy. Astron. Soc. 107, 176 (1947).

28. D. R. W. McKinley and B. M. Millman, "A Phenomenological Theory of Radar Echoes from Meteors," Proc. IRE 37, 364 (1949).

29. S. C. Lin, "Radar Echoes from a Manned Satellite During Re-entry," J. Geo. Res. 67, 3851 (1962).

30. R. N. Hollyer, Jr., "Preliminary Studies in the A.P.L. High Temperature Shock Tube," Johns Hopkins Univ. Appl. Phys. lab. Report CM-903 (1957).

31. P. Gloersen, "Some Unexpected Results of Shock Heating Xenon," Phys. Fluids 3, 857 (1960).

32. H. D. Weymann, "Electron Diffusion Ahead of Shock Waves in Argon," Phys. Fluids 3, 345 (1960).

33. H. D. Weymann and B. Troy, "Electron and Ion Density Profiles Ahead of Shock Waves in Argon." Bull. Am. Phys. Soc. 6, 212 (1961).

34. L. Wetzel, "Far Flow Approximations for Precursor Ionization Profiles," AIAA J. 2, 1209 (1964).

35. A. C. Pipkin, "Precursor Waves in Shock Tubes," Phys. Fluids 6, 1382 (1963).

36. J. P. Appleton, "Electrical Precursor of Ionizing Shock Waves," Phys. Fluids 9, 336 (1966).

37. H. D. Weymann and L. B. Holmes, "Precursors Ahead of Pressure Driven Shock Waves in Argon," Proc. VIth International Conference on Ionization Phenomena in Gases, Paris, 1962.

38. L. I. Holmes, "Plasma Density Ahead of Pressure Driven Shock Waves," U. of Rochester, Dept. of Mechanical and Aerospace Sci., Tech. Note 1 (May 1965).

39. S. Zivanovic, "Investigation of Precursor Ionization in Front of Shock Waves of Hypersonic Projectiles," G. M. Defense Research Laboratories Report TR 63-2178 (1963).

40. S. Lederman and D. S. Wilson, "Microwave Resonant Cavity Measurement of Shock Produced Electron Precursors," Polytechnic Institute of Brooklyn, Dept. of Aerospace Engineering and Appl. Mechanics, PIBAL Report No. 958 (1966).

41. J. P. Appleton and K. N. C. Bray, "The Conservation Equations for a Nonequilibrium Plasma," J. Fluid Mech. 20, 659 (1964).

42. S. Chapman and T. G. Cowling, The Mathematical Theory of Non-Uniform Gases, (Cambridge University Press, N. Y., London, 1960).

43. T. R. Morse, "Energy and Momentum Exchange Between Nonequilibrium Gases," Phys. Fluids 6, 1420 (1963).

44. L. Spitzer, Physics of Fully Ionized Gases, (Interscience, New York, 1956).

45. I. Amdur and H. A. Mason, "Properties of Gases at Very High Temperatures," Phys. Fluids 1, 370 (1958).

46. I. P. Shkarofsky, M. R. Bachynski and I. W. Johnston, "Collision Frequency Associated with High Temperature Air and Scattering Cross Sections of the Constituents," Planetary Space Science 6, 24 (1961).

47. S. C. Brown, Basic Data of Plasma Physics, (The Technology Press, Cambridge, Mass., and John Wiley, New York, 1959).

48. R. Herdan and B. S. Liley, "Dynamical Equations and Transport Relationships for a Thermal Plasma," Rev. Mod. Phys. 32, 731 (1960).

49. V. M. Zhadanov, "Transport Phenomena in Partially Ionized Gas," Appl. Math. Mech. USSR 26, 401 (1962).

50. J. M. Burgers, in Plasma Dynamics, F. H. Clauser, editor, (Addison Wesley, Reading, Mass., 1960).

51. M. Y. Jaffrin and R. F. Probstein, "Structure of a Plasma Shock Wave," Phys. Fluids 7, 1658 (1964).

52. D. R. Bates, A. E. Kingston and R. W. P. McWhirter, "Recombination Between Electrons and Atomic Ions," Proc. Roy. Soc. A267, 297 (1962) and A270, 155 (1962).

53. D. R. Bates and A. B. Kingston, "Collision-Radiative Recombination at Low Temperatures and Densities," Proc. Roy. Soc. A279, 10 and 32 (1964).

54. D. R. Bates and A. B. Kingston, "Recombination and Energy Balance in a Decaying Plasma," Proc. Phys. Soc. 83, 43 (1964).

55. R. W. P. McWhirter and A. G. Hearn, "A Calculation of the Instantaneous Population Densities of the Excited Levels of Hydrogen-Like Ions in a Plasma," Proc. Phys. Soc. 82, 541 (1963).

56. D. R. Bates and S. R. Khare, "Recombination of Positive Ions and Electrons in a Dense Neutral Gas," Proc. Phys. Soc. 85, 231 (1964).

57. R. A. Alpher and D. R. White, "Visible Emission from Shocked Noble Gases," Phys. Fluids 7, 1239 (1964).

58. F. H. Mies, "Continuum Radiation from Ionized Rare Gases in Reflected Shock Waves," J. Chem. Phys. 37, 1101 (1962).

59. A. H. Dronov, A. G. Sviridov and N. N. Sobolev, "The Continuous Emission Spectra of Krypton and Xenon Behind a Shock Wave," Optics and Spec. USSR 12, 383 (1962).

60. D. H. Menzel and C. L. Pekeris, "Absorption Coefficients and Hydrogen Line Intensities," Mon. Not. Roy. Astron. Soc. 96, 77 (1935)."

61. G. L. Weissler, "Photoionization in Gases and Photoelectric Emission from Solids," Handb. der Phys. XXI, (Springer-Verlag, Berlin, 1956).

APPENDIX A

DERIVATION OF COLLISIONAL RATE CONSTANTS

The number of collisional encounters per unit volume and time between particles of species λ having velocities in the range $\vec{v}_\lambda$, $\vec{v}_\lambda + d\vec{v}_\lambda$ and particles of species λ having velocities in the range $\vec{v}_{\lambda'}$, $\vec{v}_{\lambda'} + d\vec{v}_{\lambda'}$ is given by the following classical kinetic theory expression [42].

$$n_\lambda n_{\lambda'} f_\lambda f_{\lambda'} g b \, db \, d\theta \, d\vec{v}_\lambda d\vec{v}_{\lambda'} \tag{A.1}$$

where f_λ is the velocity distribution function

$$f_\lambda = \left(\frac{m_\lambda}{2\pi \, kT_\lambda} \right)^{3/2} e^{-\frac{1}{2} m_\lambda v_\lambda^2 / kT_\lambda} \tag{A.2}$$

b is the impact parameter, θ is the angle between the plane of motion and a reference plane, and $\vec{g}$ is the relative velocity of the particles.

Let $\Sigma_{\lambda\lambda'}^{1 \to 2}(b,g)$ be the probability that the λ particle is excited from state 1 to state 2 during the collision with the particle. The number of excitations per unit volume and time is therefore

$$n_\lambda n_{\lambda'} f_\lambda f_{\lambda'} \Sigma_{\lambda\lambda'}^{1 \to 2}(b,g) \, b \, db \, d\theta \, d\vec{v}_\lambda d\vec{v}_{\lambda'}$$

The total number of excitations for all orientations and magnitudes of the vectors $\vec{v}$ and $\vec{v}'$ is

$$\frac{n_\lambda n_{\lambda'}}{1+\delta_{\lambda\lambda'}} \int d\vec{v}_\lambda f_\lambda \int d\vec{v}_{\lambda'} f_{\lambda'} g S_{\lambda\lambda'}(g) \qquad (A.3)$$

where $S_{\lambda\lambda'}(g)$ is the diffusion cross section

$$S_{\lambda\lambda'}(g) = \int_0^{2\pi} d\theta \int_0^{\infty} db \, \Sigma_{\lambda\lambda'}^{1\to 2}(b,g) b \qquad (A.4)$$

and $\delta_{\lambda\lambda'} = 1$ if species λ is different than species λ', zero otherwise.

Consider the collisions between atoms. Except for the small number of particles that become excited, translational energy is conserved in a collision so that [42]

$$\tfrac{1}{2} m_a (v_a^2 + v_{a'}^2) = m_a [G^2 - (\tfrac{1}{2} g)^2]$$

$$d\vec{v}_a \, d\vec{v}_{a'} = d\vec{G} \, d\vec{g}$$

where $\vec{G}$ is the center of mass velocity. Substitution into equation (A.4) gives the number of excitations per unit volume and time as $n_a K_A(1,2)$ where

$$K_A(1,2) = \tfrac{1}{2} \left(\frac{m_a}{2\pi \, kT_a} \right)^{3/2} \int_{g_o}^{\infty} 4\pi g^2 \, dg \, e^{-\frac{1}{4} m_a g^2 / kT_a} g \, S_{aa}(g) \qquad (A.5)$$

g_o is defined by requiring $\frac{1}{4} m_a g_o^2$ to be the threshold energy E_{ex} required for the excitation. Since $kT_a \ll E_{ex} \leq \frac{1}{2} m_a g^2$, the cross section need only be known near the excitation threshold to obtain an accurate value of the integral in equation (A.5). Substituting

$$S_{aa} = C_A (E - E_{ex})$$

in Equation (A.5) gives the rate constant used in equation (2.73).

$$K_A(1,2) = \frac{2C_A}{\sqrt{\pi\, m_a}} (k\, T_a)^{3/2} \left(\frac{T_{ex}}{T_a} + 2 \right) e^{-T_{ex}/T_a} \qquad (A.6)$$

where $T_{ex} = E_{ex}/k$. The value of $C_A = 7.5(10^{-3})$ cm^3 erg used in this thesis is that determined by Kelley [23].

For collisions between electrons and atoms the velocity distribution functions are given by equation (A.2) at the temperatures T_e and T_a respectively. Since the electron and atom temperatures are of the same order of magnitude and the electron mass is much smaller than the atom mass, the electron velocity must be much larger than the atom velocity. This is the basis of the following approximations.

$$g = [\bar{g} \cdot \bar{g}]^{\frac{1}{2}} = [v_e^2 - 2\bar{v}_e \cdot \bar{v}_a + v_a^2]^{\frac{1}{2}}$$

$$= v_e \left[1 - \frac{2\bar{v}_e \cdot \bar{v}_a}{v_e^2} + \ldots \right] \qquad (A.7)$$

$$S_{ea}(g) = S_{ea}(v_e) + (g - v_e) \left(\frac{d\, S_{ea}}{dg} \right)_{g = v_e} + \ldots$$

$$= S_e(v_e) - \frac{\bar{v}_e \cdot \bar{v}_a}{v_e^2} \left(\frac{dS_{ea}}{dg} \right)_{g = v_e} + \ldots \qquad (A.8)$$

Using these approximations equation (A.3) becomes

$$n_e\, n_a \int_{v_{e_o}}^{\infty} 4\pi\, v_e^2\, dv_e\, f_e(v_e)\, S_{ea}(v_e) \qquad (A.9)$$

where $\frac{1}{2} m_e v_{e_o}^2$ is the threshold energy E_{ex} required for the excitation. As in the previous result, the cross section need only be known near threshold to give an accurate value for the integral in equation (A.9). Near the threshold energy the cross section may be represented by

$$S_{ea}(v_e) = C_e(\tfrac{1}{2} m_e v_e^2 - E_{ex}). \qquad (A.10)$$

With this approximation for the cross section equation (A.9) gives the number of electron-atom excitations per unit volume and time as $K_e(1,2)\, n_e n_a$ where

$$K_e(1,2) = \frac{C_e}{\sqrt{\pi\, m_e}} (2kT_e)^{3/2} \left(\frac{T_{ex}}{T_e} + 2 \right) e^{-T_{ex}/T_e} \qquad (A.11)$$

The value of the constant in the excitation cross section formula employed by Petschek and Byron [19] is $C_e = 4.4(10^{-4})$ cm^2/erg. This value is used for the computations in this thesis.

APPENDIX B

RADIATIVE REACTION TRANSFER EQUATIONS

It follows from equation (A.9) in Appendix A that the number of collisions between electrons with energy in the range η, $\eta + d\eta$ and ions per unit volume and time is $n_e\, n_i\, f_e(\eta)d\eta$ where $f_e(\eta)$ is the energy distribution function for the electrons.

$$f_e(\eta) = \frac{2\pi}{(\pi\, kT_e)^{3/2}}\ \sqrt{\eta}\ \ e^{-\eta/kT_e}$$

Let $A_{cp}\, d\omega$ be the probability that in such an encounter the electron will lose energy $h\nu = \chi_p + \eta$ by emitting radiation within a solid angle $d\omega$ of a direction specified by a unit vector $\hat{L}$. The electron will then be in the p^{th} atomic state. The total radiation intensity emitted in the frequency interval ν, $\nu + d\nu$ per unit volume and time by all such collisions is

$$h\nu\, A_{cp}\, n_e n_i\ f_e(\eta)\, h\, d\nu\, d\omega \qquad (B.1)$$

In addition to the spontaneous emission just discussed emission of radiation may be induced by the radiation field. Let B_{cp} be the probability that in an ion-electron encounter the radiation field causes the recombination. The radiation intensity emitted at point P within solid angle $d\omega$ of the direction specified by $\hat{L}$ and in the frequency range ν, $\nu + d\nu$ induced in electron-ion encounters is

$$h\nu\, B_{cp}\, I(P, \hat{L}, \nu)\, n_e\, n_i\, f_e(\eta)\, h\, d\nu\, d\omega \qquad (B.2)$$

Let B_{pc} be the probability per unit intensity that an atom in state p will be photoionized creating an electron with energy in the range η, $\eta + d\eta$ and causing a loss of radiation energy equal to $h\nu = \chi_p + \eta$ from the radiation within solid angle $d\omega$ about the direction specified by the vector $\hat{L}$. The total intensity of radiation absorbed from the radiation field within a solid angle $d\omega$ of the direction specified by $\hat{L}$ and the frequency range ν, $\nu + d\nu$ due to photoionization from atomic state p at point P is

$$h\nu\, n(p)\, B_{pc}\, I(P, \hat{L}, \nu)\, d\omega\, d\nu \qquad (B.3)$$

The rate of change of intensity at point P within solid angle $d\omega$ about the direction specified by $\hat{L}$ in the frequency range ν, $\nu + d\nu$ is the sum of the intensities given by equations (B.1), (B.2) and (B.3).

$$\frac{dI(P,\hat{L},\nu)}{ds} = -\left[n(p)\, B_{pc} - n_e n_a\, f_e(\eta)\, h\, B_{cp}\right] h\nu\, I(P, \hat{L}, \nu)$$

$$+ h\nu\, A_{cp}\, n_e n_i\, f_e(\eta) h$$

$$= -\, n(p)\, B_{pc} \left[1 - \frac{n_e n_i}{n(p)}\, f_e(\eta)\, n\, \frac{B_{cp}}{B_{pc}} \right] h\nu\, I(P, \hat{L}, \nu)$$

$$+ h\nu\, \frac{A_{cp}}{B_{pc}}\, \frac{n_e n_i}{n(p)}\, f_e(\eta)\, h \qquad (B.4)$$

Using the Einstein relations

$$\frac{B_{cp}}{B_{pc}} = \frac{g_p}{g_f} \qquad \frac{A_{cp}}{B_{cp}} = \frac{2\,h\nu^3}{c^2}$$

where g_f is the degeneracy of the free electron states [60]

$$g_f = 2\,\frac{4\pi\, m_e}{h^2}^{3/2}\sqrt{2\eta}$$

and g_p is the degeneracy of the p^{th} atomic state, equation (B.3) can be written in the form of equation (2.88)

$$\mu \frac{dI_p(x,\mu,\nu)}{dx} = \frac{1}{\ell_p(x,\nu)}\,[I(x,\mu,\nu) - S_p(x,\nu)\,] \tag{B.5}$$

where

$$\frac{1}{\ell_{pc}}(x,\nu) = n(p)\,B_{pc}\left[\,1 - \frac{n(p)_E}{n(p)}\;e^{-h\nu/kT_e}\,\right] \tag{B.6}$$

$$S(x,\nu) = \frac{n(p)_E}{n(p)}\;\frac{2h\nu^3}{c^2}\left(e^{h\nu/kT_e} - \frac{n(p)_E}{n(p)}\right)^{-1} \tag{B.7}$$

In these equations $n(p)_E$ is the population of state p which would exist if state p were in equilibrium with the ions and electrons.

$$\frac{n_e n_i}{n(p)_E} = \frac{2(2\pi\, m_e\, kT_e)^{3/2}}{h^3 g_p}\; e^{-\chi_p/kT_e} \tag{B.8}$$

The radiation energy transfer equation for radiative excitations can be derived in a similar way. Let A_{qp} be the probability for spontaneous emission, B_{qp} that for induced emission and b_{pq} that for absorption for a radiative transition between atomic states p and q. The radiation transfer equation for photoexcitation reaction between

states p and q is

$$\frac{dI_{pq}}{ds} = -n(p)B_{pq}\,\beta_{pq}(\nu)\,I(P,\hat{L},\nu) + n(g)B_{qp}\,\beta_{pq}(\nu) + n(q)\,A_{qp}\,\beta_{pq}(\nu)$$

$$= -\,n(p)\,B_{pq}(\nu)\,\beta_{pq}(\nu)\left[I(P,\hat{L},\nu) - \frac{n(q)}{n(p)}\,\frac{g_p}{g_q}\right) - \frac{n(q)}{n(p)}\,\frac{g_p}{g_q}\,\frac{2h\nu^3}{c^2}\,\Bigg] \qquad (B.9)$$

where $\beta_{pq}(\nu)$ is the line shape function. This may be written in the form of equation (2.88).

$$\mu\,\frac{dI_{pq}^{(x,\mu,\nu)}}{dx} = -\,\frac{1}{\ell_{pq}^{(x,\nu)}}\,[I(x,\mu,\nu) - S_{pq}(x,\nu)\,] \qquad (B.10)$$

where

$$\frac{1}{\ell_{pq}^{(x,\nu)}} = n(p)\,B_{pq}\,\beta_p(\nu)\,\left[\,1 - \frac{n(q)}{n(p)}\,\frac{g_p}{g_q}\,\right] \qquad (B.11)$$

$$\zeta_{pq}(x,\nu) = \frac{n(q)}{n(p)}\,\frac{g_p}{g_q}\,\frac{2h\nu^3}{c^2}\left(1 - \frac{n(q)}{n(p)}\,\frac{g_p}{g_q}\right)^{-1} \qquad (B.12)$$

APPENDIX C

AVERAGE ENERGIES OF CREATED ELECTRONS

Assume the primary way in which electrons are created in the atom-atom ionization process is by collisions between electrons and excited argon atoms. An electron of energy η on collision with an excited atom will produce an electron of energy ζ and lose energy $\zeta - \chi_2$ in the process.

$$e_\eta + A(2) \rightarrow A^+ + e_\eta - e_{(\eta - \chi_2 - \zeta)} \qquad (C.1)$$

where the energies of the electrons are indicated by their subscripts.

It follows from Appendix B that the rate at which electrons are created is

$$n_a n_e \; f(\eta) \sqrt{\frac{2\eta}{m_e}} \; S_{2 \rightarrow c}(\eta, \zeta) \, d\eta \, d\zeta$$

where $S_{2 \rightarrow c}(\eta,\zeta) \, d\eta \, d\zeta$ is the cross section for the process described by equation (C.1) and $f(\eta)$ is the electron energy distribution function.

$$f(\eta) = \frac{2\pi}{(\pi \, kT_e)^{3/2}} \sqrt{\eta} \; e^{-\eta/kT_e}$$

The total rate of production of energy in the form of created electrons is therefore

$$n_a n_e \int_{\chi_2}^{\infty} f(\eta) \sqrt{\frac{2\eta}{m_e}} \, d\eta \int^{\eta - \chi_2} \zeta \, S_{2 \rightarrow c}(\eta,\zeta) \, d\zeta$$

Dividing this by the rate of production of electrons gives the average energy of a collisionally created electron.

$$\bar{\zeta} = \frac{\int_{\chi_2}^{\infty} f(\eta)\eta^{\frac{1}{2}}\, d\eta \int_{0}^{\eta-\chi_2} \zeta\, S_{2\to c}(\eta, \zeta)\, d\zeta}{\int_{\chi_2}^{\infty} f(\eta)\, \eta^{\frac{1}{2}}\, d\eta \int_{0}^{\eta-\chi_2} S_{2\to c}(\eta, \zeta) d\zeta} \qquad (C.2)$$

Using the Thompson cross section

$$S_{2\to c}(\eta,) = \frac{\pi e^4}{\eta(\chi_2 + \zeta)^2}$$

the integration over ζ can easily be performed. The remaining integration can be carried out by noting $\eta \gg kT_e$ and expanding the integrand about the value $\eta = \chi_2$.

$$\bar{\zeta} = \frac{\int_{\chi_2}^{\infty} e^{-\eta/kT_e} \left[\ln \frac{\eta}{\chi_2} - \left(1 - \frac{\chi_2}{\eta}\right)\right] d\eta}{\int_{\chi_2}^{\infty} e^{-\eta/kT_e} \frac{1}{\chi_2}\left(1 - \frac{\chi_2}{\eta}\right) d\eta}$$

$$= \frac{e^{-\chi_2/kT_e} \int_{0}^{\infty} e^{-\eta/kT_e} \left[\frac{1}{2}\left(\frac{\eta}{\chi_2}\right)^2 + \ldots\right] d\eta}{\frac{1}{\chi_2} e^{-\chi_2/kT_e} \int_{0}^{\infty} e^{-\eta/kT_e} \left(\frac{\eta}{\chi_2} + \ldots\right) d\eta}$$

$$= \frac{e^{-\chi_2/kT_e}\, kT_e \left[\left(\frac{kT_e}{\chi_2} \right)^2 + \ldots \right]}{\frac{1}{\chi_2} e^{-\chi_2/kT_e}\, kT_e \left[\left(\frac{kT_e}{\chi_2} \right) + \ldots \right]} = kT_e \qquad (C.3)$$

Consider next the electrons produced by photoionization from the ground state. Assume the radiative intensity is given by the Planck function. The number of absorptions producing electrons with energy in the range ζ, $\zeta + d\zeta$ is then (c.f. Appendix B).

$$\frac{h(1)\, B_{1c}}{h\nu} B_\nu (T_e) \quad \frac{d\zeta}{h}$$

The average energy of photoelectrons created by photoionization from the ground state is therefore

$$\bar{\zeta} = \frac{\int_0^\infty \zeta \frac{B_{1c}}{h\nu} B_\nu(T_e) \frac{d\zeta}{h}}{\int_0^\infty \frac{B_{1c}}{h\nu} B_\nu(T_e) \frac{d\zeta}{h}} \qquad (C.4)$$

Making the following substitutions

$$\zeta = h\nu - \chi$$

$$B_{1c} = B_o \left(\frac{\nu_1}{\nu} \right)^2$$

$$B_\nu(T_e) \doteq \frac{2h\nu^3}{c^2} e^{-h\nu/kT_e}$$

equation (C.4) can be written as

$$\bar{\zeta} \qquad \frac{\int_{\nu_1}^{\infty} (h\nu - \chi)\, e^{-h\nu/kT_e}}{\int_{\nu_1}^{\infty} e^{-h\nu/kT_e}\, d\nu} = \frac{kT_e}{\chi} \qquad (C.5)$$

As in Chapter II assume the excited states are closely spaced and hydrogenic. Assuming the radiative intensity to be given by the Planck function, the rate of production of electrons with energy in the range ζ, $\zeta + d\zeta$ from a group of excited levels having energy in the range χ, $\chi + d\chi$ below the ionization limit is

$$n_e^2 \cdot \frac{h^3}{2(2\pi\, m_e kT_e)^{3/2}} \frac{K Z^2}{2h^2 R} \frac{e^{-\zeta/kT_e}}{\chi + \zeta}\, d\chi d\zeta \qquad (C.6)$$

The rate of production of electrons with energy in the range ζ, $\zeta + d\zeta$ from all the excited levels is

$$n_e^2 \frac{h^3}{2(2\pi m_e kT_e)^{3/2}} \frac{KZ^2}{2h^2 R} e^{-\zeta/kT_e}\, d\zeta \int_0^{\chi_M} \frac{d\chi}{\chi - \zeta}$$

Therefore the average energy of an electron created by photo-ionization from the excited states of the atom is

$$\bar{\zeta} = \frac{\int_0^{\infty} \zeta\, e^{-\zeta/kT_e} \ln\left(\frac{\chi_M + \zeta}{\zeta}\right) d\zeta}{\int_0^{\infty} e^{-\zeta/kT_e} \ln\left(\frac{\chi_M + \zeta}{\zeta}\right) d\zeta}$$

$$= \frac{\int_0^\infty U\, e^{-U} \ln\left(\frac{\chi_M/kT_e + U}{U}\right) dU}{\int_0^\infty e^{-U} \ln\left(\frac{\chi_M/kT_e + U}{U}\right) dU} \qquad (C.7)$$

Numerical integration of the integrals in equation (C.7) for the representative value $\chi_M/kT_e = 4$ gives

$$\bar{\zeta} = .645\ kT_e \qquad (C.8)$$

The average energy of electrons created in the atom-atom ionization process or by photoionization is of the order kT_e or les as was stated in Chapter II.

APPENDIX D

CALCULATIONAL DETAILS

As explained in Chapter II, the radiative terms are made artificially small by a multiplying factor. Such a factor multiplies each of $Q_{l\infty}$, Q_{Ml}, Q_{oM} and Q'_{oM}. Starting with the radiationless solution the factors for $Q_{l\infty}$ and Q_{Ml} may be immediately set to one since they have little effect on the solution behind the shock discontinuity. The factors for Q_{oM} and Q'_{oM} must be small, however, since these terms control the radiative cooling and ionization rate. The procedure used was to keep the factor for Q'_{oM} small (usually zero) until the solution was found for which the factor for Q_{oM} was one. In this way the long quasi-equilibrium region caused by the radiative ionization rate opposing the collisional ionization rate near equilibrium need not be calculated each time, resulting in a considerable reduction in computer time.

Successive steps in the solution are shown in Figure D.1 where the degree of ionization in the radiative cooling region is shown. The degree of ionization is only slightly affected by the excited state radiation elsewhere. Curve number 1 is the solution obtained with the Q_{oM} factor .1 and using as the previous solution that obtained with the Q_{oM} factor zero. Curves 2 and 3 show the solutions obtained when the Q_{oM} factor is increased to .3 and then to .5 each time using the previous

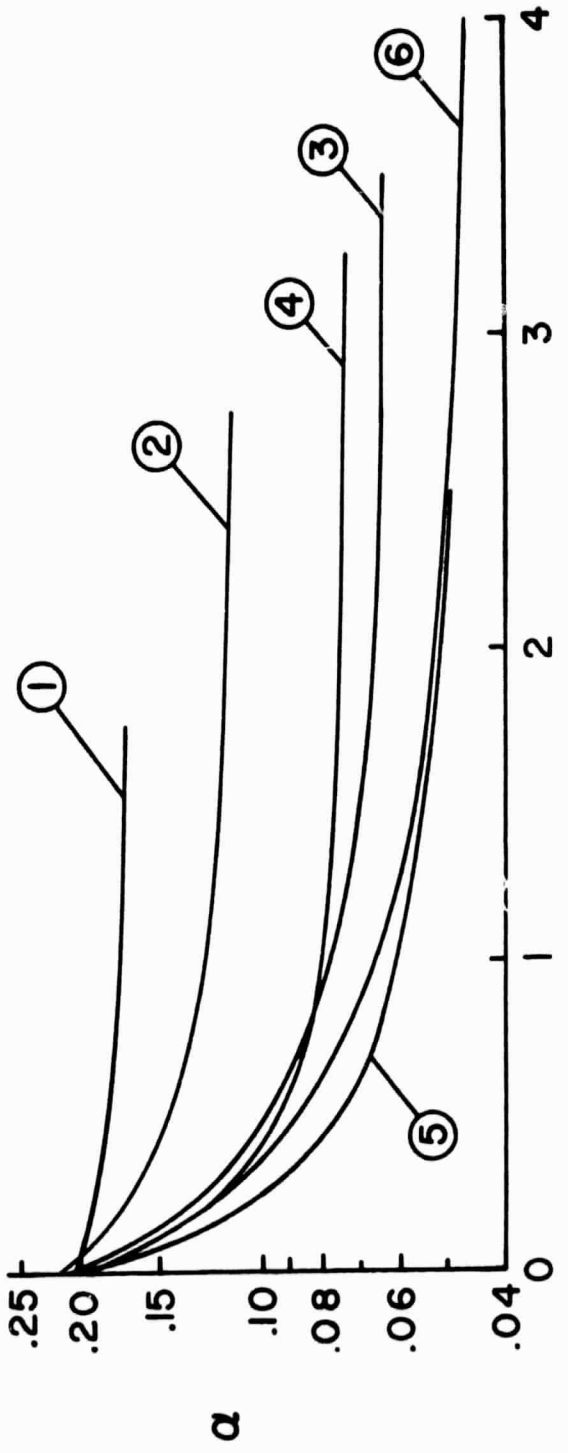

Figure D.1. Successive Steps in the Solution.

solution to estimate the radiative terms. (The larger value of the degree of ionization for curve 2 was caused by an error in the input values to the computer program, subsequently corrected.) The factor was then held at .5 and convergence was rapidly obtained resulting to curve 4. Using this solution and increasing the Q_{oM} factor to .7 results in curve 5. The Q_{oM} factor was then made one and the average of the latest solution and the previous solution was used to generate the next solution. Convergence was rapid. The factor for Q'_{oM} was then made one. The solution was little changed except for the delay of equilibrium which occurred. The result is shown as curve 6.

It required about thirty minutes of IBM 7094 computer time to reach the final solution.